View metadata, citation and similar papers at core.ac.uk

brought to you by CORE

provided by University of Saskatchewan's Research Archive

CHARACTERIZATION OF THE MOVEMENT OF SPRAY DRIFT PAST A SHELTERBELT

A thesis submitted to the College of Graduate Studies and Research
in partial fulfillment of the requirements for the Degree of Master of Science in the
Department of Civil and Geological Engineering, University of Saskatchewan

By:

Jonathan Christian Peterson

Copyright Jonathan Christian Peterson, April 2008. All rights reserved.

PERMISSION TO USE

In presenting this thesis in partial fulfillment of the requirements for a Postgraduate degree from the University of Saskatchewan, I agree that the Libraries of this University may make it freely available for inspection. I further agree that permission for copying of this thesis in any manner, in whole or in part, for scholarly purposes may be granted by the professors who supervised my thesis work or, in their absence, by the Head of the Department or the Dean of the College in which my thesis work was done. It is understood that any copying or publication or use of this thesis or parts thereof for financial gain shall not be allowed without my written permission. It is also understood that due recognition shall be given to me and to the University of Saskatchewan in any scholarly use which may be made of any material in my thesis.

Requests for permission to copy or to make other uses of materials in this thesis in whole or part should be addressed to:

Head of the Department of Civil and Geological Engineering
University of Saskatchewan
57 Campus Drive
Saskatoon, Saskatchewan S7N 5A9
Canada

OR

Dean
College of Graduate Studies and Research
University of Saskatchewan
107 Administration Place
Saskatoon, Saskatchewan S7N 5A2
Canada

DISCLAIMER

Reference in this thesis to any specific commercial products, process, or service by trade name, trademark, manufacturer, or otherwise, does not constitute or imply its endorsement, recommendation, or favouring by the University of Saskatchewan. The views and opinions of the author expressed herein do not necessarily state or reflect those of the University of Saskatchewan, and shall not be used for advertising or product endorsement purposes.

ABSTRACT

Pesticide use is an important component of the agricultural industry. Pesticides are typically applied to crops as a droplet spray, and these droplets are susceptible to off-target movement due to wind, which is called spray drift. It has recently been recognized that shelterbelts may protect vulnerable downwind areas from spray drift. There is a need to characterize the movement of spray drift past a shelterbelt to better understand the extent of this protection and the variables which affect it. The variables investigated in this research may be classified as meteorological conditions, spray application settings, and shelterbelt properties.

This research investigated the movement of spray drift past a 5 m tall carragana/chokecherry shelterbelt. Spray was applied using a conventional sprayer that travelled on a path that was upwind and parallel to the shelterbelt. A tracer substance was mixed into the spray solution, and the deposition and airborne concentration of drift was measured using a variety of collectors placed at perpendicular distances up- and downwind of a shelterbelt. The mass of drift deposit on the collectors was determined using spectrofluoremetry and standard solutions.

When the spray swath was a distance of 3H (where H is the height of the shelterbelt) upwind of the shelterbelt, it was found that the ground deposition of drift at a distance of 0.5H downwind of the shelterbelt was reduced by approximately 74%, compared to the drift deposit at 0.5H upwind. The reduction over the same downwind distances was 29% in the open field setting. The airborne drift cloud was attenuated by the shelterbelt and the airborne concentration of drift exiting the shelterbelt was reduced by approximately 85% of the entering drift. The airborne drift concentration profile indicated that there was a greater proportion of drift travelling over the top of the

shelterbelt rather than passing through the shelterbelt, with the peak concentration occurring at approximately 1.2H.

Qualitative and multiple linear regression analyses were used to determine the significance of a number of meteorological and controlled variables on the deposition of drift. It was found that the mass of drift deposited downwind of the shelterbelt increased with a higher wind speed, higher temperature, and lower relative humidity. For the range of meteorological conditions sampled, the effect of wind direction and atmospheric stability were found to be insignificant. Finer spray qualities and higher shelterbelt optical porosity produced greater airborne drift and deposition downwind of the shelterbelt. With increasing upwind sprayer distance, the mass of drift deposited within the shelterbelt decreased.

ACKNOWLEDGEMENTS

The author acknowledges the guidance and support provided by my co-supervisors, Dr. Kerry Mazurek and Dr. Tom Wolf, along with the rest of my advisory committee, Dr. Jim Bugg, Dr. Jim Kells, and Dr. Gordon Putz. The author wishes to thank Brian Caldwell, Dan Caldwell, Dave Cote, Lorelei Gress, and Adelle McIntosh for their technical support in the field. Thanks are extended to the Merlin Lee family for providing access to the land where the experiments were conducted, and to DuPont Research Farm, Hanley, Saskatchewan for providing access to their storage facilities. The author also wishes to thank Agriculture and Agri-Food Canada for providing financial support.

TABLE OF CONTENTS

LIST OF TABLES

LIST OF FIGURES

LIST OF SYMBOLS

a_i	calibration coefficients in the regression model
A	collector area
A_{LA}	leaf area index
C	concentration of dye
C_d	drag coefficient
C_{Dark}	concentration of dye on the photolysis dishes kept in the dark
C_{Light}	concentration of dye on the photolysis dishes exposed to sunlight
C_{ng/cm^2}	concentration of dye (ng/cm^2)
C_{ppb}	concentration of dye (ppb)
C_o	concentration of particles entering the shelterbelt
C_1	concentration of particles exiting the shelterbelt
D	upwind sprayer distance
D_b	total deposition of particles to a windbreak
$D_{V0.1}$	diameter which contains 10% of the spray volume
$D_{V0.5}$	diameter which contains 50% of the spray volume
$D_{V0.9}$	diameter which contains 90% of the spray volume
g	gravitational acceleration
H	shelterbelt height
k_r	resistance coefficient
$M_{Applied}$	mass of spray delivered by the sprayer
N_L	number of light pixels
N_T	total number of pixels
P_h	photolysis correction factor

Q	spray quality
$\dot{Q}$	flow rate of spray delivered by the sprayer
Ri	Richardson number
RH	relative humidity
s	shelter parameter
T	temperature
ΔT	wet bulb depression
T_K	absolute temperature
T_{wb}	wet bulb temperature
u'	root mean squared velocity
U	wind speed
U_m	minimum wind speed downwind of the shelterbelt
U_o	approach wind speed
v	travel speed of the sprayer
V_{wash}	wash volume
W	boom width of the sprayer
x	distance perpendicular to shelterbelt
x_b	distance to the back edge of the shelterbelt
x_f	distance to the front edge of the shelterbelt
x_i	independent variables in the regression model
Y	dependent variable in the regression model
z	height
α	shelterbelt aerodynamic porosity
β	shelterbelt optical porosity
γ	wind direction relative to perpendicular to the shelterbelt
Γ	dry adiabatic lapse rate
ξ	potential temperature
ρ	density of spray solution
σ	transmittance of particles

Chapter 1

INTRODUCTION

1.1 Background

Pesticide use is an important component of the agricultural industry because it allows the producer to control insects, weeds, and disease that may otherwise infest the crop. These pesticides are most commonly applied to crops as a polydisperse droplet spray where the median sized droplets are typically in the order of 100 µm in diameter (Bache and Johnstone, 1992). Droplets of this size are susceptible to off-target movement due to wind and this is termed "spray drift". Spray drift occurs when droplets are swept downwind from the application area or when the active ingredient in particles that land in the treated area later volatize and travel downwind (Miller, 1993). Modern pesticides are formulated to have a low vapour pressure so that the proportion of volatile particle drift is minimal compared to droplet drift.

Although the deposition of spray drift decreases with the logarithm of distance from the point of application (Carlsen et al., 2006), a sufficient amount may be carried downwind and harm vulnerable areas, particularly neighbouring crops, water bodies, and residential areas. While this may not necessarily be lethal to the affected downwind area, it could delay growth of vegetation and disrupt the competitive balance of an ecosystem (Marrs et al., 1992).

Current strategies to mitigate the negative effects of spray drift include the use of buffer zones and low-drift sprayer components. Buffer zones are located on the downwind edge of a field and may be composed of mixed vegetation in the field boundary or the crop itself. Buffer zones are not treated with pesticide and thus provide a separation for vulnerable organisms downwind from the treated area.

Low-drift sprayer components include air induction, twin-fluid, and electrostatic nozzles and shrouds. Air induction nozzles mix air with the spray liquid in a pre-orifice chamber and produce droplets with an internal air cavity. These droplets are larger in size than those produced by a conventional nozzle, and are thus less prone to drift (Miller and Lane, 1999). Twin-fluid nozzles issue an air jet within the nozzle orifice that propels the droplets towards the crop canopy. Electrostatic nozzles are used to improve deposition to the crop canopy. The droplets are electrically charged and are attracted to the ground, which enhances deposition and reduces drift (Bache and Johnstone, 1992). Shrouds may be placed on the sprayer boom and act to shield the spray nozzle from cross winds and, in some cases, are designed to propel the droplets downwards to the crop canopy (Ozkan et al., 1997; Wolf et al., 1993).

There has been recent interest in the use of shelterbelts to mitigate spray drift. A shelterbelt, also referred to as a windbreak, is composed of trees in a single or series of rows. Figure 1.1 is an example of a typical shelterbelt found in Saskatchewan. They are designed to be tall (5-10 m) in order to provide the greatest shelter extent and narrow to minimize the crop area occupied (Loeffler et al., 1992; Nord, 1991). Shelterbelts are typically used to combat wind-induced soil erosion, trap snow to improve soil moisture, shelter livestock, protect roadways and yard sites from dangerous cross winds, and improve biodiversity (Jones and Sudmeyer, 2002). Previous research has also shown that a shelterbelt may modify the temperature, humidity, and solar radiation in its vicinity, which may benefit the crop in the up- and downwind areas of the shelterbelt (Cleugh, 2002). The potential of shelterbelts for trapping particulate matter and odour from intensive livestock operations has also been recently realized (Adrizal et al., 2008).

It is suggested that spray drift past a shelterbelt is reduced through two mechanisms as it moves past a shelterbelt: (1) a reduction in local wind velocity that allows droplets to settle out; and (2) a “scrubbing” of the droplet-laden flow as it passes through the canopy of the shelterbelt (Ucar and Hall, 2001; Raupach et al., 2001). This observation is supported by previous studies that have examined the movement of drift past other types of field boundaries including natural grass strips (Miller and Lane,

Figure 1.1 Typical shelterbelt found in Saskatchewan

1999), vinyl snow fences (Brown et al., 2004), and riparian zones (Wolf et al., 2004). These studies have all shown a reduction in drift downwind of the barrier.

The flow around a shelterbelt is complex and depends on the width, porosity, and uniformity of the vegetation. When the flow encounters the shelterbelt, some passes through the vegetation (bleed flow) while the majority is diverted over the top (displaced flow) (Judd et al., 1996). The displaced flow reattaches to ground level at a distance of approximately 25H downwind of the shelterbelt, where H is the height of the shelterbelt (Cleugh, 1998). Previous studies, such as Davis et al. (1994) and Wolf et al. (2004), have found drift deposit to decrease in the immediate downwind vicinity of a hedge, and then increase farther downwind. This suggests that the drift droplets that are diverted over the top of the hedge return to ground level with the displaced flow.

These studies have examined the movement of spray drift past a barrier of different types, but there is limited information on the movement of spray drift near a live shelterbelt as it is defined. Also, previous studies have described the movement of spray drift past a barrier, but there is a lack of knowledge of how meteorological conditions, spray application settings, and shelterbelt properties interact to affect the movement of drift past a shelterbelt.

1.2 Objectives

The objective of this research is to assess the movement and deposition of spray drift past a live vegetated shelterbelt in field conditions. A qualitative and quantitative analysis is performed first on the effect of meteorological conditions, including wind

speed, wind direction, temperature, relative humidity, and atmospheric stability. This analysis is followed by a qualitative and quantitative assessment of the following controlled variables:

1. spray quality;
2. shelterbelt optical porosity;
3. upwind sprayer distance from the shelterbelt.

1.3 Scope

The scope of this research is defined by the labour-intensive nature of conducting field experiments. Three spray qualities are investigated, Fine, Medium, and Very Coarse, with a single shelterbelt optical porosity and upwind sprayer distance. Only one experimental shelterbelt is used, with varying optical porosity examined by sampling the shelterbelt in varying stages of foliation through the autumn season, with a single spray quality and upwind sprayer distance. Three upwind sprayer distances are sampled with a single spray quality and shelterbelt optical porosity. The meteorological conditions naturally vary while sampling the above controlled variables and this is the basis for the analysis of the meteorological variables. In other words, there is not a specific effort made to conduct experiments to assess any particular meteorological variable, other than what is due to the normal fluctuation in weather conditions.

1.4 Organization of the Thesis

The remainder of the thesis document is organized as follows. Chapter 2 presents the literature review which describes the movement of spray drift and the flow around a shelterbelt, and is followed by a review of the research conducted on the interaction of spray drift and vegetation. Chapter 3 describes the experiment design for measuring the movement and deposit of drift and the meteorological conditions around a live shelterbelt. Chapter 4 presents results from the field experiments and discussion of the data analysis. Finally, concluding remarks and recommendations for future research are given in Chapter 5.

Chapter 2

LITERATURE REVIEW

2.1 Introduction

This chapter provides a review of the two main areas in the literature that are pertinent to this research: (1) the movement of spray drift; and (2) the flow of wind past a shelterbelt. The movement of spray drift is described followed by an explanation of the factors affecting spray drift. Next, the flow of wind past a shelterbelt is described, along with the methods of characterizing a shelterbelt's porosity. Finally, specific studies that have investigated the movement of spray drift in the presence of vegetation are discussed.

2.2 Spray Drift

2.2.1 Movement of spray drift

Spray drift is the wind-mediated movement of pesticide droplets away from the treated area (Miller, 1993). Most agricultural sprayers are of the boom-type, and are fitted with hydraulic nozzles (Robinson, 1993). The spray liquid is emitted as a thin sheet as it is forced through the orifice of the nozzle. The sheet, due to drag from the surrounding air, becomes unstable and disintegrates into droplets. The nozzles produce a polydisperse spray, with droplet median diameters ranging from 50 μm to greater than 400 μm (Bache and Johnstone, 1992). The size of the droplets is dependent on operating settings and the spray mixture which include nozzle pressure and surface tension and viscosity of the spray mixture (Matthews, 2000). It is generally accepted that droplets less than 150 μm in diameter are at greatest risk of off-target displacement by wind, which results in spray drift (Miller, 1993; Hewitt, 2001).

The trajectory of a spray droplet, once it has reached terminal velocity, is dependent on its sedimentation velocity, the wind velocity, and the mechanical and thermal turbulence of the atmosphere (Matthews, 2000). The spray exits the nozzles as a thin, fan-shaped sheet which quickly disintegrates into droplets (CISRO, 2002). The droplet decelerates due to drag from the surrounding air and eventually reaches a constant fall velocity, termed the sedimentation velocity (Crowe et al., 1998). The sedimentation velocity of a liquid droplet in still air is dependent on the density of the liquid and the surrounding medium, air viscosity, and the droplet size. In pesticide applications, all of the variables are relatively constant except for the droplet size. Fine droplets (<100 µm) have a low sedimentation velocity and their movement is thus more susceptible to convective and thermal currents than larger droplets (Miller, 1993). For example, the sedimentation velocity for a 100 µm diameter droplet is 0.28 m/s, compared to 2.14 m/s for a 500 µm diameter droplet (CSIRO, 2002). Except in instances where the droplet has a high initial velocity (such as with twin-fluid nozzles), the most important factors affecting spray drift from conventional nozzles are the droplet size and meteorological conditions.

The impact of spray droplets onto a surface is termed deposition (Bache and Johnstone, 1992). It is expressed as mass of deposit, mass of droplets per unit area, or percentage of the applied dose (Caldwell and Wolf, 2006). The downwind deposit of drift typically follows a logarthmic decay (Caldwell and Wolf, 2006; Carlsen et al., 2006; Holterman et al., 1997; Nuyttens et al., 2006a), and a significant amount falls out within a short distance. Maybank et al. (1978) reported that approximately 1-8% of the pesticide applied using a tractor-drawn sprayer and conventional flat-fan nozzles drifted out of the treated area. Carlsen et al. (2006) found that the ground deposit was 0.1% – 9% of applied at 2 m downwind of the sprayed area and decreased to 0.02% - 4% at 3 m downwind. Caldwell and Wolf (2006) measured a ground deposit of 0.092% of applied at 10 m downwind of the treated area. The ground deposit at 400 m downwind of the treated area had decreased to 0.0011% of applied. They also found that the ground deposit with respect to downwind distance decreased linearly on a logarithmic scale ($r^2 = 0.99$).

2.2.2 Factors affecting spray drift

Considering the factors that affect spray drift, the droplet size within the spray is of concern because the size affects the droplets' trajectory. Generally, only droplets smaller than 100 to 200 µm are susceptible to off-target movement due to wind; sedimentation dominates for larger droplets. As described earlier, conventional hydraulic nozzles produce a polydisperse spray that have a wide range of droplet sizes. The droplet size spectrum for a particular nozzle may be defined by the $D_{V0.1}$, $D_{V0.5}$, and $D_{V0.9}$, which corresponds to the diameter that contains the cumulative volume fraction of 10, 50, and 90% of the total spray volume. For example, 10% of the total spray volume contains droplets with diameters smaller than the $D_{V0.1}$. The droplet sizes produced by a particular nozzle are compared to a reference nozzle and given a classification of, in increasing droplet size, Very Fine (VF), Fine (F), Medium (M), Coarse (C), Very Coarse (VC), or Extremely Coarse (XC) (ASAE, 2005b). This classification is termed the spray quality, and the droplet size spectra for the above spray qualities are shown in Figure 2.1. Spray quality is affected by a number of application settings such as operating pressure, nozzle type, fan angle, and surface tension and viscosity of the spray mixture (Grover et al., 1997; Lefebvre, 1993).

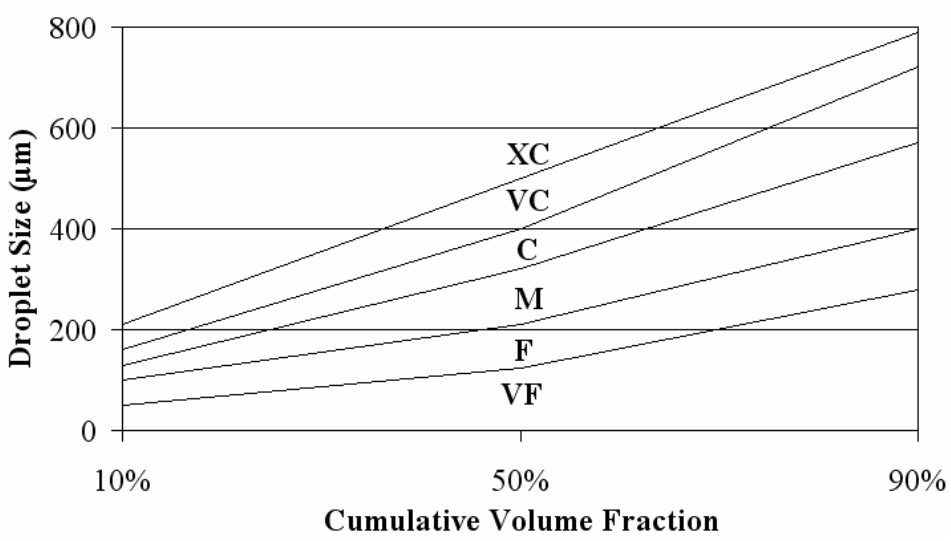

Figure 2.1 Spray quality classification based on droplet size spectrum (Adapted from ASAE, 2005b)

It has been found that spray drift is reduced using nozzles that produce coarser (larger) droplet sizes (Wolf et al., 1993; Grover et al., 1997; Carlsen et al., 2006; Nuyttens et al., 2006b). A coarser spray quality may be produced by decreasing the fan angle, which is defined as the angle of the spray sheet as it exits the nozzle. Wolf et al. (1993) found that a fan angle of 110^{o} increased airborne drift by 29% compared to an angle of 80^{o}. Grover et al. (1997) compared a conventional nozzle to a commercially-marketed "low-drift" nozzle. The volume median diameters of the droplets produced by the conventional and low-drift nozzles were 169 µm and 258 µm, respectively. The low-drift nozzle reduced airborne drift 5 m downwind of the spray swath by 51% compared to the conventional nozzle. Carlsen et al. (2006) found that, at 3 m downwind of the spray swath, low-drift nozzles reduced the ground deposition of drift by 24% compared to conventional nozzles. Nuyttens et al. (2006b) found that low-drift nozzles reduced the ground deposition of drift by 51% compared to conventional nozzles.

The meteorological factors that affect spray drift include wind speed, atmospheric stability, turbulence, temperature, and humidity (Johnstone, 1985). Wind speed is important because the wind carries droplets downwind from the treated area. A high wind speed increases drift in two ways: (1) air-borne droplets travel a longer distance downwind from the area of application before they deposit; and (2) larger droplets that would normally settle in the treated area are subjected to drift. The movement of spray drift is governed by winds produced by horizontal pressure gradients and by those produced by convective currents, which are driven by atmospheric instability (Bache and Johnstone, 1992).

Atmospheric stability is a method to characterize the thermal turbulence of the atmosphere, and is classified as stable, unstable, or neutral (Miller, 1993). In a stable atmosphere, mechanical wind effects dominate and thermal turbulence is suppressed. In this situation, drifting droplets may be carried far downwind before depositing. Turbulence is enhanced in unstable conditions due to convective currents, and droplets may be carried upwards and downwards, enhancing both near-field deposition and loss to the atmosphere. Neutral conditions, though rare, are optimal for pesticide application

because they allow for adequate mixing and deposition to the plant canopy through the action of eddies produced by mechanical turbulence (CSIRO, 2002).

The stability of the atmosphere is the ratio of the temperature and velocity gradients and may be characterized by the Pasquil stability chart or the Richardson number (*Ri*). The Pasquil stability chart classifies the atmospheric stability based on a visual assessment of the cloud cover in the sky and the wind speed measured at 10 m. The classification ranges from A through F, which corresponds to extremely unstable to moderately stable (ASAE, 2005a). The Richardson number is presented in Oke (1987) and Bache and Johnstone (1992), and expressed as:

$$Ri = \frac{g\left(d\xi/dz\right)}{T_K\left(dU/dz\right)^2} \qquad [2.1]$$

$$\xi = T_K + \Gamma z \qquad [2.2]$$

where g is the gravitational acceleration, ξ is the potential temperature, T_K is the absolute temperature, U is the wind speed, Γ is the dry adiabatic lapse rate ($\approx 0.01^{o}$C/m), and z is height. A negative Richardson number represents the case of unstable atmospheric conditions where thermal turbulence dominates over mechanical turbulence, and a decreasing Richardson number represents increasing thermal turbulence (Bache and Johstone, 1992). An explanation of the range of Richardson number and its effect on stability is provided by Oke (1987). Over the range of Richardson numbers of -0.05 to +0.05, the stability is classified as "fully forced convection" and thermal and mechanical turbulence is approximately balanced. For Richardson numbers outside this range, the effect of either thermal or mechanical turbulence dominates, corresponding to a negative or positive Richardson number.

Temperature and humidity only indirectly influence the movement of spray drift. The evaporation rate of a water droplet is dependent on the atmospheric temperature and humidity and the vapour pressure of the bulk liquid. The droplet size becomes progressively smaller as it evaporates and drifting droplets are more likely to remain air-borne. This effect becomes important when the temperature is high (greater than 30^{o}C) and the humidity is low (wet bulb depression greater than 10^{o}C) (CSIRO, 2002).

2.3 The Flow around a Shelterbelt

2.3.1 Flow regions around a shelterbelt

Considering the wind profile around shelterbelts, there have been many studies of both field and wind-tunnel experiments (see for example, Nord, 1991; Davis et al., 1994; Cleugh, 1998; Cleugh, 2002). The field studies have analyzed the wind profile around both vegetative and artificial windbreaks. Most studies have classified the wind profile at distances in units based on the height of the shelterbelt, H, which gives distance in terms of dimensionless height. This allows for comparisons to be made between the field and laboratory studies and between shelterbelts of different heights.

The flow in the vicinity of a shelterbelt, shown in Figure 2.2, is characterized by a reduction in wind speed on the windward and leeward sides (Judd et al., 1996). The approaching wind begins to slow at a distance of 5H upwind of the shelterbelt. When the flow encounters the shelterbelt, some air passes through it, which is referred to as bleed flow, while the majority of the flow passes up and over the shelterbelt. From the point at the top of the shelterbelt, there is a triangular zone that descends to ground level at a distance of about 5H downwind, bracketing what is termed the quiet zone. There is a mixing layer of high turbulence above the quiet zone, where the wind begins to return to its approach speed. Finally, there is the re-equilibration zone, starting at approximately 25H downwind of the shelterbelt, where the wind returns to its approach profile.

In the quiet zone downwind of the shelterbelt, the wind speed does not reach a minimum until some distance behind the shelterbelt, usually between 1-3H (Nord, 1991). Immediately downwind of the shelterbelt, the flow accelerates as it converges through the pores of the shelterbelt. Upon exiting the shelterbelt, the jets diverge and the wind speed decreases. At the point of the minimum wind speed, the displaced flow begins to combine with the bleed flow and the wind speed increases. Simplistically, the sheltered zone downwind of a windbreak is influenced by the proportion of bleed flow compared to displaced flow (Caborn, 1965). Where there is a large amount of bleed flow, there is less reduction in wind speed. However, the bleed flow acts to “cushion” the displaced flow as it returns to ground level, which produces a farther-reaching

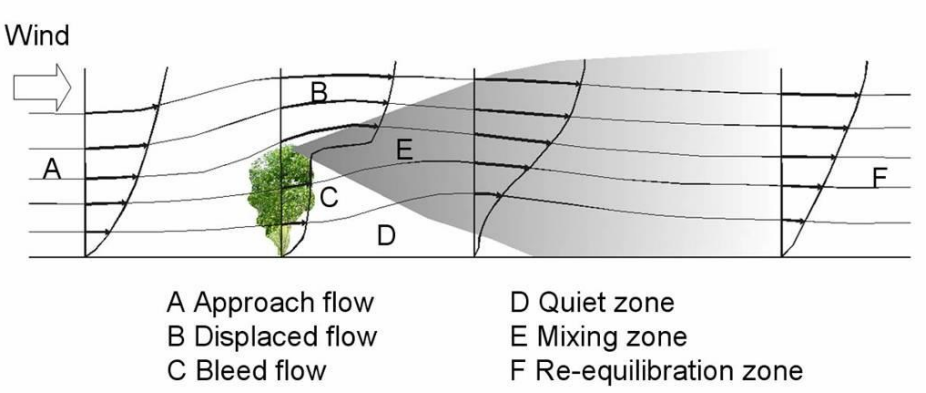

Figure 2.2 Wind profile around a shelterbelt
(Adapted from Judd et al., 1996)

sheltered zone. In the situation of little bleed flow, there is a greater maximum reduction in wind speed, but the extent of the sheltered zone is shorter because the displaced flow is able to return to ground level in a shorter distance. The bleed flow is influenced by the resistance to the flow within the shelterbelt and atmospheric turbulence. Thus, the proportion of bleed and displaced flow, and hence the shelter provided by the shelterbelt, is dependent on the shelterbelt characteristics and meteorological conditions (Caborn, 1965).

2.3.2 Effect of shelterbelt characteristics and meteorological conditions on flow

The shelter provided by a shelterbelt is usually expressed in terms of the following values: (1) the maximum reduction in wind speed (or minimum relative wind speed) compared to the approach wind speed; (2) the distance downwind of the shelterbelt where the maximum reduction in wind speed occurs; or (3) the distance in which the wind speed is reduced by some factor of the approach wind speed, usually 0.2 (Cleugh, 1998; Heisler and Dewalle, 1988). These values are dependent on a number of variables such as shelterbelt width, porosity, and uniformity, and approach wind speed, direction, and turbulence (van Eimern et al., 1964).

The shelterbelt width (perpendicular to the oncoming wind) affects the shelter provided by a shelterbelt because the bleed flow has a longer distance to pass through the shelterbelt; this causes more flow to be diverted over the shelterbelt. The width is often designed on economic and forestry principles (van Eimern et al., 1964). Economically, it is desired to minimize the agricultural land that is taken out of rotation

in order to establish the shelterbelt; in this case, a shelterbelt of one row is recommended (Jones and Sudmeyer, 2002). Conversely, a wide tree stand is easier to establish and maintain, may be self-rejuvenating, and there is the opportunity for timber harvest. Previous studies have investigated the wind reduction of shelterbelts of various widths; however the experiments were confounded by other variables such as shelterbelt species and porosity. For example, Nord (1991) compared a multiple row shelterbelt of birch and spruce (width = 20 m) and a single row shelterbelt of poplar (width = 10 m), and found the minimum wind speed behind the shelterbelt (relative to the approach wind speed) was 0.11 and 0.40, respectively. Heisler and Dewalle (1988) concluded that the sheltered distance is shorter behind a wide shelterbelt consisting of a number of rows of trees compared to a narrow shelterbelt consisting of one row.

The shelter provided by a shelterbelt is also affected by the resistance of the shelterbelt to bleed flow, which is typically characterized by the shelterbelt porosity. It is recognized that shelterbelt porosity is the most important characteristic determining the shelter extent (van Eimern et al., 1964; Bean et al., 1975). Shelterbelt porosity is characterized by the "openness" within the shelterbelt, and the shelterbelt optical porosity is sometimes used to classify a shelterbelt's porosity. A highly porous shelterbelt will allow for more bleed flow, decreasing the maximum reduction in wind speed but increasing the extent of the sheltered zone (Cote et al., 2006). Nord (1991) sampled a carragana and a poplar shelterbelt with respective optical porosities of 16% and 51%. The corresponding minimum wind speed behind the shelterbelts was 0.23 and 0.63 of the approach wind speed.

The flow is also affected by the uniformity of a shelterbelt, which affects the porosity and describes the presence and size of gaps (porosity is often assumed to be homogeneous). Gaps commonly occur along the top of the tree line and along the bottom where lower branches are pruned or where there is no undergrowth. Gaps along the top can increase the turbulence of the displaced flow, causing a more rapid return to the free-stream wind speed, and jetting may occur in gaps along the bottom causing high local wind speeds (Loeffler et al., 1992). van Eimern et al. (1964) reported that bleed flow may be 1.2 times greater than the approach wind speed through wide gaps (width $\approx$1H) where the flow accelerates through the gap.

The shelter effect may also indirectly depend on the approach wind speed. As the wind speed increases, the leaves and twigs of the trees align with the flow and increase the porosity of the shelterbelt (Bean et al., 1975). Zhang et al. (1995) found that the minimum relative wind speed increased from 0.30 to 0.50 for wind speeds of 1 m/s to 5 m/s, respectively, and that for wind speeds greater than 5 m/s, the minimum relative wind speed was constant. They explained that, at lower wind speeds, the leaves and twigs of the trees start to flutter and this changes the shelterbelt porosity. At wind speeds greater than the threshold value of 5 m/s, the shelterbelt's canopy is in full motion and the porosity is thus unchanged.

The deviation of the oncoming wind direction from perpendicular to the shelterbelt, referred to as wind obliqueness, also appears to have a significant effect on the sheltered zone behind a windbreak. Wind obliqueness changes the flow in three ways (Wang and Takle, 1996): (1) the resistance of the shelterbelt increases due to increased flow depth within the shelterbelt; (2) the wind reduction caused by the shelterbelt on the parallel component of an oblique wind is less pronounced than for the perpendicular component; and (3) the rotation of the wind direction in the sheltered zone. It has been reported that, for an increasingly oblique wind, the location of the minimum wind speed moves closer to the lee of the windbreak, the reduction in wind speed is greater, and the sheltered zone is not as far reaching (Cleugh, 2002; Nord, 1991; Seginer, 1975a). Nord (1991) found the minimum wind speed was 0.6 of the approach wind speed when the wind was perpendicular to the shelterbelt and decreased to 0.2 for a wind direction of 60^o from perpendicular. It was also observed that the distance of the minimum wind speed downwind of the shelterbelt was 4H for a perpendicular wind and 1H for a wind direction of 60^o from perpendicular. Cleugh (2002) determined that the wind speed reduction varied linearly with $\cos(\gamma)$, where γ is the angle between the wind and a line perpendicular to the shelterbelt and that the length of the sheltered zone (where wind was reduced by 20%) decreased from greater than 20H to 12H to 4H for angles of 0^o, 30^o, and 60^o from normal to the shelterbelt, respectively. A study by Seginer (1975a) found that, behind a thin, porous fence, the length of the sheltered zone decreased from 20H to 5H for a wind direction of 0^o and 60^o from perpendicular, respectively.

Another consideration is the turbulence of the approach flow, which is produced by the surface roughness of the upwind terrain, obstacles upwind of the shelterbelt, and thermal instability (Heisler and Dewalle, 1988). In stable conditions, the atmosphere is thermally stratified and turbulence is suppressed. As the wind approaches the shelterbelt, the upward movement of the displaced flow is resisted by the thermal stratification resulting in more bleed flow (van Eirmen et al., 1964). However, Seginer (1975b) found that, in increasingly unstable conditions (Richardson number corresponding to 0.0 and -1.5), the minimum relative wind speed increased from 0.30 to 0.55 and the extent of the sheltered zone (where wind speed was reduced by 20%) decreased from 22H to 8H. The work of Seginer (1975b) was conducted around a thin model windbreak, which would have had different bleed flow characteristics compared to the observations by van Eirmen et al. (1964), who investigated the effects of vegetated windbreaks. Surface roughness upwind of the shelterbelt also affects turbulence in the approaching flow. Seginer (1975a) found that, behind a thin, porous fence, increased surface roughness slightly increased the minimum relative wind speed from 0.35 to 0.40 for aerodynamic roughness heights of 0.3 cm and 2.4 cm, respectively.

2.3.3 Characterizing shelterbelt porosity

The porosity or resistance of a shelterbelt has been suggested to be the most important measure to describe wind reduction behind a shelterbelt (van Eirmen et al., 1964; Bean et al., 1975). However, there is still much debate in the literature on how to assess the characteristics of a shelterbelt's resistance to bleed flow, and previous studies have used optical porosity (Kenny, 1987; Loeffler et al., 1992), aerodynamic porosity (Bean et al., 1975; Nelmes et al., 2001), drag coefficient (Guan et al., 2003; Seginer, 1975b), and resistance coefficient (Heisler and Dewalle, 1988; Wang and Takle, 1996) to assess the shelterbelt's resistance.

Optical porosity (β) is the ratio of the frontal area of the open spaces in a profile view of a shelterbelt divided by the total frontal area of the shelterbelt. To estimate the optical porosity of a shelterbelt, Kenney (1987) developed a method where a two-dimensional picture is scanned into a computer and converted to a binary (black and

white) image, which produces a silhouette. The optical porosity is then calculated by taking the ratio of light pixels to total pixels:

$$\beta = \frac{N_L}{N_T} \qquad [2.3]$$

where N_L is the number of light pixels and N_T is the total number of pixels. While this method works well for characterizing a thin, two-dimensional fence, it may not be applicable to a live shelterbelt because it does not take into account the shelterbelt's width. A wide shelterbelt would likely appear less porous than a thin fence, but would not necessarily provide a greater resistance to the bleed flow.

Zhou et al. (2002 & 2004) attempted to address this issue by developing a numerical model that relates the two-dimensional optical porosity of a shelterbelt to its three-dimensional structure by using surface area density (surface area of vegetation per unit shelterbelt volume) and cubic density (volume of vegetation per unit shelterbelt volume). Another issue with using optical porosity to characterize a shelterbelt is that the optical porosity of a live shelterbelt changes with the season, as well as for different wind speeds as high winds can cause the leaves of the trees to align themselves with the wind making it appear to be more open. Also, gaps along the top of the tree line may artificially increase the porosity. Loeffler et al. (1992) attempted to remove this potential source of error in determining shelterbelt porosity by relating the wind reduction to the optical porosity for the bottom half and bottom three-quarter height of the shelterbelt.

A measure of the aerodynamic porosity (α) has been proposed by Bean et al. (1975) and used by Cleugh (2002). The aerodynamic porosity takes into account the three-dimensional nature of the shelterbelt, and is calculated as the minimum wind speed downwind of the shelterbelt divided by the open field wind speed:

$$\alpha = \frac{U_m}{U_o} \qquad [2.4]$$

where U_m is the minimum wind speed and U_o is the approach wind speed, both measured at the same height. In a wind tunnel study, Cote et al. (2006) calculated the aerodynamic porosity of a model windbreak as the height-averaged velocity at a

distance of 1H downwind of the windbreak divided by the height-averaged velocity at the same location with no model in place. An empirical relationship was developed by Guan et al. (2003) for a wind tunnel model that related the aerodynamic porosity to the optical porosity:

$$\alpha = \beta^{0.4} \qquad [2.5]$$

and was deemed valid except near the values of $\alpha = 0.5$ and $\beta = 0.2$, where the divergence of the equation was the greatest.

It was recognized by Nelmes et al. (2001) that the above calculation of aerodynamic porosity does not take into account local terrain features which affect the turbulence and shear of the approach flow. They defined a shelter parameter, *s*, which takes into account the wind speed and turbulence:

$$s = \sqrt{\frac{U^2 + u'^2\big|_{D/W}}{U^2 + u'^2\big|_{U/W}}} \qquad [2.6]$$

where U is the average wind speed, u' is the root mean squared wind speed, and $U^2 + u'^2\big|_{U/W}$ and $U^2 + u'^2\big|_{D/W}$ are the corresponding turbulent wind speeds on the up- and downwind sides of the shelterbelt, measured at a distance of 1H and height of 0.4H.

An interesting measure of porosity was used by Nord (1991) to calculate the effective porosity of live shelterbelts. For this method, the wind speed was measured at distances along a perpendicular line on the upwind and downwind sides of the shelterbelt. The particular graph of the wind speed reduction with respect to distance measured in the field was compared to those of two-dimensional windbreak models of known optical porosity. The graph of the wind speed reduction of the live shelterbelt which most closely matched the one of the wind tunnel model was chosen as the "effective porosity" of the shelterbelt. It was found that the optical porosity was always less than the porosity of the wind tunnel model. For example, a carragana shelterbelt with optical porosity of 10% matched closely to a wind tunnel model of porosity ranging from 23% to 53%.

The drag of a windbreak has been studied by Guan et al. (2003) and Seginer (1975b). A wind tunnel study by Guan et al. (2003) attempted to measure the drag

coefficient of a model wind break and related the drag coefficient, C_d, to the aerodynamic porosity:

$$C_d = 1.08\left(1-\alpha^{1.8}\right) \quad [2.7]$$

They found the drag coefficient ranged from 0.6 to 1.0 for corresponding aerodynamic porosities of 0.1 to 0.7. Seginer (1975b) found similar values in measuring drag on a shelter fence; the drag coefficient was approximately 0.77 for an optical porosity of 50%.

Wang and Takle (1996) introduced the resistance coefficient, k_r, into a numerical model for predicting the wind speed reduction and the sheltered distance behind a shelterbelt. The k_r coefficient was calculated by:

$$k_r = \int_{x_f}^{x_b} C_d A_{LA} dx \quad [2.8]$$

where x_f and x_b are the locations of the front and back edges of the windbreak, respectively, x is the distance perpendicular to the windbreak, and A_{LA} is the leaf area index. The resistance coefficient in this study varied from 0.25 to 3.0. They found that the minimum wind speed decreased and the sheltered distance increased with an increasing resistance coefficient. The minimum relative wind speed was 0.65 and 0.10 and the sheltered distance was 12H and 20H for k_r corresponding to 0.25 and 3.0.

2.4 Effect of a Shelterbelt on Spray Drift

The movement of spray drift around shelterbelts has been studied in the field using live trees (Davis et al., 1994; Wolf et al., 2004; Wolf et al., 2005) and snow fence (Brown et al. 2004), in the wind tunnel (Ucar et al. 2003), and numerically (Bouvet et al., 2006; Raupach et al., 2001; Wilson, 2005). It has been recognized that the most important factors influencing the movement of drift past a shelterbelt is wind speed and direction and shelterbelt height, type, and porosity (Ucar et al., 2003; Wolf et al., 2005).

Davis et al. (1994) studied the movement of spray drift past a 1.6 m tall hawthorn hedge. Drift was measured using a tracer dye as well as herbicide and insecticide bioassays. The effect of the hedge was compared to open field

measurements; the open field was characterized by a 16 m (10H) wide gap cut into the hedge. This relatively narrow opening may have been susceptible to effects of the hedge for winds that were not perpendicular to the shelterbelt. Spray was delivered with a tractor-mounted boom that was 6 m wide. Four adjacent passes were made starting 6 m upwind of the hedge (covering an area 24 m wide), extending 50 m on either side of the sampling line. In the open field, they found that the logarithm of drift deposition followed a linear decay with respect to downwind distance. In the presence of the hedge, the ground deposit of drift decreased by an order of magnitude directly behind the hedge and then increased with downwind distance. The authors expected that the deposit would eventually decrease further downwind, but deposition still increased past the furthest measurement point (12.5H downwind of the spray application). It was not indicated at which distance downwind of the hedge that the deposit was expected to decrease. The deposition of drift immediately downwind of the hedge was less than in the open field setting, but increased to more than in the open field at approximately 10 – 16 m (6 – 10H) downwind.

Wolf et al. (2004) measured the ground deposition of drift behind three types of riparian vegetation and in an open field. The types of vegetation were classified based on their height: low (grass – 0.75 m tall), medium (willow shrubs – 3 m tall), and high (aspen trees – 8 m tall). The willow shrubs were uniformly dense along their height compared to the aspen trees that were open at the bottom and relatively porous. Each vegetation type was located adjacent to each other along the same riparian area; the length of each type was not reported. The riparian vegetation may have been relatively wide and short in length and of variable width compared to a shelterbelt, which is characteristically long and narrow and of constant width. Spray application was by a self-propelled ground driven sprayer with a boom width of 10 m. The spray swath was located immediately upwind of the riparian vegetation. The sheltered zone extends 5H upwind of a shelterbelt (Judd et al., 1996); this corresponds to a distance of 15 m and 24 m upwind of the willow shrubs and aspen trees, respectively. Thus, the spray was likely released within the sheltered region for the willow shrubs and aspen trees. It was found that, at a downwind distance of 15 m, drift deposition was reduced by 63.5%, 98.6%, and 94.6% for grass, willow shrubs, and aspen trees, respectively, compared to

the open field. There was an increase in deposit at a downwind distance of 26 m (8.7H) behind the willow shrubs, which could have been due to droplets within the displaced flow returning to the ground surface. The decrease in deposition with respect to downwind distance behind the aspen trees was similar to the open field setting. This may have been because the aspens were open near the bottom and allowed a large proportion of bleed flow so that the drift movement through the bottom of the aspen trees mimicked the open field setting.

It was reported by Davis et al. (1994) that the drift deposit increased downwind of the hedge, while Wolf et al. (2005) found the drift deposit to decrease downwind of the riparian vegetation. This discrepancy in observations may be due to the location of the spray swath with respect to the tree stand. In Davis et al. (1994), the spray was released in four adjacent swaths upwind of the shelterbelt, of which three swaths would have been upwind of the sheltered zone on the windward side of the hedge. However, in Wolf et al. (2005), the spray was released directly upwind of the trees in the sheltered zone. Thus the spray would not have been subjected to the displaced flow over the top of the shelterbelt, as it was for Davis et al. (1994). This suggests that the location of the spray release may be an important factor of how the droplets move past the shelterbelt.

Brown et al. (2004) studied the movement of spray drift past two snow fences of different porosity that were 2.4 m tall and 200 m long. The snow fence was classified as porous (50% optical porosity) and dense (25% optical porosity). It was found that the ground deposit of drift was reduced by 47% and 72% behind the porous and dense windbreaks, respectively. They recommended that the dense fence is more effective than the porous fence at protecting downwind areas from spray drift.

Miller et al. (2000) studied the airborne movement of drift through field boundaries of different structure, composed of tall grass and a cut grass/flower mixture. They found that drift was reduced by 70% over the tall grass (1.3 m tall) compared to the cut mixture (0.15 m tall). The majority of the drift cloud was found to move above the top of the vegetation with relatively little movement within the canopy and that it shifted upwards with the taller vegetation. This suggests that, as the drift cloud encounters a strip of taller vegetation, such as a shelterbelt, the majority of the cloud is shifted up and travels along the top of the vegetation.

A study by Richardson et al. (2002) investigated the airborne drift past a windbreak boundary around an apple orchard. Spray was delivered using an axial-fan orchard sprayer. The height of the apple trees and windbreak were 2.49 m and 6.03 m, respectively, and the length of the windbreak was 77 m. The drift reduction through the windbreak was greater than 50%. The wind direction was approximately 47^{o} from perpendicular to the shelterbelt, and may have experienced considerable veering within the orchard due to the presence of the orchard trees and boundary windbreaks. There was no explanation given to account for the obliqueness and veering of the wind. In a later study at the same site, Richardson et al. (2004) found that the airborne drift was reduced by 80% in the summer when the trees were fully leaved, compared to 50% in early spring before the canopy of the trees was foliated. This larger reduction in drift in the summer because of the growth of leaves on the windbreak may have been due to two effects: (1) differences in bleed flow due to changes in porosity; and (2) differences in collection characteristics of the windbreak because leaves have a different collection efficiency of droplets than bare branches.

Raupach et al. (2001) developed a numerical model to relate the transmittance of particles through a windbreak (σ) to the optical porosity (β). The theory was developed for a particle-laden flow normal to a long, uniform windbreak of constant porosity. The transmittance of particles is given by:

$$\sigma = \frac{C_1}{C_o} \qquad [2.9]$$

where C_1 is the airborne concentration of particles exiting the windbreak and C_o is the airborne concentration of particles entering the windbreak. For particle sizes larger than 30 µm and vegetative elements smaller than 30 mm, the approximation $\sigma = \beta$ was found to compare well with experimental data. The total deposition of particles to the windbreak per unit length (D_b) is given by:

$$D_b \approx U_m H C_o (1-\sigma) \qquad [2.10]$$

where H is the windbreak height. The theoretical analysis was found to agree well with field experiments. In an extension of the work of Raupach et al. (2001), Wilson (2005)

determined that the presence of gaps in the windbreak did not change the bleed flow directly behind the windbreak, which in turn did not affect the particle deposition.

Bouvet et al. (2006) numerically modeled the movement of heavy particles in windbreak flow using a Lagrangian stochastic particle trajectory model. It was found that the particles followed the flow over the windbreak with maximum ground deposition occurring at a distance of 3-6H downwind of the windbreak.

2.5 Summary

From the above review, it is evident that both the movement of spray drift and the wind flow past a shelterbelt are dependent on meteorological conditions which include wind speed, turbulence, wind direction, and atmospheric stability. Drift is also dependent on the temperature and humidity, which affects the evaporation of the spray droplets. The flow around a shelterbelt is also affected by the shelterbelt's width, porosity, and uniformity.

As the droplets in the drift cloud approach the shelterbelt, they may be diverted over the top of the shelterbelt with the displaced flow, or pass through the shelterbelt with the bleed flow and be scrubbed by the vegetation. The proportion of droplets that travel through the shelterbelt compared to over the top is dependent on the resistance of the shelterbelt to flow. If a significant proportion of the drift cloud is displaced over the top of the shelterbelt, deposition directly behind the shelterbelt may be reduced but may increase farther downwind, as shown by Bouvet et al. (2006), Davis et al. (1994), and Wolf et al. (2005).

There has been previous research that investigated the movement of spray drift in an open field and around barriers of different types. However, there is limited information available on the movement of spray drift past a live shelterbelt. Also, as previously explained, both the movement of spray drift and the flow around a shelterbelt are dependent on a number of meteorological conditions. There is not a clear understanding of how these variables interact to influence the movement of spray drift past a shelterbelt.

Chapter 3

METHODOLOGY

3.1 Overview

The experiments were carried out around a live shelterbelt in an alfalfa field. Spray was applied using a conventional self-propelled farm sprayer that travelled upwind and parallel to the shelterbelt. A tracer substance was mixed in the spray solution, and the movement of spray drift was determined by measuring the mass of the tracer that landed on surfaces arranged at perpendicular distances up- and down-wind of the shelterbelt.

In this chapter, the experimental method and details of the experiments are discussed. First, a description of the experimental site and characteristics of the shelterbelt is given. This is followed by an explanation of the spray measurement technique, including the collectors that were used to sample the spray drift, the measurement of meteorological conditions, the layout of collectors, and the determination of drift deposit. Finally, the testing program and experimental conditions are presented.

3.2 Shelterbelt Site

The experiments were conducted at a shelterbelt composed of carragana and chokecherry trees in an alfalfa field located near Hanley, Saskatchewan, approximately 70 km southeast of Saskatoon, Saskatchewan (Latitude $51^{o}37'45.04"$; Longitude $106^{o}34'6.38"$). The shelterbelt was the westernmost row in a series of straight and parallel shelterbelts oriented approximately 12^{o} counterclockwise from North-South (Figure 3.1). The field gently sloped downwards to the northeast. The west side of the shelterbelt was clear of obstacles for more than 500 m; the east side was clear of

obstacles except for the next shelterbelt 200 m to the east. As a result, this shelterbelt was only suitable for testing in westerly winds as only on the west side was the field free of obstacles. Easterly winds would have been influenced by the shelter effect of the upwind shelterbelt. The downwind shelterbelt, located 200 m (40H) downwind, was not expected to influence the wind profile of the leading shelterbelt since the effect of a shelterbelt on the oncoming flow extends only 5 H upwind (Judd et al., 1996).

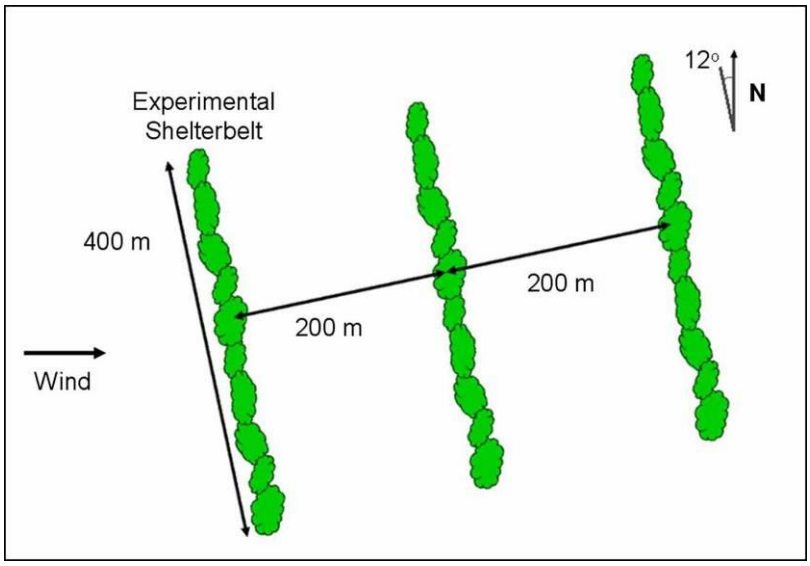

Figure 3.1 Series of shelterbelts at the test site

The field in which the shelterbelt was situated was cropped to alfalfa, which is a perennial crop grown for forage in Saskatchewan. In this region, alfalfa is harvested once throughout the summer, usually in July or August. The crop ranged in height from less than 50 mm soon after harvesting to approximately 300 mm prior to harvesting. Alfalfa has a dense ground cover, so the potential funnelling effect of the plant rows on the wind and drift cloud was assumed to be negligible.

The shelterbelt was approximately 5 m tall with branches extending 2.5 m on either side; the carragana and chokecherry trees were the same height. The shelterbelt was 400 m long with no significant gaps. The optical porosity of the shelterbelt varied from approximately 20% to 50%, corresponding to when the shelterbelt was in full leaf and bare of leaves (Figures 3.2 and 3.3). Details of the calculation of the optical porosity of the shelterbelt are given in Section 3.8.

Figure 3.2 Shelterbelt in full leaf

Figure 3.3 Shelterbelt bare of leaves

3.3 Spray Measurement Technique

Spray drift around the shelterbelt was measured using the fluorescent dye technique detailed by the International Standard 22866:2005 (ISO, 2005), where a recoverable tracer material is mixed in the solution to be sprayed. With this technique, after the spray is applied, the dye lands on collection surfaces (collectors) placed downwind of the site of application. The collectors are later washed and the volume of dye in the wash quantified.

The spray mixture followed that used by Caldwell and Wolf (2006), and was composed of 0.2% v/v Rhodamine WT (Paterson Company Ltd., North York, ON), 0.1% v/v AgSurf (Interprovincial Cooperative Ltd., Saskatoon, SK), 0.3% w/v Tinopal CBS-X (Ciba Specialty Chemicals Canada Inc., Mississauga, ON), and tap water as the carrier liquid. Rhodamine WT is a fluorescent dye and was used as the tracer material. AgSurf is a surfactant and was used to lower the surface tension which makes the atomization of the spray solution similar to that of a commercial pesticide. Tinopal CBS-X was used to absorb ultraviolet rays in order to protect the Rhodamine WT from photodegradation.

The spray was applied using a Melroe Spra-Coupe 220 (AGCO, Bismarck, ND) (Figure 3.4), which is a self-propelled crop sprayer commonly used on the Canadian prairies. The sprayer was equipped with a 14.5 m wide boom set at a height of 0.75 m above the ground. The length of the spray swath ranged from 150 m to 300 m. The operating pressure at the nozzle was 275 kPa. Three hydraulic nozzles were used: a TeeJet XR8001, a TeeJet XR8003 (Spraying Systems, Wheaton, IL), and a Turbo-Drop TD11003/06 (Greenleaf Technologies, Covington, LA). Each of these nozzles provided a different droplet size spectrum at this operating pressure (Table 3.1). The driftable fraction is the percentage of droplets smaller than 150 μm, which is generally accepted as the size of droplets susceptible to spray drift (Hewitt, 2001). According to the ASAE S572 standard (ASAE, 2005b), the XR8001, XR8003, and TD11003/06 nozzles produced a Fine, Medium, and Very Coarse spray quality, respectively. The travel speed of the sprayer was approximately 12 km/h, resulting in application rates of 33 L/ha for the XR8001 nozzle and 100 L/ha for the XR8003 and TD11003/06 nozzles. The sprayer made three passes on the same swath, which ranged from 100 m to 300 m long. This was done to average the fluctuations in wind speed and direction and to ensure the furthest collectors were adequately dosed with dye.

Figure 3.4 Melroe Spra-Coupe

Table 3.1 Spray nozzle classification (Caldwell, 2005)

Nozzle	Spray quality	$D_{V0.1}$	$D_{V0.5}$	$D_{V0.9}$	Driftable fraction[1]
XR8001	Fine	77 μm	141 μm	313 μm	56%
XR8003	Medium	101 μm	221 μm	596 μm	26%
TD11003	Very Coarse	183 μm	547 μm	971 μm	7.2%

1. Proportion of volume of droplets with diameter smaller than 150 μm

3.4 Sampling of Spray Drift

3.4.1 Spray droplet collectors

The collectors used in the experiments included plastic Petri-plates, polyethylene line, and U-shaped brass rods. These three collectors are recommended by the ISO Standard 22866 as suitable surfaces to collect drift droplets. The Petri-plates were 150 mm in diameter and are shown in Figure 3.5. They were placed on wooden stakes in order to be at the same height as the crop, and used to sample drift deposition to the ground. The polyethylene line was 2 mm in diameter and 30 m long and was suspended in the air by a helium blimp (Figure 3.6). The line sampled airborne drift concentration from ground level to a vertical height of 30 m. The Petri-plate and polyethylene line are classified as passive collectors, which sample an unknown volume of air that flows past the collector. The U-shaped brass rods, called rotorods, were 1.52 mm wide square rods and the two tines were 63 mm long. They were mounted on electric motors, spun in the horizontal plane at a rate of 2400 rpm (Figure 3.7), and

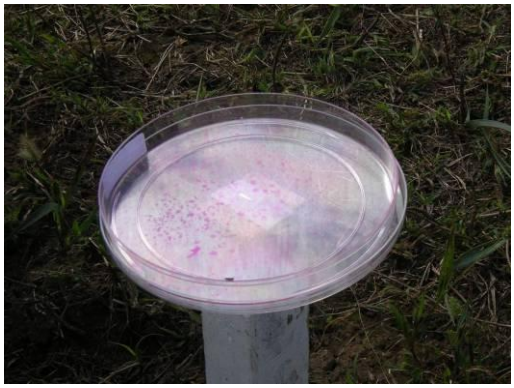

Figure 3.5 Petri-plate collectors

Figure 3.6 Polyethylene line suspended by the helium blimp

placed beside a cup anemometer. The rotorods and anemometers were mounted on poles at heights of 1, 2, 3, and 4 m. The wind speed at the same height as the rotorod, measured by the anemometer, was used to calibrate the sampling volume of the rotorod. The collection surface of the rotorod was the frontal area of the two tines that swept the air as it rotated. Rotorods are classified as active collectors, because they actively sweep a known volume of air. The rotorods were used to sample the airborne drift concentration entering and exiting the shelterbelt. The mode of sampling, orientation, and sampling area of the three types of collectors are given in Table 3.2.

Table 3.2 Spray drift collectors

Type	Mode of Sampling	Orientation	Sampling Area (cm^2)
Petri-plate	Passive	Horizontal	156.1
Polyethylene Line	Passive	Vertical	600
Rotorod	Active	Vertical	1.9

Figure 3.7 Rotorod collector mounted on the electric motor

An issue associated with the use of Rhodamine WT as a tracer material is its degradation by ultraviolet light, also called photolysis. This potential reduction in observed dye concentration was addressed by preparing four pairs of Petri-plates for each experiment as control samples. The four pairs of Petri-plates were spiked with a known dose of spray mixture in the laboratory prior to conducting field trials and were kept in the dark while in the field. When a trial began, one set of control samples were exposed to the sunlight while the other set was kept in the dark. At the end of the trial, the exposed plates were returned to the dark. Since both sets of plates initially had the same quantity of dye, measuring the reduction of dye on the exposed plates allows calculation of a photolysis correction factor (P_h):

$$P_h = \frac{C_{Light}}{C_{Dark}} \qquad [3.1]$$

where C_{Light} and C_{Dark} are the corresponding concentrations of dye on the plates that were placed in the sunlight and kept in the dark, respectively. All drift deposit data were corrected for photolysis by dividing the measured deposit by the photolysis correction factor. The average photolysis correction factor in the experiments was approximately 0.70.

The background level of naturally occurring fluorescent particles was determined by measuring the fluorescence intensity of samplers that were placed upwind of the spray swath and exposed only to the atmosphere. Any measured background deposit was subtracted from the deposit data.

3.4.2 Collector layout

Collectors were placed at perpendicular distances starting from the sprayer path to 170 m downwind of the spray swath. Blank collectors and photolysis plates were placed upwind of the sprayer's path. The ground area that was covered by the sprayer boom, called the "spray swath", extended from 30 m to 15 m upwind of the shelterbelt. The deposit of spray within the spray swath, called "onswath deposition", was measured using three rows, spaced 5 m apart, of four Petri-plates (total of 12 plates) placed directly underneath the spray swath. The deposit of spray drift to the ground downwind of the spray swath, called "offswath deposition", was measured using three rows of Petri-plates, spaced 5 m apart, downwind of the spray swath. Petri-plates were placed at 5, 10, and 15 m downwind of the spray swath (2H, 1H, and 0H upwind of the shelterbelt respectively) and 20, 35, 50, 65, 80, 95, 110, 125, 140, 155, and 170 m downwind of the spray swath (0H, 3H, 6H, 9H, 12H, 15H, 18H, 21H, 24H, 27H, and 30H downwind of the shelterbelt respectively). Rotorods were placed in rows of three, spaced 5 m apart, on the immediate up- (0.5H) and downwind (0.5H) sides of the shelterbelt. The rotorods were mounted on poles at 1, 2, 3, and 4 m heights (Figure 3.8). One polyethylene line collector was suspended by a blimp on the immediate up- and down-wind sides of the shelterbelt. The collector layout is shown in Figure 3.9.

Figure 3.8 Rotorod poles alongside the shelterbelt

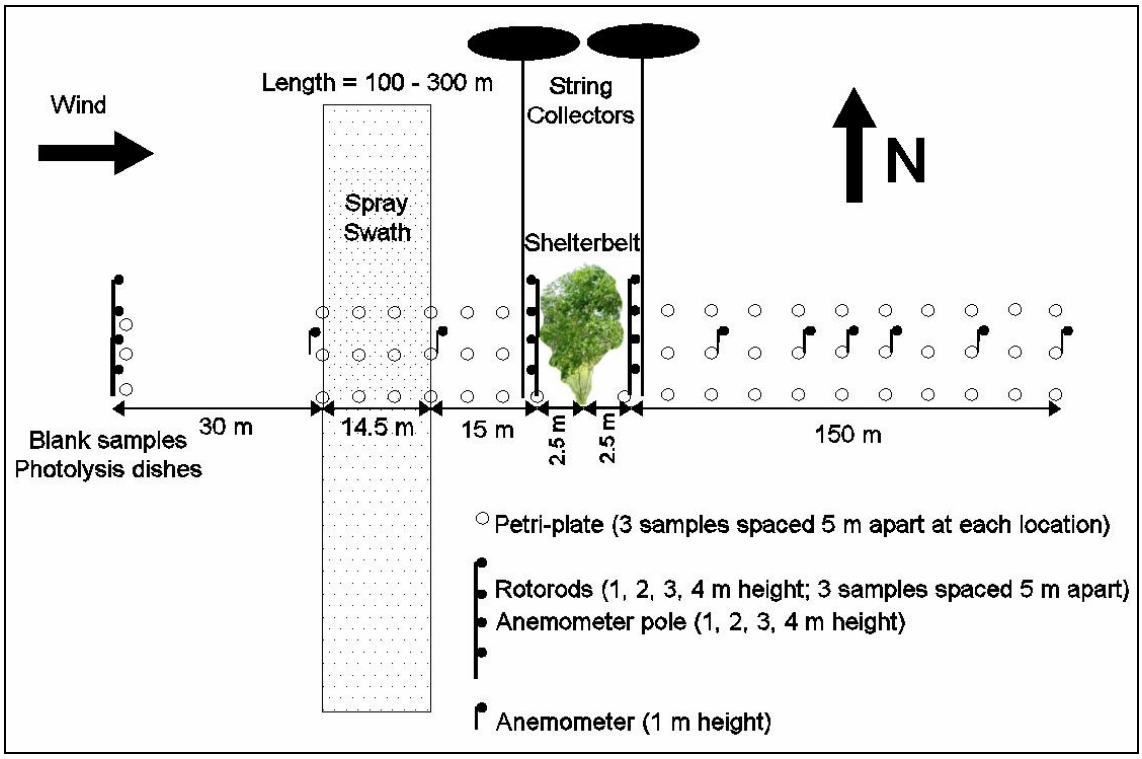

Figure 3.9 Collector layout

3.4.3 Meteorological equipment and layout

For each trial, wind speed, wind direction, temperature, temperature differential at heights of 1 m and 5 m, and relative humidity (RH) were monitored and measured. Each meteorological instrument collected data at a 0.1 Hz sampling rate that was recorded by a data logger. The meteorological conditions were recorded for a 10 minute period commencing from initiation of spraying.

The approach wind speed was measured using cup and ultrasonic anemometers. Cup anemometers only measure wind speed in the horizontal plane while ultrasonic anemometers are capable of measuring the three dimensional components of the wind velocity as well as the wind direction.

The approach flow was measured to a height of 4 m at a distance of 60 m upwind of the shelterbelt. Cup anemometers were placed alongside the rotorod motors on an aluminium pole at heights of 1, 2, 3, and 4 m. The vertical wind profile was also measured at the same heights at distances of 0.5H upwind and downwind of the shelterbelt. The wind speed reduction profile on either side of the shelterbelt was

measured using cup anemometers placed at a height of 1 m. The anemometers were placed at a 1 m height alongside the Petri-plates at 0, 15, 30, and 60 m (0H, 3H, 6H, and 12H, respectively) upwind and 0, 30, 45, 60, 75, 90, 120, and 150 m (0H, 6H, 9H, 12H, 15H, 18H, 24H, and 30H, respectively) downwind of the shelterbelt. The wind direction was measured by the ultrasonic anemometer at 60 m upwind of the shelterbelt as well as by a wind vane at 150 m downwind of the shelterbelt.

Temperature was measured using thermocouples 60 m upwind of the shelterbelt. The thermocouples were shielded from solar radiation and vented to allow natural air flow. Thermocouples were placed at 1 and 5 m to assess the atmospheric stability. Relative humidity was measured with a humidity probe at 60 m upwind of the shelterbelt.

3.4.4 Trial procedure

The handling of the collectors followed a strict procedure because contamination of the collectors could easily occur in the field. All samplers were covered and kept in the dark prior to the drift trial. At the start of each trial, collectors were laid out in order according to their susceptibility to contamination, with the most susceptible collectors laid out last. The Petri-plates were the most prone to contamination compared to the polyethylene string and rotorod collectors.

After all the collectors were laid out, the rotorod motors were turned on and the sprayer was signalled to start. Photolysis and blank samples were laid out upwind of the spray swath once spraying started. After spraying was completed, the collectors were kept out for another 5 minutes to ensure the drift cloud had travelled past the furthest collectors. At this time, the rotorod motors were turned off. Petri-plates were collected first, starting at the furthest downwind location, then the rotorods were picked up, and lastly the string. The collectors were covered and placed in bins to keep them in the dark and new collectors were laid out for the next trial.

3.5 Determination of Spray Concentration

To determine the concentration of spray on the drift collectors, the collectors were washed with a 95% ethanol wash. Each collector had its own method for washing in order to recover the dye. The Petri-plates were rinsed three times with 15 mL of

ethanol and the wash made up to 50 mL. The rotorods were placed so each tine was in a vial of 7 mL ethanol and sonicated for 30 seconds; the individual vials were combined to make a total wash volume of 14 mL. The polyethylene line was fed through a glass U-tube that was filled with 20 mL of ethanol. The U-tube immersed a length of 0.5 m of string in ethanol. The U-tube was sonicated for 30 s and then another 0.5 m of line was strung through and sonicated. The wash was then evacuated from the tube. This gave an average value of deposit over 1 m height increments of the string. These wash procedures have been found to give greater than 95% recovery of Rhodamine WT in similar experiments (Caldwell and Wolf, 2006). After washing, the solution was stored in the dark until analyzed by spectrofluorophotometry.

The fluorescence intensity of the wash was then measured with a Shimadzu RF-1501 spectrofluorophotometer (Shimadzu Instruments, Columbia, MD). The spectrofluorophotometer measured the fluorescence intensity of the wash, which was converted to concentration of dye using standard curves. The spray solution was decanted from the tank and diluted to give three standard curves: 0 to 15 ppb, 0 to 150 ppb, and 0 to 1500 ppb. The standard curves were used to convert the fluorescence intensity readings to concentration of dye in the wash (parts per billion).

The average concentration of dye was calculated from the three individual samples at each collector distance. The average dye concentration was then converted to mass per unit area (C_{ng/cm^2}) by:

$$C_{ng/cm^2} = \frac{C_{ppb} V_{wash} \rho}{A} \qquad [3.2]$$

where C_{ppb} is the concentration of the dye in the wash, V_{wash} is the wash volume, ρ is the density of the spray solution, and A is the collector area.

3.6 Testing Program

The variables that were investigated in this research may be defined as meteorological and controlled variables. The meteorological variables included wind speed (U), wind direction (γ), temperature (T), relative humidity (RH), and atmospheric stability. The wind direction was expressed as the angle between the oncoming wind

and the sampling line (perpendicular to the shelterbelt); an angle of 0º would be normal to the shelterbelt. The atmospheric stability was assessed by calculating the Richardson number (Ri) at a height of 1 m; a negative Ri would represent unstable conditions. The controlled variables were spray quality (Q), shelterbelt optical porosity (β), and upwind sprayer distance (D). The wind speed reduction behind the shelterbelt, expressed as the aerodynamic porosity (α), was also calculated for each trial.

Experiments were conducted at the shelterbelt site on September 1, 13, 19, and 29, 2005, July 31, 2006, and August 24 and 25, 2006. The experiment dates were chosen to provide a range of optical porosities (to coincide with the time when the shelterbelt was losing its leaves in the autumn). The effect of spray quality was sampled during the trials in September 2005 and the effect of upwind distance of the spray swath was investigated during the trials in July and August 2006. Table 3.3 gives the details of the experimental conditions. Each sampling day, and each individual drift trial, took place under unique meteorological conditions, as is the nature of field experiments. Depending on weather conditions, a maximum of six trials could be conducted on one day, and replicate trials were performed each day if conditions allowed.

The aerodynamic porosity was close to 1.0 on September 29, 2005, and greater than 1.0 for Trial 10. These trials took place when the shelterbelt was at its highest optical porosity (close to being bare of leaves). It is not reasonable that a shelterbelt would have an aerodynamic porosity greater than 1.0. These high aerodynamic porosities may be due to anemometer error or an error in placement of the anemometers (perhaps behind a gap in the shelterbelt, which would have accelerated flow).

The effect of shelterbelt porosity was investigated by conducting drift trials during the autumn when the shelterbelt was losing its leaves. This approach assumed that the shelterbelt properties, such as height, width, and uniformity, remained constant through September 2005 to August 2006 and that only the shelterbelt optical porosity was variable. Spray quality and upwind distance of the spray swath were sampled by keeping the controlled variables constant and conducting trials on the same day so meteorological conditions would be similar. Wind speed, wind direction, temperature,

Table 3.3 Experimental Conditions

Date	Trial #	Time	U (km/h)	γ (°)	T (°C)	RH (%)	Ri	Q	β	α	D	Drift Data[1]
01-Sep-05	1	13:00	8.8	33	18.5	42.2	-0.019	M	0.204	0.457	3H	○ + *
	2	13:32	7.3	57	18.1	42.7	-0.015	VC	0.204	0.445	3H	○ + *
	3	14:11	6.8	52.7	18	42	-0.005	M	0.204	0.385	3H	○ + *
	4	15:09	7.9	52	19.2	35.3	0.014	VC	0.204	0.497	3H	○ + *
13-Sep-05	5	13:20	15.8	25.7	13.2	42.6	-0.009	M	0.204	0.489	3H	○ +
	6	13:55	15.9	33.1	13.4	42.7	-0.02	F	0.204	0.548	3H	○ +
	7	14:22	13	37	13.6	42.5	-0.028	M	0.204	0.535	3H	○ +
	8	14:51	15.3	33.3	13.5	41	-0.007	F	0.204	0.523	3H	○ +
	9	15:19	12.9	30.5	14.5	40.5	-0.03	VC	0.204	0.506	3H	○ +
19-Sep-05	10d	12:29	7	2.4	17.3	37.7	-0.079	F	------	0.581	3H	○ *
	11d	13:00	9.1	5.9	17	37	-0.011	F	------	0.618	3H	○ *
	12d	13:23	8.5	4.4	16.8	36	-0.004	F	------	0.6	3H	○ *
29-Sep-05	10	10:59	11.4	13.5	14.6	42.1	-0.03	F	0.483	1.005	3H	○ *
	11	11:25	9.9	15.5	15.3	40.8	-0.022	M	0.483	0.937	3H	○ *
	12	11:50	9.4	4.2	15.6	40.4	-0.004	VC	0.483	0.942	3H	○ *
	13	12:48	10.5	11.2	17.9	34	-0.026	F	0.483	0.933	3H	○ *
	14	13:13	10.3	14.4	17.7	33.5	-0.035	M	0.483	0.974	3H	○ *
	15	13:37	11.5	0.9	18.9	30.2	-0.034	VC	0.483	0.908	3H	○ *
31-Jul-06	16	13:54	24.1	2.2	16.6	64.9	-0.02	M	------	0.634	1H	○ +
	17	13:29	25.5	7.1	16.4	73.4	-0.02	M	------	0.528	3H	○ +
	18	12:38	27.6	5.2	17.9	55.7	-0.025	M	------	0.612	6H	○ +
24-Aug-06	19	13:56	13.2	28	22	-----	-0.061	M	0.292	0.513	1H	○ = *
	20	14:22	15.8	47.7	22.9	-----	-0.051	M	0.292	0.299	3H	○ = *
	21	14:49	18.1	49.4	21.9	-----	-0.024	M	0.292	0.283	6H	○ = *
25-Aug-06	22	10:27	11.5	12.6	20	53.5	-0.107	M	0.292	0.628	1H	○ + = *
	23	10:55	11.3	3.5	20.9	50.2	-0.087	M	0.292	0.614	3H	○ + = *
	24	11:21	12.6	11.2	22.1	45.6	-0.089	M	0.292	0.605	6H	○ + = *
	25	12:38	15.9	13.6	24.8	33	-0.07	M	0.292	0.634	1H	○ + = *
	26	13:03	16	39	23.9	31.5	-0.032	M	0.292	0.473	3H	○ + = *
	27	13:29	18.2	17.6	25.5	26.7	-0.047	M	0.292	0.608	6H	○ + = *

1. Drift data available:
   ○ Petri-plate data
   + Rotorod data
   = String data upwind of the shelterbelt
   * String data downwind of the shelterbelt

RH, and atmospheric stability were meteorological variables that could not be controlled so, to determine the effects of the meteorological variables, trials were chosen for which the controlled variables were constant.

Trials through the month of September 2005 investigated the effects of spray quality. The spray qualities sampled were Fine, Medium, and Very Coarse. The upwind distance of the spray swath was evaluated in the experiments carried out on July 31 and August 24 and 25, 2006. The distances sampled, measured from the downwind edge of the swath, were 5 m (1H), 15 m (3H), and 30 m (6H) upwind of the shelterbelt.

The effect of shelterbelt optical porosity was investigated by sampling the shelterbelt with varying degrees of foliage as the shelterbelt was losing its leaves in the autumn. The shelterbelt was in full leaf on September 1, and became more porous through the month and was mostly bare of leaves on September 29. The foliation of the shelterbelt on September 1 (Figure 3.10), 13 (Figure 3.11), 19 (Figure 3.12), and 29 (Figure 3.13) are shown below.

Figure 3.10 Shelterbelt in full foliaton (September 1, 2005)

Figure 3.11 Shelterbelt in full foliation (September 13, 2005)

Figure 3.12 Shelterbelt in moderate foliation (September 19, 2005)

Figure 3.13 Shelterbelt bare of leaves (September 29, 2005)

A number of photographs of the profile view of the shelterbelt were taken at random intervals along the shelterbelt's length on each day of experiments in order to calculate the optical porosity. However, suitable photographs were not taken on September 19, 2005 and July 31, 2006. The evaluation of optical porosity of the shelterbelt followed the technique described by Kenney (1987). A colour digital photograph of the profile view of the shelterbelt was loaded into the computer program Photoshop (Adobe Systems, Inc., San Jose, CA). The photograph was converted first to greyscale (Figure 3.14), then to black and white (Figure 3.15). The number of black pixels and white pixels was computed by the Photoshop program. The shelterbelt profile view was truncated at a height of approximately 4 m so that the gaps along the top of the tree line were not included in the porosity calculation. The optical porosity was calculated using Equation 2.3.

Figure 3.14 Shelterbelt profile view converted to greyscale

Figure 3.15 Shelterbelt profile view converted to black and white

The aerodynamic porosity of the shelterbelt was calculated using Equation 2.4, based on the research of Bean et al. (1975). The approach wind speed was measured at a distance of 60 m (12H) upwind of the shelterbelt and it was assumed the minimum wind speed occurred at a distance of 2.5 m (0.5H) downwind of the shelterbelt. Although the minimum wind speed may occur at a distance from 1H to 4H downwind of a shelterbelt (Nord, 1991), the nearest wind speed measurement in these experiments was at a distance of 0.5H downwind of the shelterbelt. From the wind speed data for each trial, the aerodynamic porosity was calculated for heights of 1, 2, 3, and 4 m for each 10 second measurement using Equation 2.4. The average aerodynamic porosity of the shelterbelt was calculated by integrating the porosity first over the time interval, then over the height of the shelterbelt.

Chapter 4

RESULTS AND ANALYSIS

4.1 Introduction

The analysis of the spray drift data is presented in this chapter. First, the general characteristics of the movement of spray drift around the shelterbelt are described. Next, the movement of spray drift in the shelterbelt setting is compared to the open field setting. This is followed by a mass balance analysis, which accounts for the mass of drift deposited to ground and captured within the shelterbelt. An analysis of the repeatability of the drift trials is then presented in order to assess the random variability inherent in the field trials. The next two sections examine the effects of the meteorological conditions and the controlled variables on the ground deposition and the airborne movement of drift near the shelterbelt. The meteorological variables are wind speed, wind direction, temperature, relative humidity, and atmospheric stability. The controlled variables are spray quality, shelterbelt optical porosity, and upwind distance of the spray swath. A qualitative assessment is performed first, followed by a quantitative analysis using multiple linear regression analysis. Finally, an analysis of the errors in the experiments is presented.

4.2 General Movement of Spray Drift around the Shelterbelt

The movement of spray drift around the shelterbelt was characterized using three types of drift collectors: Petri-plates, rotorods, and string. These collectors measured the drift deposit to the ground, airborne concentration of drift entering and exiting the shelterbelt, and the airborne concentration of drift over the top of the shelterbelt, respectively.

Figures 4.1 and 4.2 show the ground deposit of drift around the shelterbelt for two typical drift trials, Trials 11 and 23. These trials were chosen as typical trials because the wind speed was moderate (less than 15 km/h) and the wind direction was close to normal to the shelterbelt (less than 15^{o} from perpendicular). It is seen that there was a sharp reduction in deposition immediately downwind of the shelterbelt compared to the deposition upwind. For Trials 11 and 23, this reduction was 74.0% and 74.4%, respectively. This observation was likely due to the reduction of wind speed within the shelterbelt so that the drift droplets settled out earlier, deflected over the top of the shelterbelt, or collected on the shelterbelt canopy. This was comparable to findings by Davis et al. (1994), who found that the deposit directly behind a windbreak decreased by an order of magnitude relative to the upwind deposit. In Trial 11 (Figure 4.1), the drift deposit was relatively constant over the distance of 15 to 30 m (3H to 6H) downwind of the shelterbelt and then slightly increased further downwind from the shelterbelt. This increase may have been due to the displaced flow over the top of the shelterbelt returning to ground level. Further downwind of this, the drift deposit decreased at a relatively constant rate on a logarithmic scale, which may have been where the flow again followed the same trend as it had upwind of the shelterbelt.

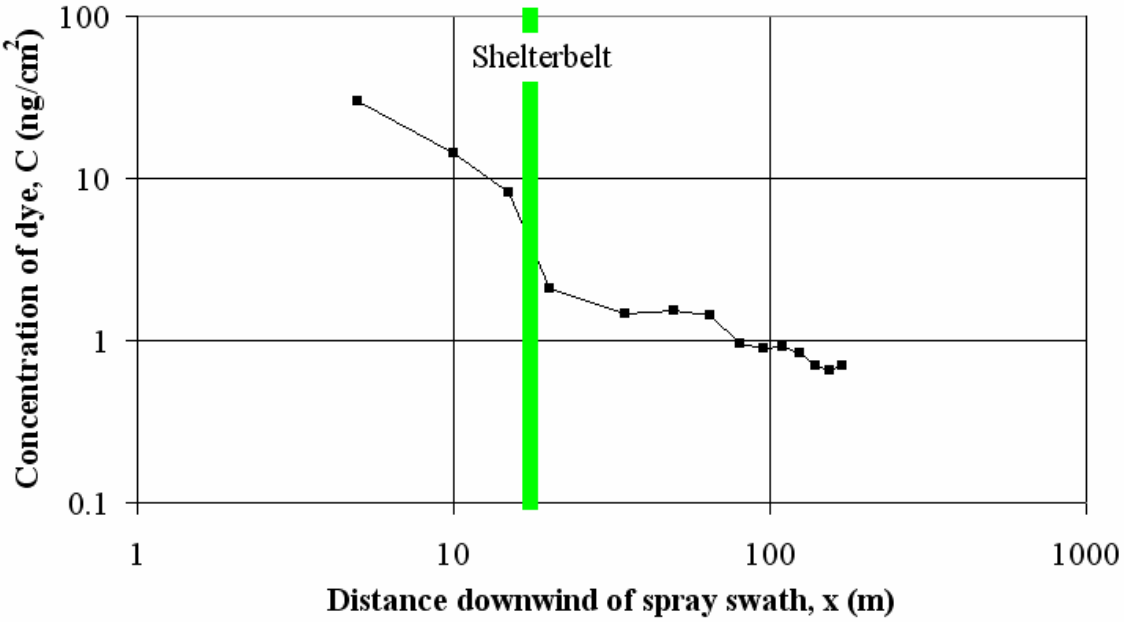

Figure 4.1 Ground deposit upwind and downwind of the shelterbelt (Trial 11)

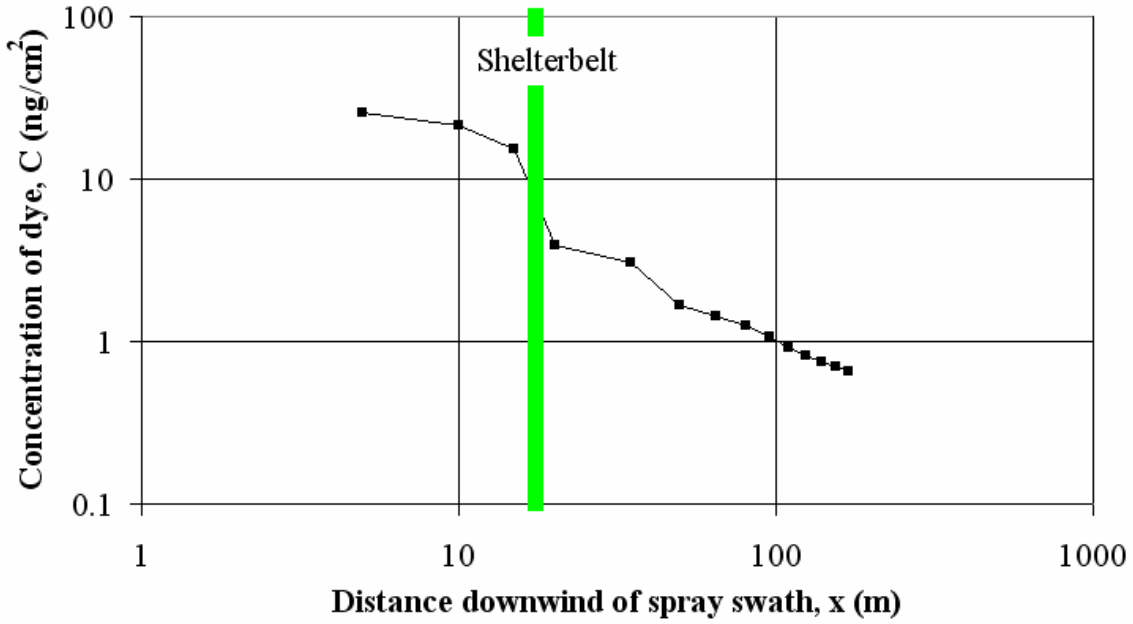

Figure 4.2 Ground deposit upwind and downwind of the shelterbelt (Trial 23)

Figures 4.3 and 4.4 show the airborne movement of spray drift through the shelterbelt for Trials 5 and 17. Both figures show a typically significant reduction in the airborne concentration exiting the shelterbelt (67.5% and 85.1%, respectively) relative to the upwind concentration profile. This indicated that a large proportion of drift droplets may have collected on the surfaces of the shelterbelt canopy as the drift cloud passed through the shelterbelt (the filtering effect of the shelterbelt). The reduction in drift exiting the shelterbelt was comparable to research by Richardson et al. (2002) where they found the airborne concentration of drift exiting a windbreak was reduced by 50% compared to the drift entering the windbreak.

The airborne concentration profile of drift above the shelterbelt for two typical trials (Trials 14 and 23) is shown below in Figures 4.5 and 4.6. Although the string collector used for the measurements was suspended 30 m in the air, the concentration profiles were truncated to a height of 20 m because, as was for most of the drift trials, there was usually no measurable drift at heights greater than 10 m. The shape of the profiles up to a height of 4 m was similar to that seen in Figures 4.3 and 4.4. There were two local maxima in the concentration profile exiting the shelterbelt, occurring at heights of approximately 2 m and 6 m, with the greater concentration occurring

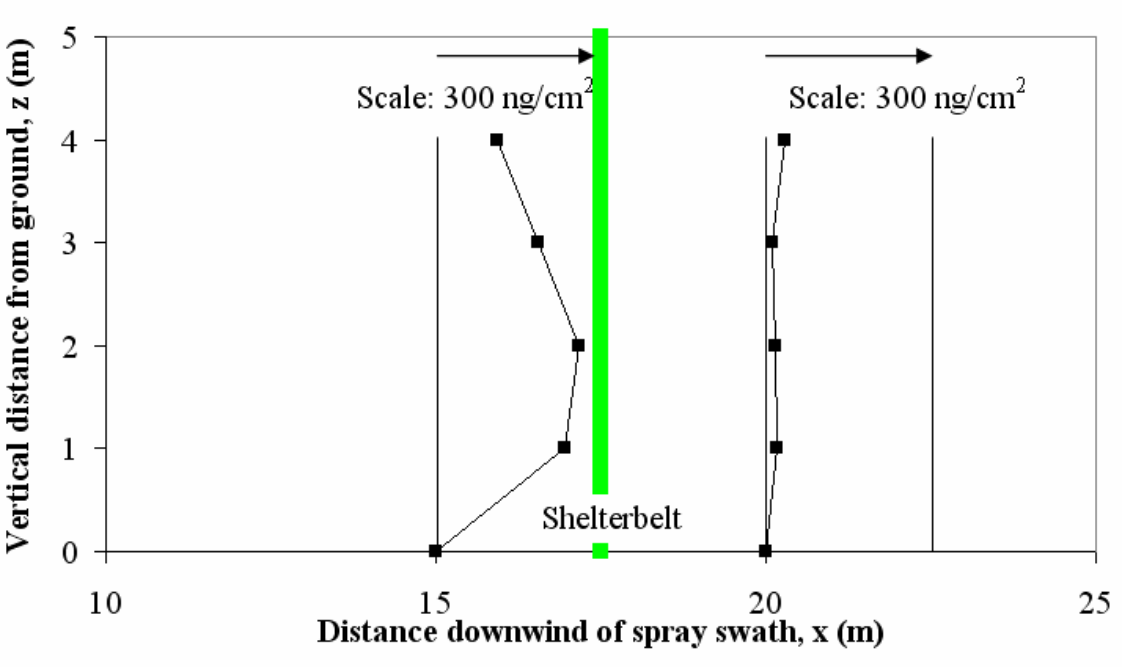

Figure 4.3 Airborne concentration profile entering and exiting the shelterbelt (Trial 5)

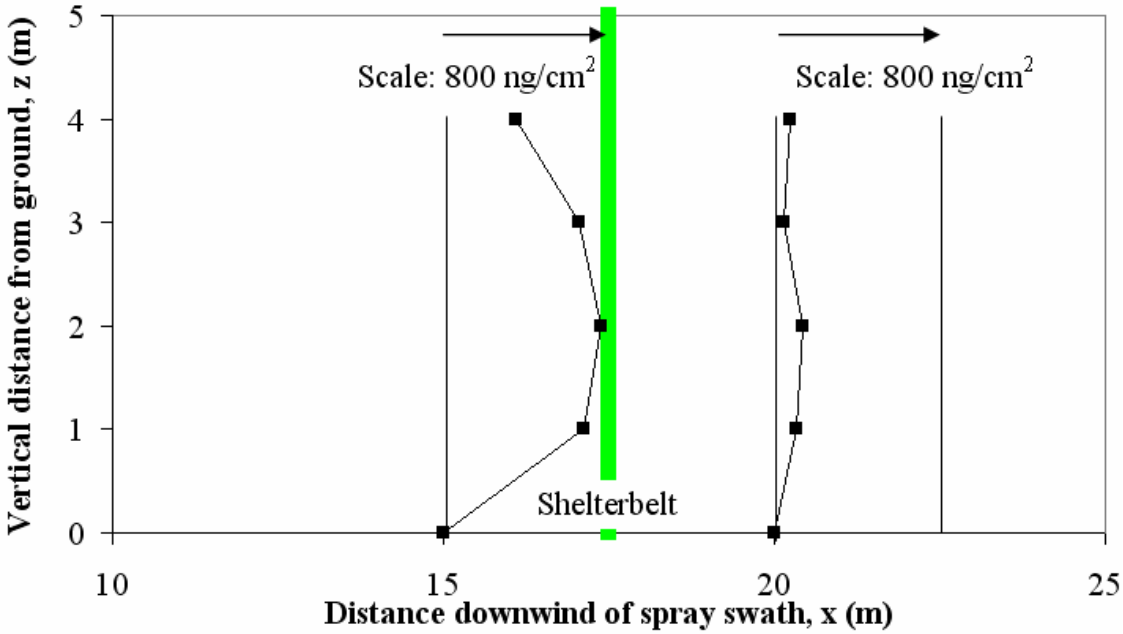

Figure 4.4 Airborne concentration profile entering and exiting the shelterbelt (Trial 17)

at 6 m (Figure 4.5). The shape of the concentration profile suggested that the drift cloud was split into two components and that there was a greater proportion of drift traveling over the top of the shelterbelt rather than through it. This observation was also reported by Miller et al. (2000) and Raupach et al. (2001).

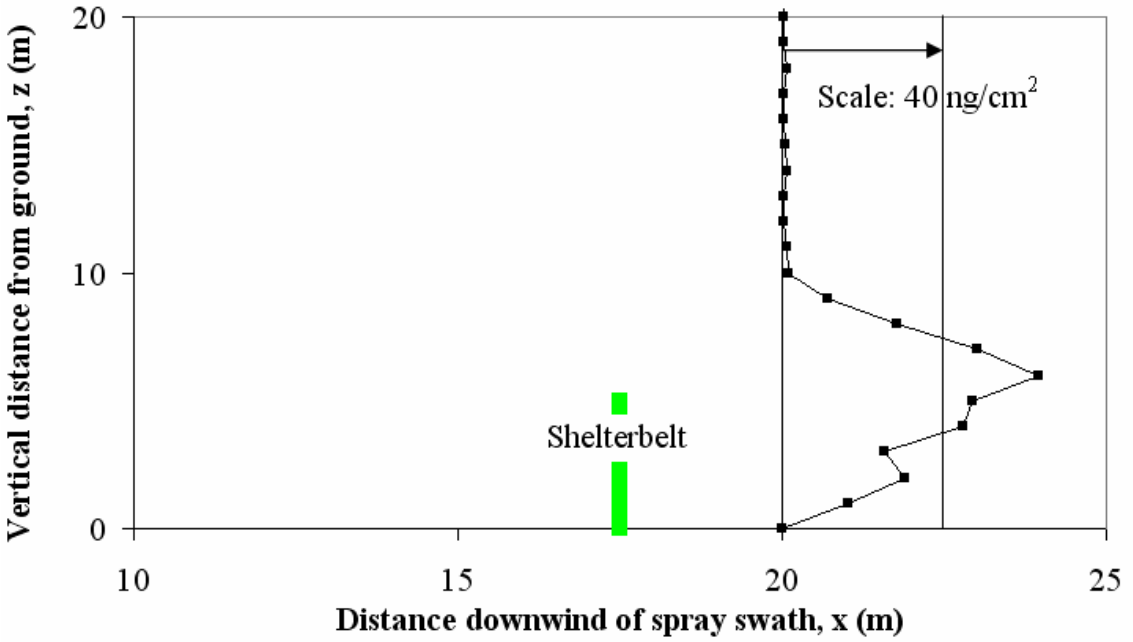

Figure 4.5 Airborne concentration profile over the top of the shelterbelt (Trial 14)

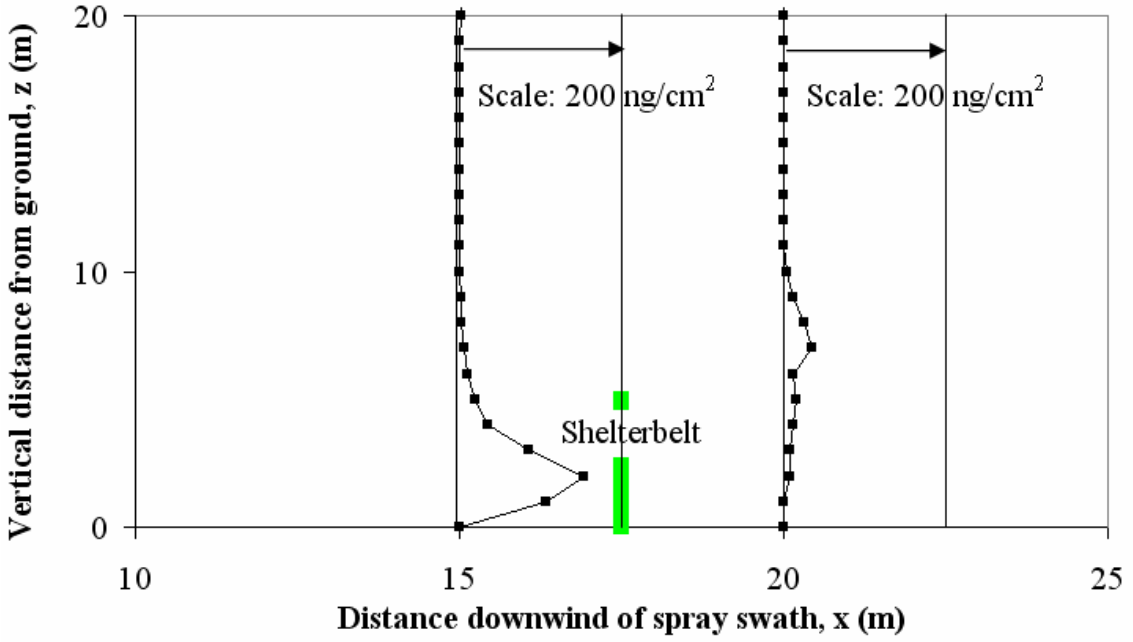

Figure 4.6 Airborne concentration profile over the top of the shelterbelt (Trial 23)

4.3 Comparison of the Shelterbelt and Open Field Setting

A comparison of the movement of spray drift in an open field and around the shelterbelt may provide insight into whether the shelterbelt does indeed protect downwind areas as was reported by Wolf et al. (2005). The open field data presented here is unpublished data from Wolf (2006). Three trials were conducted at a different site than the shelterbelt experiments, and were done in an immature barley field that was free of obstacles. The collectors were at the same locations as in the shelterbelt trials and a Medium spray quality was used. The average wind speed was 11.7 km/h and was oriented at 17.3º from the sampler line. Figure 4.7 shows the ground deposition with respect to distance downwind of the spray swath. A line of best fit (r^2 = 0.99) was drawn based on the nine data points at each measurement distance (3 trials with 3 samples at each location). The equation of the line is given as:

$$C = \frac{3.926}{x^{1.116}} \qquad [4.1]$$

where C is the normalized concentration of dye (% of Applied) at a downwind distance, x.

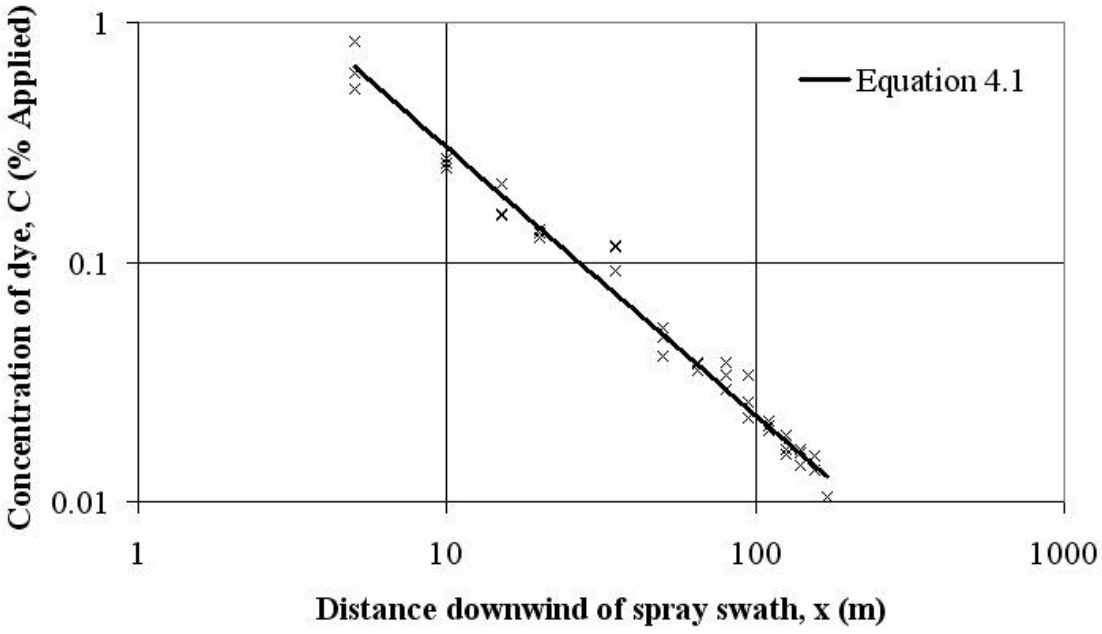

Figure 4.7 Open field drift deposit (Wolf, 2006)

To compare the shelterbelt experiments to the open field setting, a subset of three trials, Trials 5, 11, and 14, were identified that had a Medium spray quality and meteorological conditions similar to the open field experiments. Table 4.1 gives a comparison of the meteorological conditions. The following qualitative analysis focuses more on the movement of the drift cloud and characteristics of deposition near the shelterbelt relative to the open field setting rather than the amounts of drift deposition. Although the wind conditions for Trial 5 and the open field trials were not as similar as for Trials 11 and 14, this trial was included in the analysis because it was the only trial in this subset that had rotorod data available. Thus, although the meteorological conditions were different between the trials, it was assumed that the effect was slight and that the nature of the movement and deposition of drift was still comparable between the trials.

Table 4.1 Open field and comparative shelterbelt trials

Trial #	U (km/h)	γ (^{o})	T (^{o}C)	RH (%)	Ri
Open Field	11.7	17.3	26.9	35.0	-0.109
5	15.8	25.7	13.2	42.6	-0.009
11	9.9	15.5	15.3	40.8	-0.022
14	10.3	14.4	17.7	33.5	-0.035

The downwind ground deposition for Trials 11 and 14 compared to the open field setting is shown in Figures 4.8 and 4.9. The total mass of deposition measured downwind of the shelterbelt was 63% and 44% less than in open field setting for Trials 11 and 14, respectively. The corresponding deposition at 0.5H downwind of the shelterbelt was reduced by 74% and 72%, compared to the deposit at 0.5H upwind. In the open field setting, the deposit was reduced by 28% for the same distances downwind of the spray swath.

On the upwind side of the shelterbelt, the rate of deposition with distance was similar to the open field setting; however, from the shelterbelt to a distance of approximately 10H downwind of the shelterbelt, the rate of deposition was less than in the open field. At distances greater than 10H downwind of the shelterbelt, the rate of

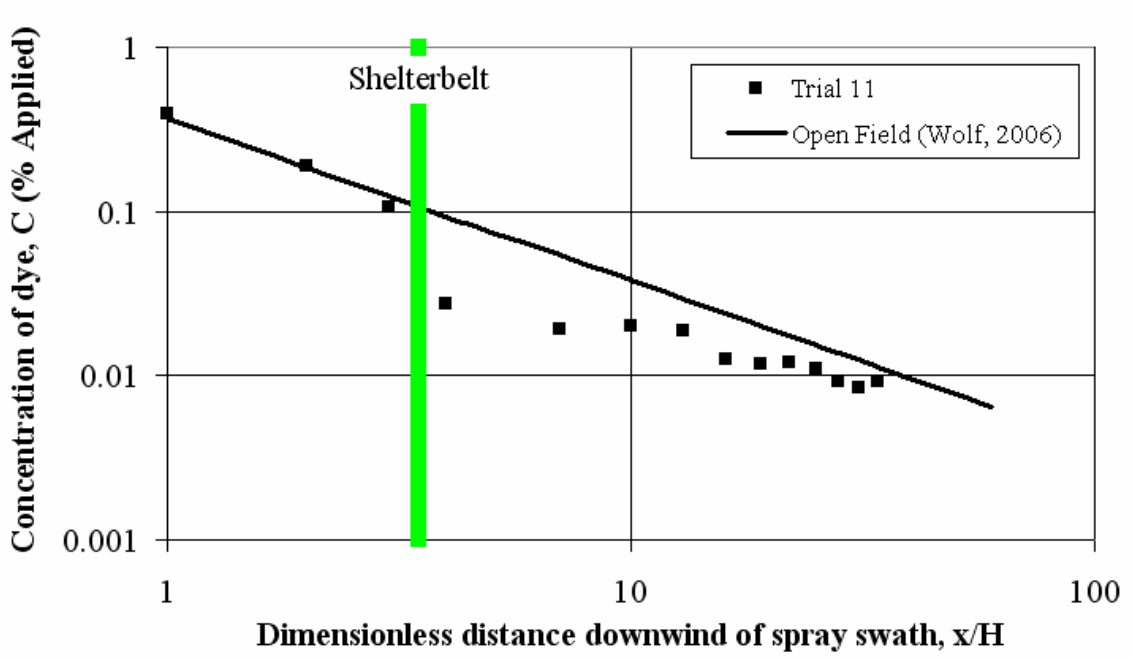

Figure 4.8 Comparison of deposit in the shelterbelt and open field settings (Trial 11)

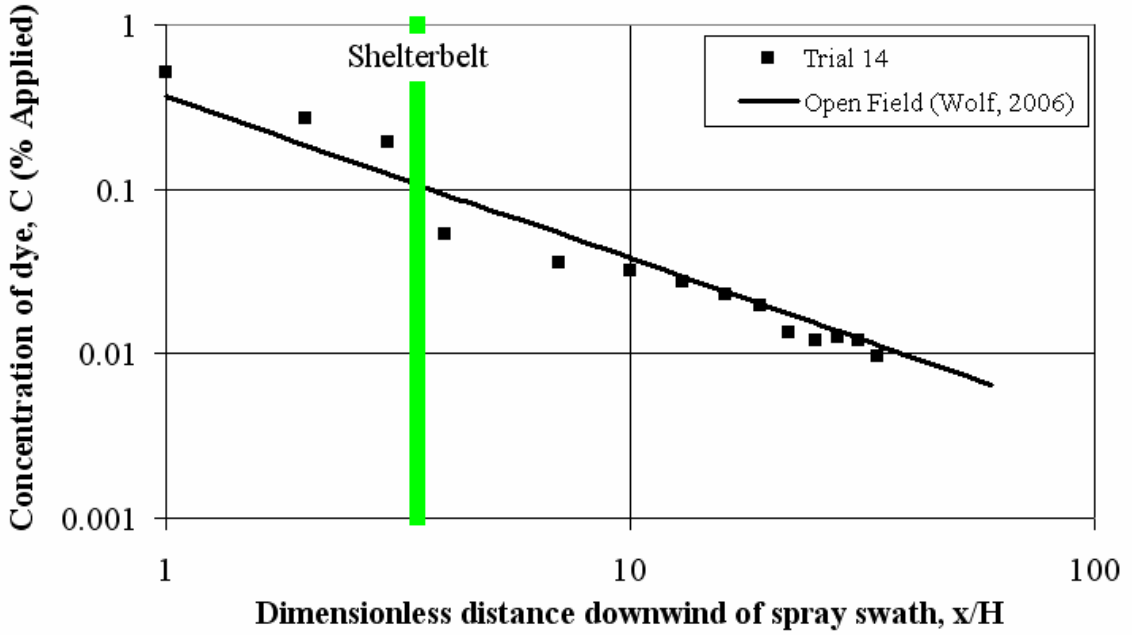

Figure 4.9 Comparison of deposit in the shelterbelt and open field settings (Trial 14)

deposition was again similar to the open field. In Trial 14, the mass of deposition was nearly the same as the open field setting at distances greater than 10H downwind of the shelterbelt, but for Trial 11, the mass of deposition was less than in the open field at all of the measurement distances downwind of the shelterbelt. Thus, it was not definitively

observed that the shelterbelt typically had reduced deposition in its far lee (further than 10H downwind of the shelterbelt), compared to the open field setting.

Figure 4.10 shows the airborne concentration of drift entering and exiting the shelterbelt compared to the open field setting. On the upwind side of the shelterbelt, the profile of the drift concentration was similar in both the shelterbelt and open field settings, with the peak concentration occurring at a height of 0.4H. However, downwind of the shelterbelt, the drift cloud was attenuated and the profile was nearly constant over the 4 m height compared to the open field. This behaviour was also described in the theory developed by Raupach et al. (2001).

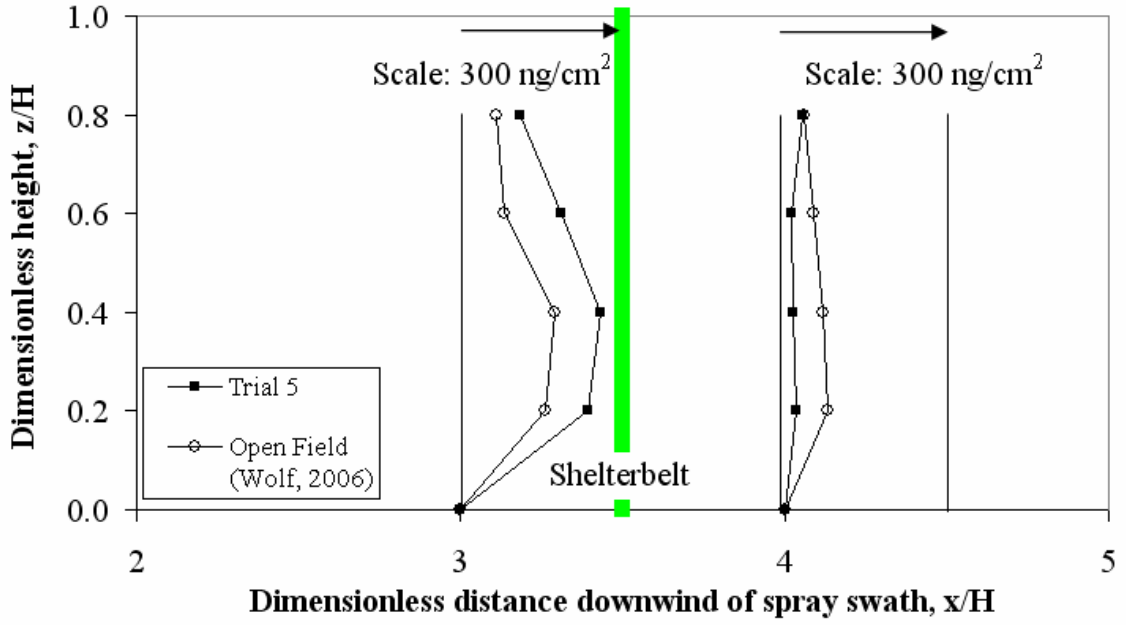

Figure 4.10 Airborne concentration profile for the open field and shelterbelt site (Trial 5)

The airborne concentration above the shelterbelt is shown in Figures 4.11 and 4.12. The profile of drift concentration upwind of the shelterbelt (Figure 4.12) was similar in shape to that seen in the open field experiments with the peak concentration occurring at a height of approximately 0.4H. However, on the downwind side of the shelterbelt, the peak concentration had risen by a height of approximately 1H compared to the open field setting. This was also found by Miller et al. (2000), who observed that the majority of airborne drift moved above a relatively wide stand of grass.

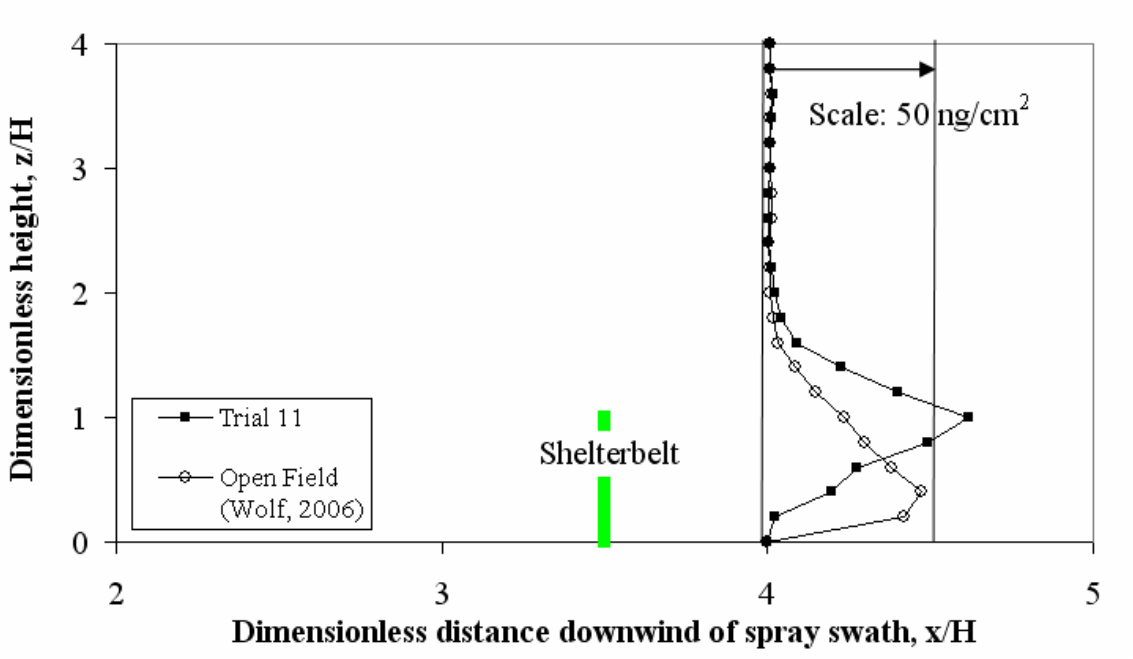

Figure 4.11 Airborne concentration profile for the open field and shelterbelt site (Trial 11)

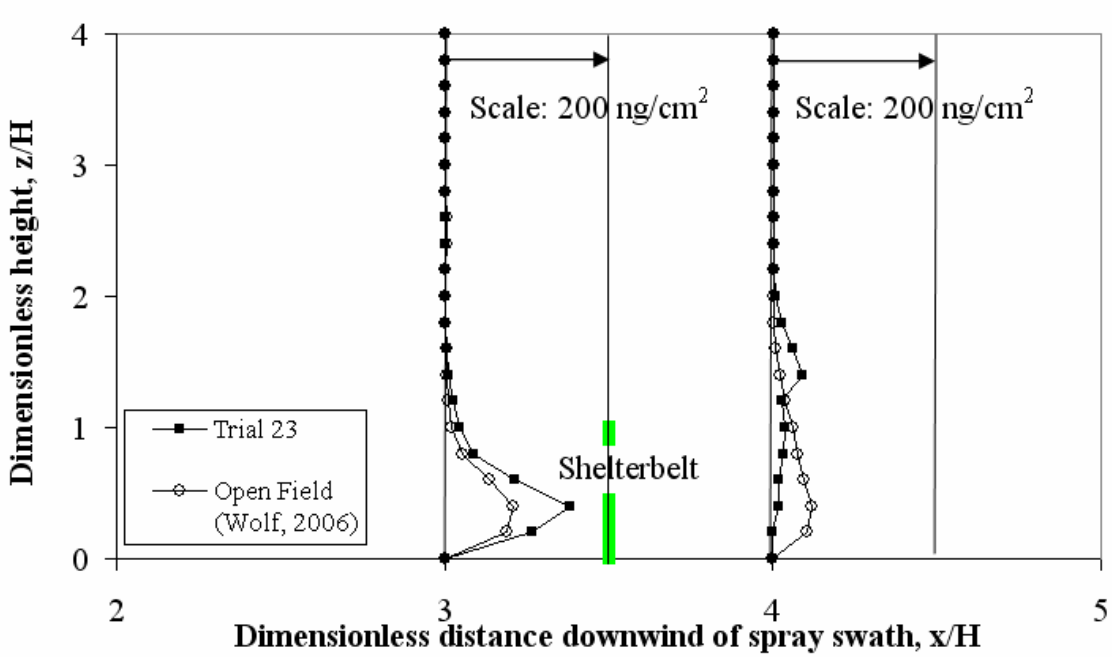

Figure 4.12 Airborne concentration profile for the open field and shelterbelt site (Trial 23)

4.4 Mass Balance Analysis

In spray drift studies, a mass balance analysis may be used to account for the total mass of drift. In these experiments, although the mass of drift can not be completely accounted for because there was some portion of drift that deposits downwind of the furthest measurement point and is lost to the atmosphere, a mass balance may provide comparison between drift trials for the mass of drift that deposited to ground upwind and downwind of the shelterbelt and the drift that was captured within the shelterbelt.

The drift samplers used in these experiments were able to measure the drift deposition in three locations: (1) onswath ground deposition; (2) offswath ground deposition on the upwind side of the shelterbelt (WSB), and; (3) offswath ground deposition on the downwind side of the shelterbelt to a distance of 150 m (the furthest measurement point) (LSB). The mass of drift deposited within the shelterbelt (SB) was not directly measured; however, the airborne concentration of drift entering and exiting the shelterbelt was measured. The mass of deposit within the shelterbelt was calculated as the difference between the mass entering and exiting the shelterbelt, and was based on the assumption that the reduction in drift was caused by droplets collecting on the shelterbelt's canopy or settling to the ground within the shelterbelt. There may have been some component of the drift cloud that entered the shelterbelt but deflected over the top of the highest collector; however, this was assumed to be minor compared to the mass collected and deposited within the shelterbelt. Figure 4.13 shows the four locations of deposit relative to the spray swath.

The drift deposit data in the Onswath, WSB, and LSB locations were integrated with distance using the trapezoidal rule to determine the total mass of ground deposit in their respective areas. The WSB deposit was integrated starting from the downwind edge of the spray swath, using the Onswath deposit as the deposit at distance $x = 0$ m. The airborne concentration profile of drift entering and exiting the shelterbelt was measured to a height of 4 m (0.8H) using the rotorod data and the slope of the concentration profile was linearly extrapolated to a height of 5 m (1H) based on the slope of the profile between 3 m and 4 m. This was done in order to match the height of

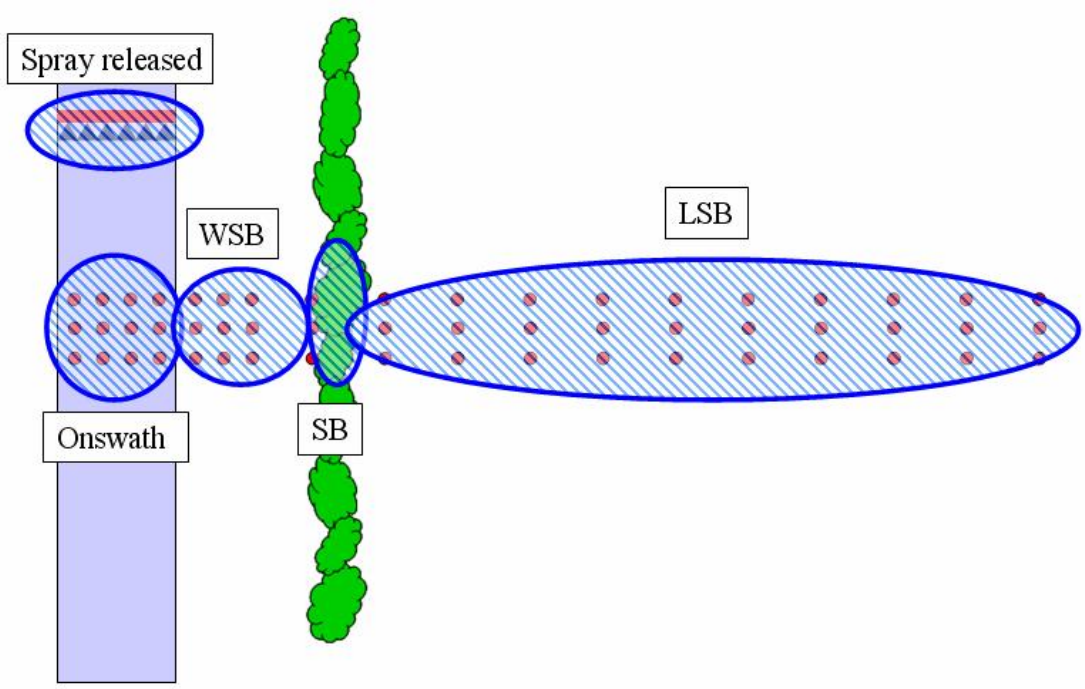

Figure 4.13 Locations of drift deposit accounted for in the mass balance

the concentration profile with the height of the shelterbelt. The mass of drift entering and exiting the shelterbelt was determined by integrating the concentration profile over the height of the shelterbelt based on the assumption that the airborne concentration of drift was zero at the ground (z = 0 m).

The mass of deposit in these four locations was normalized by the mass of spray applied by the sprayer in order to account for varying application rates of the sprayer. The mass of spray applied, $M_{Applied}$, in ng/cm^2, was calculated using the following equation:

$$M_{Applied} = \frac{\dot{Q}}{vW} C\rho \qquad [4.2]$$

where $\dot{Q}$ is the flow rate of spray delivered by the sprayer, v is the travel speed of the sprayer, W is the width of the sprayer boom, C is the concentration of dye in the spray solution, and ρ is the density of the spray solution. The results of the mass balance are presented in Table 4.2.

Table 4.2 Mass balance results

Trial	Onswath (% of Applied)	WSB (% of Applied)	SB (% of Applied)	LSB (% of Applied)	Total (% of Applied)	Spray Quality	Upwind Sprayer Distance
1	84.7	14.7	0.01	0.08	99.5	M	3H
2	86.1	14.9	0.05	0.02	101.1	VC	3H
3	75.5	13.1	0.01	0.05	88.6	M	3H
4	77.7	13.4	0.01	0.02	91.3	VC	3H
5	82.5	14.6	0.60	0.12	97.8	M	3H
6	56.7	10.8	1.78	0.35	69.6	F	3H
7	74.7	13.2	0.57	0.12	88.6	M	3H
8	59.8	11.1	1.80	0.30	73.1	F	3H
9	79.4	13.8	0.53	0.02	93.8	VC	3H
16	90.5	16.4	3.40	0.20	110.4	M	1H
17	105.1	19.9	1.76	0.18	126.9	M	3H
18	75.9	15.3	1.31	0.23	92.7	M	6H
21	80.7	14.4	0.20	0.16	95.5	M	6H
22	91.8	--------	2.33	0.16	94.3	M	1H
23	79.3	14.0	0.43	0.24	93.9	M	3H
24	121.1	21.4	0.29	0.32	143.1	M	6H
25	100.8	18.0	4.20	0.35	123.3	M	1H
26	79.3	14.2	1.30	0.52	95.3	M	3H
27	87.0	16.0	0.52	0.29	103.8	M	6H

A number of trials were omitted from the mass balance analysis because they did not have rotorod data available. Also, there were a number of trials where the mass balance yielded greater than 100% of the spray applied. This may be attributed to the photolysis correction factor. All of the drift deposit measurements were corrected for photolysis while the mass of applied spray was based on a theoretical calculation. In some instances, the loss due to photolysis was more than 40% over approximately 15 minutes of exposure to sunlight, which was much higher than anticipated. All the deposit data for each trial were corrected by the same photolysis factor calculated for that particular trial. Thus, the length of time the samples were exposed before being picked up proved to be significant, and assuming the same photolysis factor for all deposits likely overestimated the deposit on some of the samples that were picked up first.

For the subset of trials that examined a Fine and Medium spray quality on the same day (Trials 5 – 8), the ground deposition onswath was 26% greater and the deposition on the upwind side of the shelterbelt was 15% greater for the Medium spray quality compared to the Fine spray quality. The deposit on the downwind side of the shelterbelt was 63% less for the Medium spray quality compared to the Fine spray quality. The deposit within the shelterbelt for the Medium spray quality was 67% less than for the Fine spray quality. This suggested that, as was expected, coarser sprays were more likely to deposit onswath or within a short distance downwind, while finer sprays drifted further downwind and had increased deposition within the shelterbelt and on the leeward side of the shelterbelt.

It was also seen that, for the subset of trials that varied the upwind distance of the sprayer from the shelterbelt on the same day (Trials 22 – 27), the greatest capture of drift within the shelterbelt occurred when the spray swath was 1H upwind of the shelterbelt. The calculated deposit captured within the shelterbelt for the 3H distance was 74% less than the 1H distance. This was likely because the sprayer traveled within the sheltered zone upwind of the shelterbelt. This sheltered zone extends 5H upwind of a shelterbelt (Judd et al., 1996) and the spray swath extended from approximately 1H to 4H upwind of the shelterbelt. When the spray was released entirely in the sheltered zone, the droplets likely were not subjected to the displaced flow traveling over the top of the shelterbelt. Therefore, the offswath movement of drift was channeled through the shelterbelt. Also, when the spray swath was closest to the shelterbelt, there was decreased deposition in the lee of the shelterbelt. The deposition downwind of the shelterbelt for the 1H distance was 33% less than the 3H distance. This was likely because more of the drift cloud traveled through the shelterbelt than over the top of the shelterbelt, and the drift cloud was filtered by the shelterbelt. Thus, there was a lower amount of drift available to deposit downwind of the shelterbelt.

4.5 Repeatability of Trials

When conducting the field experiments, it was accepted that there was some random variability between trials although considerable effort was put into duplicating experimental conditions. In these field experiments, the sources of variability could

have been from meteorological conditions, application settings, or operator control. An assessment of the variability of trials with quite similar conditions may provide insight into the value of comparisons between trials with greater variation in experimental conditions. Two sets of trials were identified, Trials 6 & 8 and Trials 10d, 11d, & 12d, in which the meteorological and controlled variables were similar (Table 4.3). In this analysis, repeatability is assessed strictly by visually comparing the plots of the trials within the particular subset. For this comparison, the mean and standard deviation for each data point were calculated based on the three sub-samples at each measurement distance for the Petri-plate and rotorod data. Error bars were drawn to denote ± 1 standard deviation from the mean value.

Table 4.3 Conditions of trials that examine repeatability

Subset	Trial #	U (km/h)	γ (°)	T (°C)	RH (%)	Ri	Q	β	α	D
1	6	15.9	33.1	13.4	42.7	-0.020	F	0.204	0.548	3H
	8	15.3	33.3	13.5	41.0	-0.007	F	0.204	0.523	3H
2	10d	7.0	2.4	17.3	37.7	-0.079	F	--------	0.581	3H
	11d	9.1	5.9	17.0	37.0	-0.011	F	--------	0.618	3H
	12d	8.5	4.4	16.8	36.0	-0.004	F	--------	0.600	3H

The Petri-plate data for Trials 6 & 8 and Trials 10d, 11d, & 12d are shown in Figures 4.14 and 4.15, respectively. Each trial was mostly within ± 1 standard deviation of the other comparative trials most of the measurement distances, but there was a noticeable divergence of the ground deposition beyond a distance of approximately 28H downwind of the spray swath. The overall shape of the plots was mostly preserved between the replicate trials.

The repeatability was also assessed using the rotorod data for Trials 6 & 8 (Figure 4.16). The two concentration profiles were within ± 1 standard deviation for all of the measurement heights. For Trials 10d, 11d, & 12d, there was only one string collector in each trial, so the mean and standard deviation could not be calculated for the trials. However on a strictly visual basis, the three trials did show variability in the concentration profiles (Figure 4.17). The shapes of the profiles in both

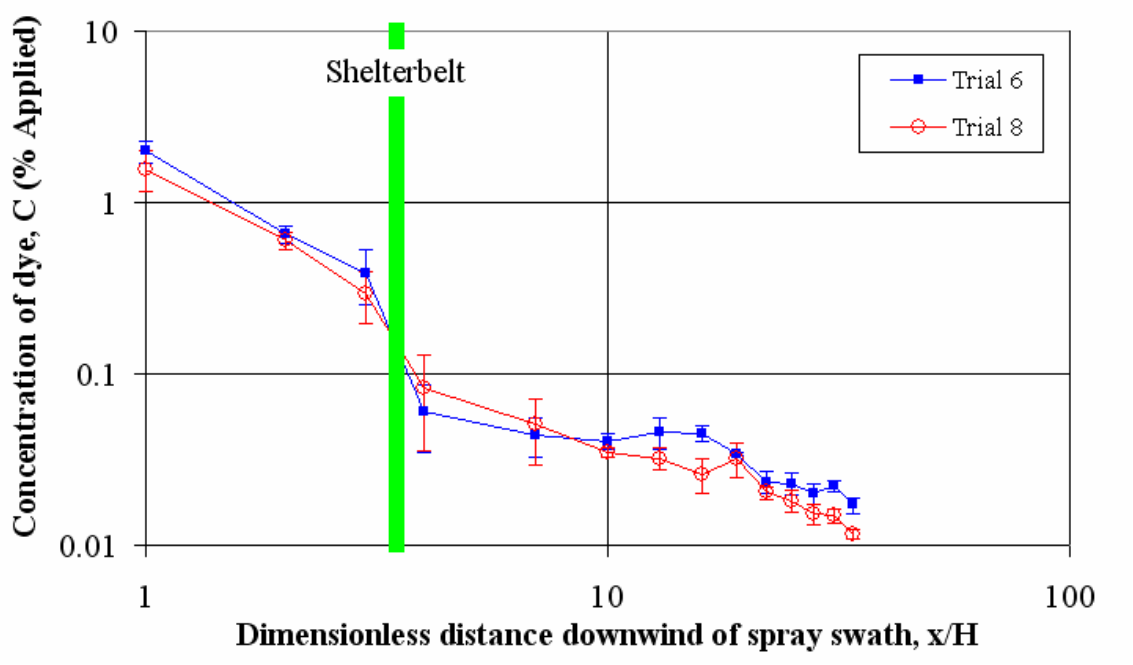

Figure 4.14 Repeatability of Petri-plate data for Trials 6 & 8

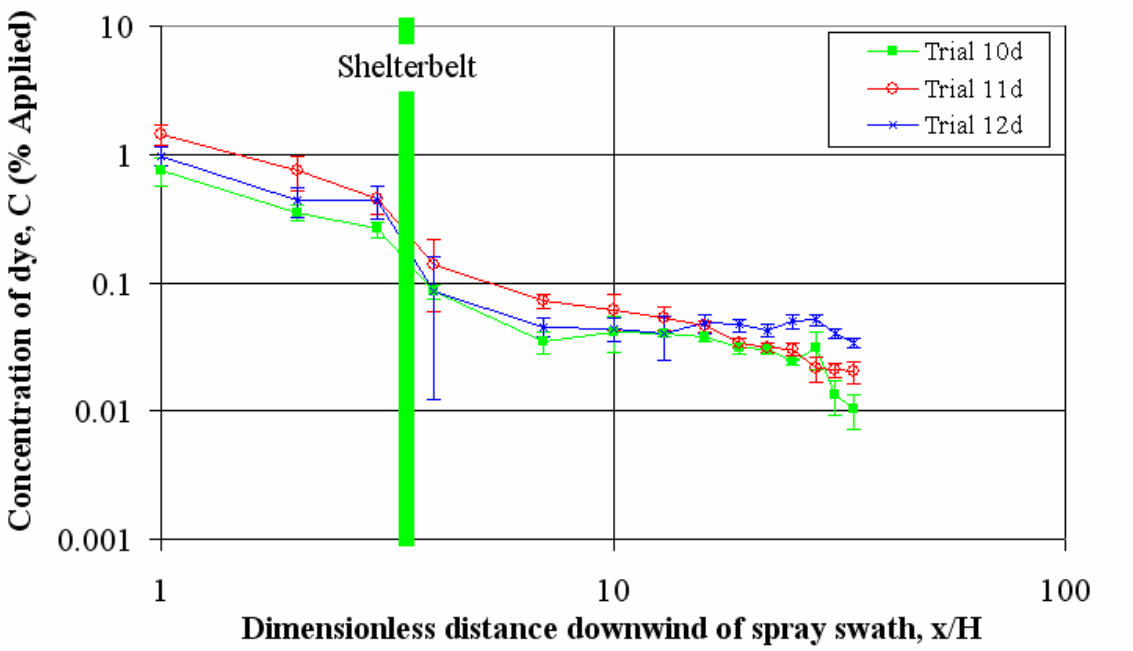

Figure 4.15 Repeatability of Petri-plate data for Trials 10d, 11d, & 12d

Figures 4.16 and 4.17 were similar, showing two local maxima in the concentration profile occurring at heights of approximately 0.4H and 1.4H.

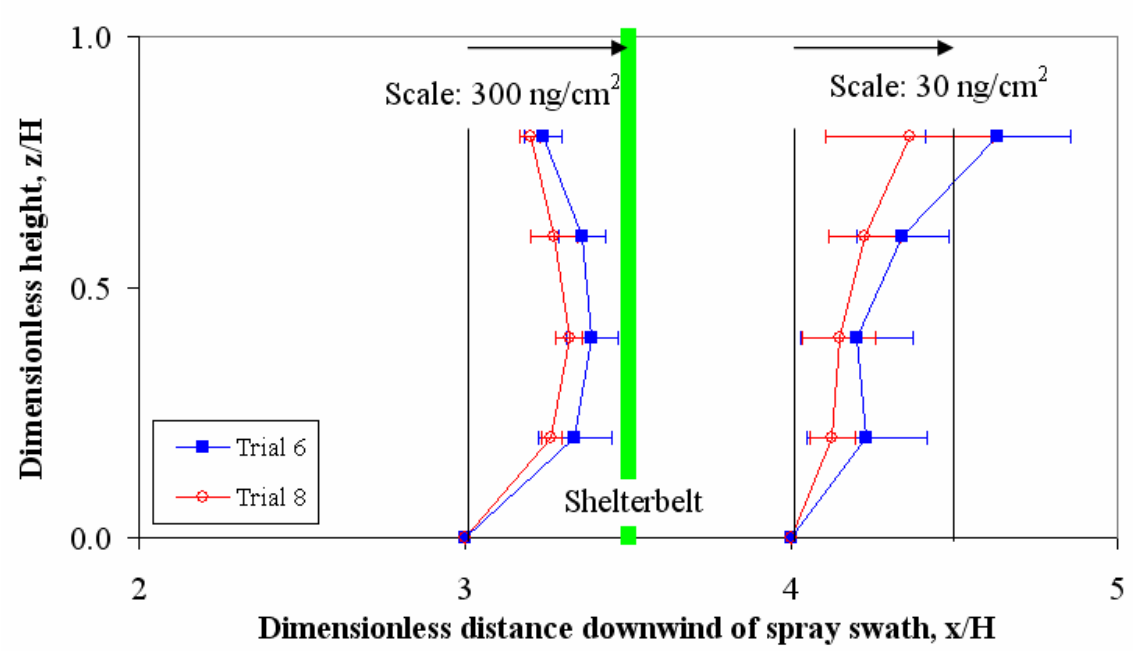

Figure 4.16 Repeatability of rotorod data for Trials 6 & 8

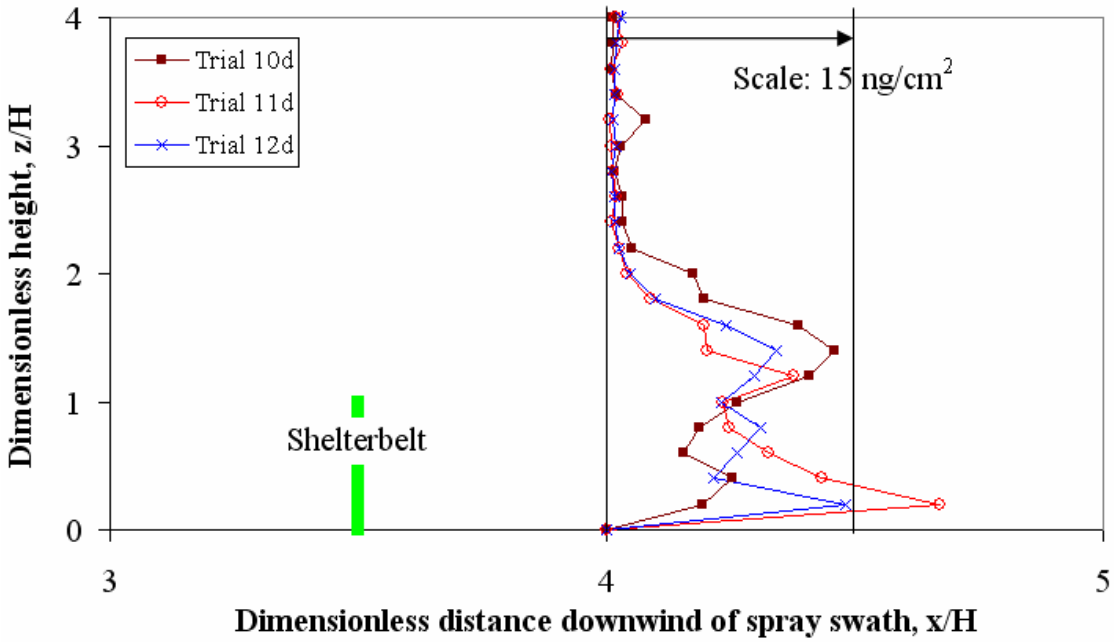

Figure 4.17 Repeatability of string data for Trials 10d, 11d, & 12d

For the three types of collectors, there was variability between the amounts of deposition at any particular distance or height, but the shapes of the profiles were similar between the trials. This suggested that, in the following sections examining the

meteorological and controlled variables, the relative shapes of the profiles were important to consider.

4.6 Assessment of the Effect of Meteorological Variables

As discussed earlier, the movement of spray drift and the flow around a shelterbelt are both dependent on a number of meteorological conditions including wind speed, wind direction, atmospheric stability, temperature, relative humidity, and turbulence. Turbulence was not measured in these experiments. A qualitative assessment of the effect of these variables on the deposition and airborne concentration of spray drift was done first, followed by a quantitative assessment using multiple linear regression analysis.

The qualitative analysis was performed by choosing two experiments where the variable in question differed but all other measured variables were similar. There were comparative trials identified to examine the effect of wind direction, wind speed, temperature, and relative humidity; however, comparative trials with differing atmospheric stability (with all other meteorological conditions similar) were not found.

4.6.1 Qualitative analysis of the effect of wind direction

Two pairs of trials were identified that had similar meteorological conditions except for wind direction; these trials were Trials 1 & 3 and Trials 19 & 22 (Table 4.4). In Trials 1 & 3, there was decreased deposition beyond 10H downwind of the spray swath for the more oblique wind (Figure 4.18). This was contradicted in Figure 4.19, which shows the ground deposit for Trials 19 & 22, where the more oblique wind had more deposition for a distance of 5H to 17H downwind of the shelterbelt. Beyond a distance of 17H downwind of the shelterbelt, it was observed that the deposition was similar for both trials (0.066% and 0.054% of Applied for Trials 19 and 22, respectively).

The airborne concentration profiles of drift entering and exiting the shelterbelt for Trials 1 & 3 shows there was greater airborne drift for the more oblique wind (Figure 4.20). The shape of the concentration profiles for Trials 1 & 3 was similar, which suggested that the movement of drift through the shelterbelt was not affected by

Table 4.4 Conditions of trials that examine wind direction

Subset	Trial #	U (km/h)	γ (°)	T (°C)	RH (%)	Ri	Q	β	α	D
1	1	8.8	33.0	18.5	42.2	-0.025	M	0.204	0.457	3H
	3	6.8	52.7	18.0	42.0	-0.005	M	0.204	0.385	3H
2	19	13.2	28.0	22.0	------	-0.061	M	0.292	0.513	1H
	22	11.5	12.6	20.0	53.5	-0.107	M	0.292	0.628	1H

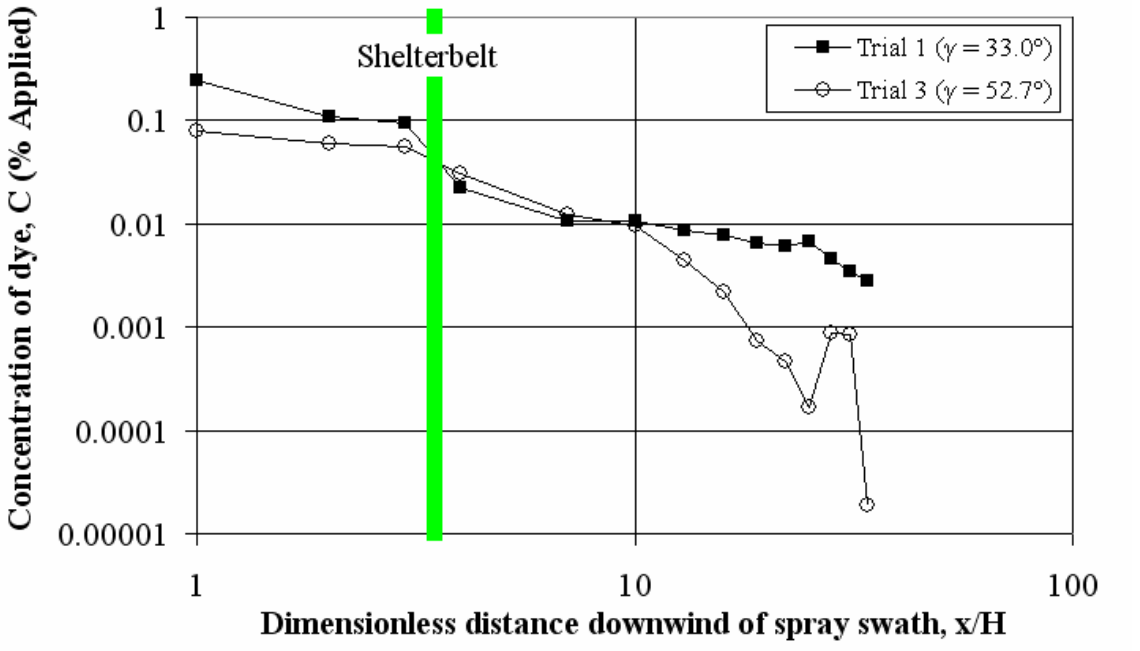

Figure 4.18 Effect of wind direction on the downwind ground deposition of drift for Trials 1 & 3

the wind direction. For Trials 19 & 22, this data was only available for the string collector (Figure 4.21), and shows the less oblique wind had a higher concentration of drift over the height of the shelterbelt on both the up- and downwind sides of the shelterbelt. The airborne drift concentration profiles for Trials 19 & 22 were similar, with the peak concentration on the up- and downwind sides of the shelterbelt both occurring at 0.4H.

The effect of wind direction is usually not investigated in spray drift research in the open field because the collector distances may be adjusted to account for an oblique wind (ASAE, 2005a). In these experiments, it was thought that adjusting the collector distance to account for wind obliqueness was not applicable to the shelterbelt site

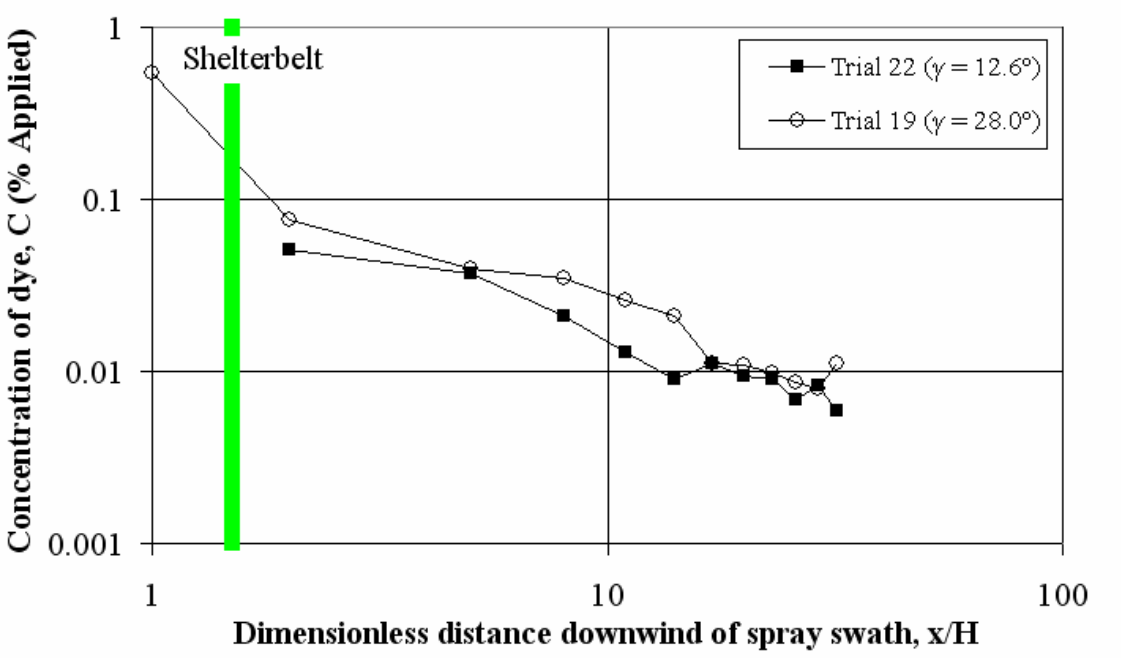

Figure 4.19 Effect of wind direction on the downwind ground deposition of drift for Trials 19 & 22

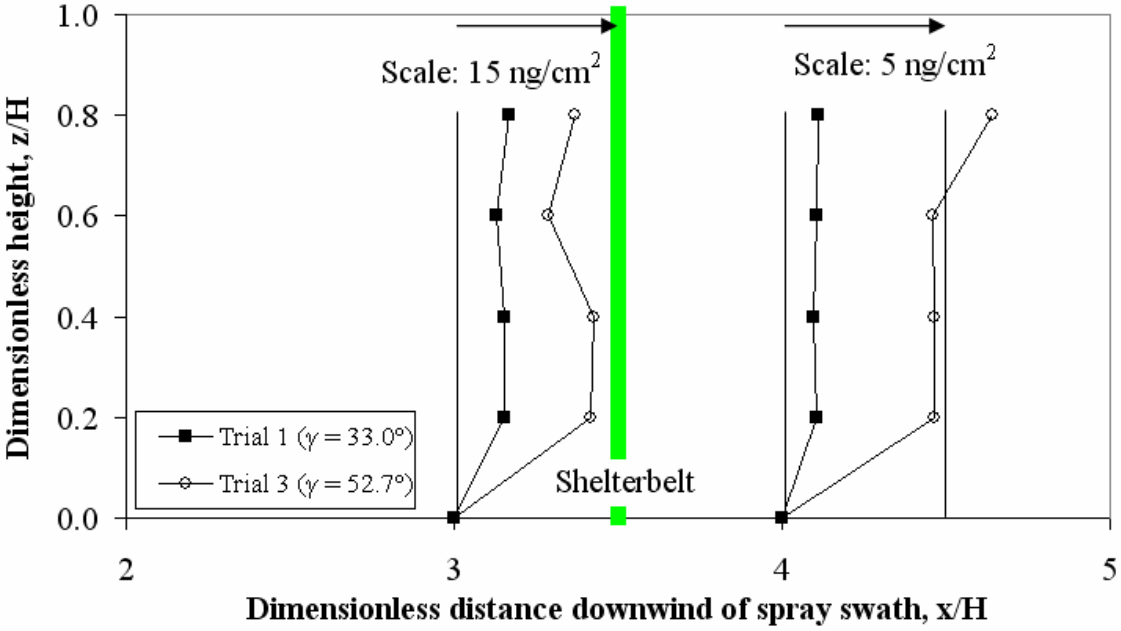

Figure 4.20 Effect of wind direction on the airborne drift concentration profiles for Trials 1 & 3

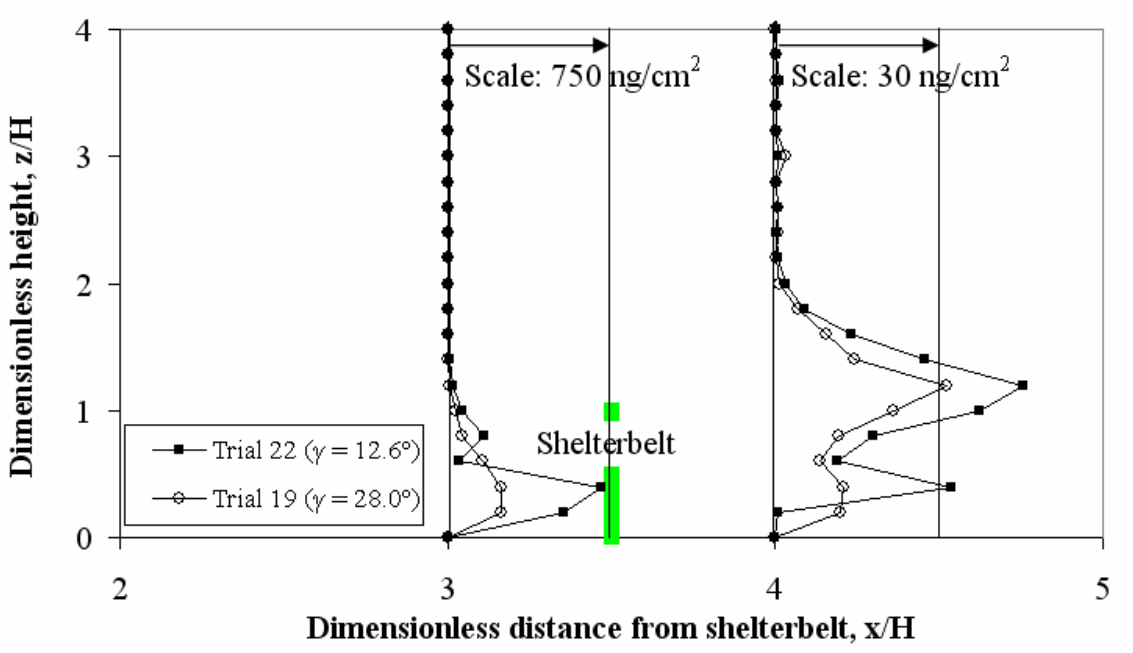

Figure 4.21 Effect of wind direction on the airborne drift over the shelterbelt for Trials 19 & 22

because of potential veering of the wind direction near the shelterbelt caused by an oblique wind. There is limited information available regarding the nature of the wind veering near a shelterbelt, but Nord (1991) found that the wind direction was affected by the shelterbelt for a distance of approximately 11H downwind of the shelterbelt.

4.6.2 Qualitative analysis of the effect of wind speed

Trials 18 and 24 were the only pair of trials that had a different wind speed with all other variables being similar. Table 4.5 gives a summary of the conditions for the two trials. The downwind ground deposition of spray drift for these two trials is shown in Figure 4.22. The deposition of drift on the upwind side of the shelterbelt for the higher wind speed was 75% greater than for the lower wind speed. Immediately downwind of the shelterbelt, the deposition was significantly less for the higher wind speed compared to the lower wind speed (91% and 37% of the deposit at 0.5H upwind of the shelterbelt, respectively). The drift deposition with respect to downwind distance increased for the higher wind speed and decreased for the lower wind speed for a distance of 0H to 6H downwind of the shelterbelt. Further downwind than 15H, the deposition decreased at a similar rate for both trials.

Table 4.5 Conditions of trials that examine wind speed

Trial #	U (km/h)	γ (°)	T (°C)	RH (%)	Ri	Q	β	α	D
18	27.6	5.2	17.9	55.7	-0.025	M	-------	0.612	6H
24	12.6	11.2	22.1	45.6	-0.089	M	0.292	0.605	6H

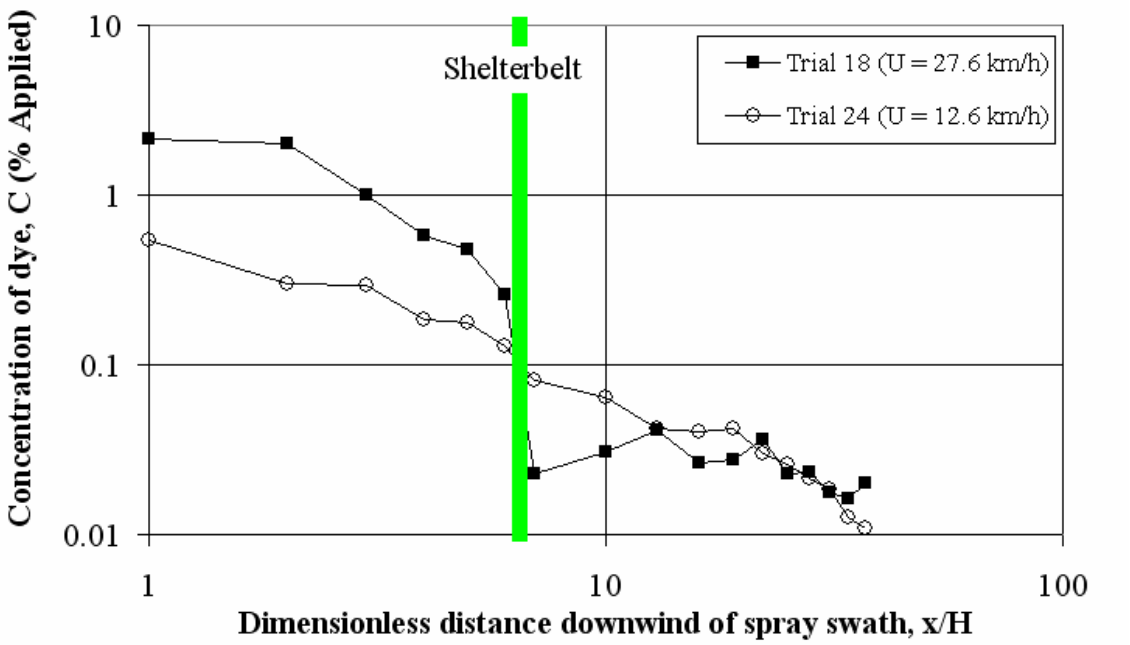

Figure 4.22 Effect of wind speed on the downwind ground deposition of drift for Trials 18 & 24

Figure 4.23 shows the airborne drift concentration profiles for Trials 18 & 24. The mass of airborne drift entering the shelterbelt was 4.7 times greater for the higher wind speed, which was likely due to the higher wind speed. This is comparable to research by Grover et al. (1997) who found that the mass of airborne drift was approximately 5 times greater for a 30 km/h wind compared to a 10 km/h wind. There was a greater mass of drift exiting the shelterbelt (relative to the mass entering) for the higher wind speed. The mass of drift exiting the shelterbelt was 16.6% and 6.1% of the mass entering the shelterbelt for Trials 18 and 24, respectively. However, the mass of drift captured within the shelterbelt was 78% greater for Trial 18 compared to Trial 24. This indicated that the shelterbelt was more efficient at capturing drift droplets in the higher wind speed. For the higher wind speed, the shelterbelt's canopy would have swayed more and swept a greater volume of air compared to a lower wind speed. The

ground deposit and airborne concentration data both indicate that wind speed has a noticeable effect on the movement of spray drift past the shelterbelt.

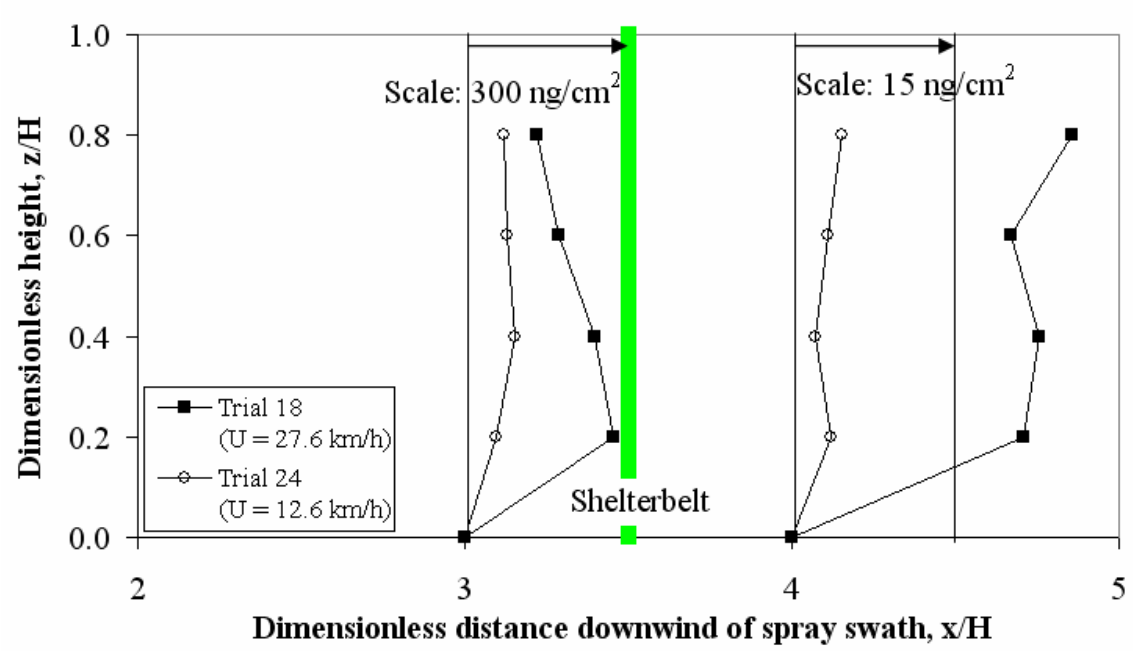

Figure 4.23 Effect of wind speed on the airborne drift concentration profiles for Trials 18 & 24

4.6.3 Qualitative analysis of the effect of temperature and relative humidity

Trials 10 & 13 and 12 & 15 had a varied temperature and RH with the other meteorological variables similar. Table 4.6 gives a summary of the experimental conditions for these two sets of trials. Temperature and relative humidity were examined together, as both variables influenced the evaporation rate of the drift droplets. The effect of temperature and humidity on spray drift is considered significant when the temperature or wet bulb depression is greater than 30^{o}C and 10^{o}C, respectively (CSIRO, 2002). The temperatures in these experiments were mild (15 to 20^{o}C) and the greatest wet bulb depression was 9.0^{o}C during Trial 15 (Table 4.7), so the effect of temperature and RH may not be apparent for the conditions observed in these two sets of trials.

Table 4.6 Conditions of trials that examine temperature and relative humidity

Subset	Trial #	U (km/h)	γ (°)	T (°C)	RH (%)	Ri	Q	β	α	D
1	10	11.4	13.5	14.6	42.1	-0.030	F	0.483	1.005	3H
	13	10.5	11.2	17.9	34.0	-0.026	F	0.483	0.933	3H
2	12	9.4	4.2	15.6	40.4	-0.004	VC	0.483	0.942	3H
	15	11.5	0.9	18.9	30.2	-0.034	VC	0.483	0.908	3H

Table 4.7 Temperature and humidity for Trials 10, 12, 13, and 15

Trial	T (°C)	RH	T_{wb} [1] (°C)	ΔT [2] (°C)
10	14.6	42.1%	8.3	6.3
13	17.9	34.0%	9.7	8.2
12	15.6	40.4%	8.8	6.8
15	18.9	30.2%	9.9	9.0

1. Wet bulb temperature
2. Wet bulb depression = $T - T_{wb}$

Figure 4.24 shows that there was no clear difference in the mass of ground deposition of drift for Trials 10 & 13 except for distances further than 13H downwind of the spray swath. The rate of deposition past this distance decreased for Trial 13 and was relatively constant for Trial 10. Trial 13 had a greater rate of evaporation and this indicated that, when the drift cloud had traveled downwind a distance of 13H, the droplets would have been smaller and less prone to deposition. This was contradicted in Figure 4.25 where the mass of drift deposition was greater for Trial 15, which had the greater rate of evaporation. The greater rate of evaporation in Trial 15 would have caused the droplets to decrease in size quicker than in Trial 12. These finer droplets would have been more prone to remain airborne, and this may have led to greater downwind drift deposition.

Figures 4.26 and 4.27 show the airborne drift concentration profiles for Trials 10 & 13 and Trials 12 & 15, respectively. In both pairs of trials, there was less airborne drift for the trial with the lower rate of evaporation. The airborne drift was 43% less for Trial 10 compared to Trial 13 and 42% less for Trial 12 compared to Trial 15. The shapes of the concentration profiles in both pairs of trials were similar. This suggested

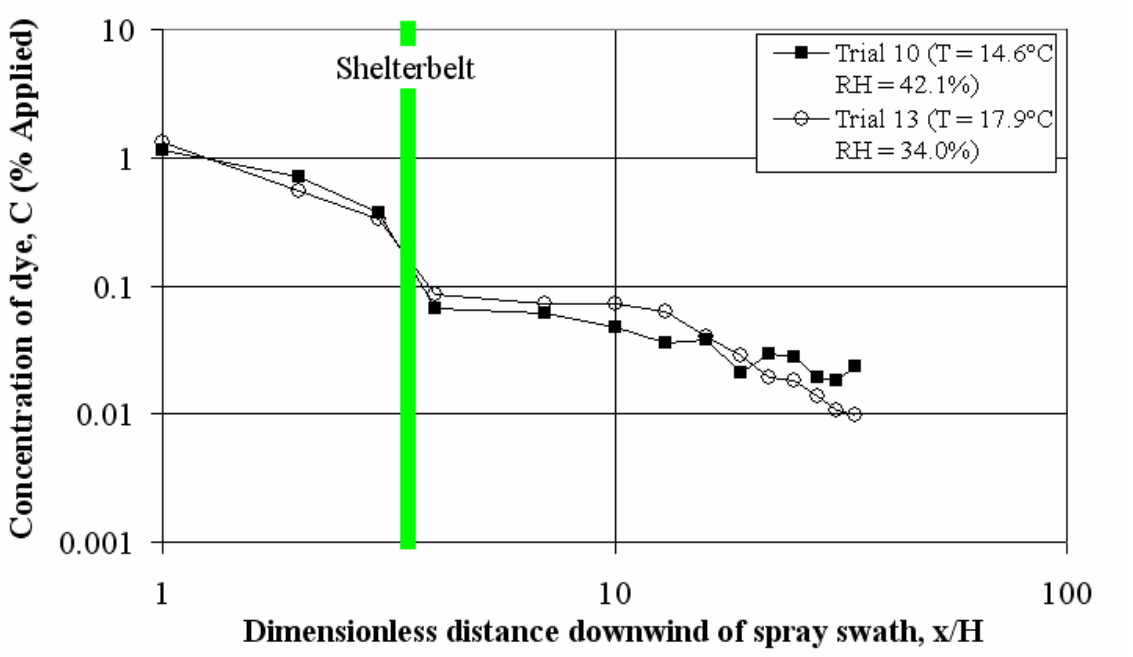

Figure 4.24 Effect of temperature and RH on the downwind ground deposition of drift for Trials 10 & 13

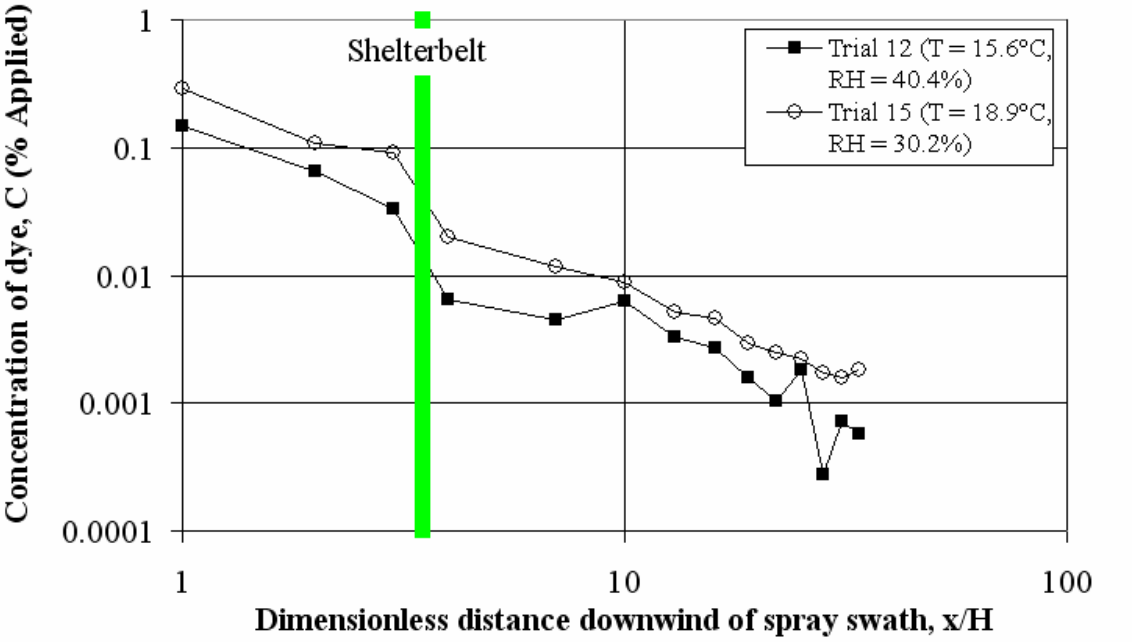

Figure 4.25 Effect of temperature and RH on the downwind ground deposition of drift for Trials 12 & 15

that, while temperature and RH had an effect on the mass of airborne drift, the movement of the drift cloud was similar for the range of temperature and RH observed.

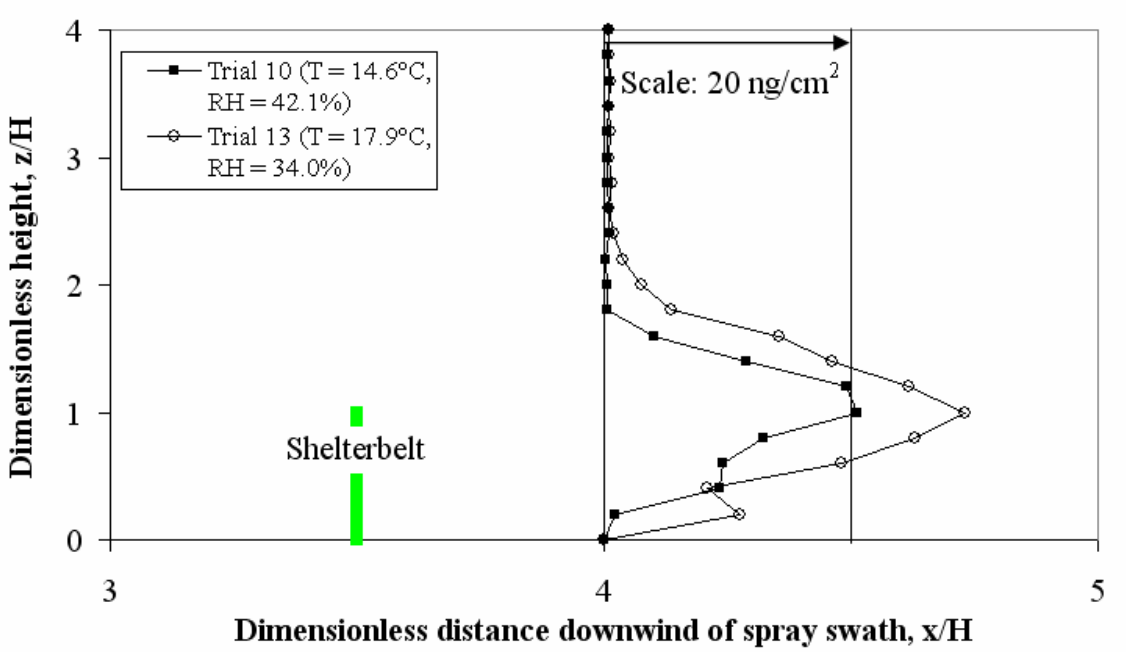

Figure 4.26 Effect of temperature and RH on the airborne drift concentration profiles for Trials 10 & 13

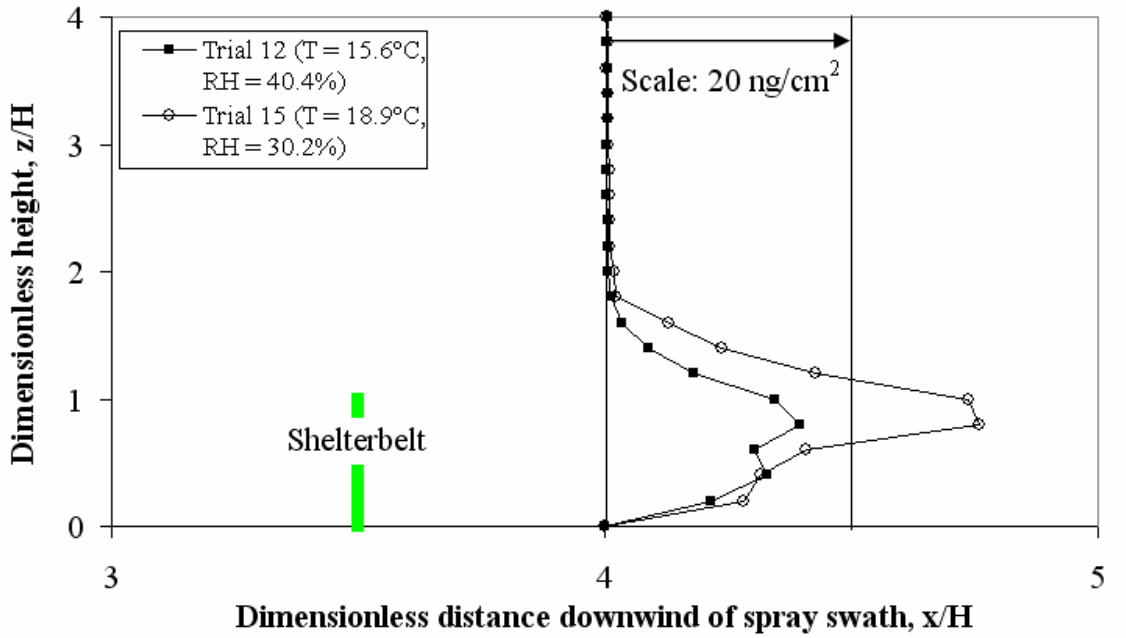

Figure 4.27 Effect of temperature and RH on the airborne drift concentration profiles for Trials 12 & 15

The effect of atmospheric stability was not investigated in the preceding qualitative analysis because there were no trials that had different Richardson numbers with the other meteorological conditions being similar. The Richardson numbers for all of the trials were negative, which denotes unstable conditions, except for Trial 4 where

the Richardson number was 0.014. It is rare for stable conditions to occur in the afternoon (CSIRO, 2002), so the calculation of a positive Richardson number may be due to instrument error. The range of negative Richardson numbers was -0.004 to -0.107. For Richardson numbers between approximately -0.05 and 0.05, the atmospheric stability is classified as fully forced convection (Oke, 1987). The stability conditions experienced during these field experiments only varied slightly and the effects of stability on the movement of spray drift past the shelterbelt may not have been apparent. Fritz (2004) sampled a relatively wide range of atmospheric stabilities, including very stable conditions at the first light of dawn, and found that atmospheric stability did have a significant effect on the ground deposition of spray drift. Although the effect of atmospheric stability on the movement and deposition of drift was not included in the preceding qualitative analysis, it was included in the following quantitative assessment.

4.6.4 Quantitative analysis of the meteorological variables

Regression analysis has been used in field experiments by other researchers (Adrizal et al., 2008; Brown et al., 2004; Fritz, 2004; Hoffman et al., 2003) as a way of determining the significance of a certain variable when there are confounding effects from other variables. Therefore, for this study, multiple linear regression analysis was used to determine the significance of each of the meteorological variables on the movement of spray drift past a shelterbelt. In the preceding qualitative analysis, there were few definite conclusions that could be made because of the inherent variability of the meteorological conditions in each trial. The regression analysis may provide insight into which of the above variables has a significant effect on the movement and deposition of spray drift past the shelterbelt, although the model is only applicable to the range of variables sampled.

The standard stepwise method was chosen to perform the regression analysis. This method is different than the commonly used forward and backward-elimination stepwise methods because it introduces all of the variables in one step (Statistica User Manual, 2001). Both the forward and backward-elimination techniques have a threshold F value to enter and remove a variable from the regression. The F statistic determines the likelihood that, when adding a variable into the regression model, the

variable is within the population of the model. So, if the computed F value of a variable is greater than the F value to enter it into the model or less than the F value to remove it from the model, the variable is removed from the regression (Montgomery et al., 2004). Thus, both the forward or backward-elimination stepwise methods may have removed variables from the regression model if the variable did not meet the F value criteria. Thus, the standard step method was chosen instead of the forward or backward-elimination stepwise methods because it preserved all of the variables in the analysis.

In order to perform the regression analysis, it was hypothesized that each independent variable had a statistically significant effect on the dependent variable. The p value is the probability that a hypothesis is false, and a threshold p value can be arbitrarily set. A threshold p value of 0.05 has been used in previous field experiments to identify the significance of variables (see for example, Adrizal et al., 2008; Brown et al., 2004; Hoffman et al., 2003). The p value was computed by the model for each independent variable. If the p value was less than 0.05 for a particular variable, the variable was identified as statistically significant. In other words, there was at least a 95% probability that the independent variable in question had a significant effect on the dependent variable.

The software program Statistica (StatSoft, Inc., Tulsa, OK) was used to perform the regression analysis. The input data were the meteorological conditions of the trials that had a Medium spray quality and an upwind sprayer distance of 3H (10 trials). The shelterbelt optical porosity was not available for all of the trials in this subset, so the aerodynamic porosity was introduced into the regression to account for the variation in shelterbelt porosity.

The multiple linear regression analysis generated an empirical equation of the form:

$$Y = a_0 + a_1 x_1 + a_2 x_2 + a_3 x_3 \ldots \qquad [4.3]$$

where Y is the dependent variable, a_i are the coefficients used to calibrate the model, and x_i are the independent variables. The sign of the calibration coefficient (positive or negative) provides insight into how the independent variable was affected the dependent variable. For instance, a negative coefficient for a certain independent variable suggests that the dependent variable varied inversely with respect to that particular variable.

In this regression model, the meteorological variables were the independent variables. The dependent variable was the integrated mass of drift deposited to ground downwind of the shelterbelt to a distance of 30H. This dependent variable was chosen because the effect of the shelterbelt on the deposition of spray drift would likely be most pronounced downwind of the shelterbelt. Also, it was anticipated that the drift cloud would have recovered from any effect the shelterbelt had by the time it had traveled 30H downwind from the shelterbelt. The results of the regression analysis are shown in Table 4.8. The adjusted r^2 value, which takes into account the number of independent variables (Montgomery et al., 2004) was 0.87.

Table 4.8 Regression analysis to determine significant meteorological variables

x_i	a_i	p value
Intercept	-0.862	0.018
U	0.025	0.016
γ	0.006	0.069
T	0.024	0.041
RH	-0.004	0.046
Ri	-2.796	0.123
α	0.380	0.062

The multiple linear regression analysis determined that the wind speed, temperature, and relative humidity were statistically significant variables; the p values corresponded to 0.016, 0.041, and 0.046. The effects of wind direction, atmospheric stability, and shelterbelt aerodynamic porosity were not statistically significant. The sign of the calibration coefficients (a_i) indicated that a higher wind speed (0.025), higher temperature (0.024), or lower relative humidity (-0.004) would increase the deposition of drift downwind of the shelterbelt. This was comparable to observations by Fritz (2004), who found that, using regression analysis, wind speed had a significant effect on the deposition of drift at distances further than 35 m downwind of the spray swath.

4.7 Assessment of the Effect of Controlled Variables

In the following section, the effect of the controlled variables on the movement of spray drift past a shelterbelt is investigated. The controlled variables include spray quality, shelterbelt optical porosity, and upwind sprayer distance. First, a qualitative analysis is carried out that examines the effect of the controlled variables on the ground deposition and airborne concentration profile of drift around the shelterbelt. This is followed by a quantitative assessment that uses multiple linear regression analysis to determine the significance of the effect the controlled variables have on the movement of spray drift.

In the previous qualitative analysis that examined the effect of the meteorological conditions, the method was to choose two trials in which the variable in question was different but all other variables were similar. In the following qualitative analysis, the same method is employed; subsets of trials are compared that have similar meteorological conditions. Using multiple linear regression analysis, it was determined that wind speed, temperature, and RH had statistically significant effects on the quantity of drift deposited downwind of the shelterbelt, while wind direction and atmospheric stability was found to be statistically insignificant. Thus, a greater difference in wind direction and Richardson number is tolerated in the analysis herein than in the previous section.

4.7.1 Qualitative analysis of the effect of spray quality

Three different spray nozzles were used to produce a varied spray quality. The three spray qualities were, in ascending order of drift potential, Very Coarse, Medium, and Fine. Three sets of trials were identified that had similar experimental conditions except for spray quality (Table 4.9).

Figure 4.28 shows the downwind ground deposition of drift for Trials 2 and 3, which had Very Coarse and Medium spray qualities, respectively. The ground deposition upwind of the shelterbelt for the Very Coarse spray quality was 80% less than for the Medium spray quality. On the downwind side of the shelterbelt to a distance of 19H downwind of the spray swath, the ground deposit was 71% less for the Very Coarse spray quality compared to the Medium spray quality. This increased mass

Table 4.9 Conditions of trials that examine spray quality

Subset	Trial #	U (km/h)	γ (°)	T (°C)	RH (%)	Ri	Q	β	α	D
1	2	7.3	57.0	18.1	42.7	-0.015	VC	0.204	0.445	3H
	3	6.8	52.7	18.0	42.0	-0.005	M	0.204	0.385	3H
2	5	15.8	25.7	13.2	42.6	-0.009	M	0.204	0.489	3H
	6	15.9	33.1	13.4	42.7	-0.020	F	0.204	0.548	3H
3	15	11.5	0.9	18.9	30.2	-0.034	VC	0.483	0.908	3H
	14	10.3	14.4	17.7	33.5	-0.035	M	0.483	0.974	3H
	13	10.5	11.2	17.9	34.0	-0.026	F	0.483	0.933	3H

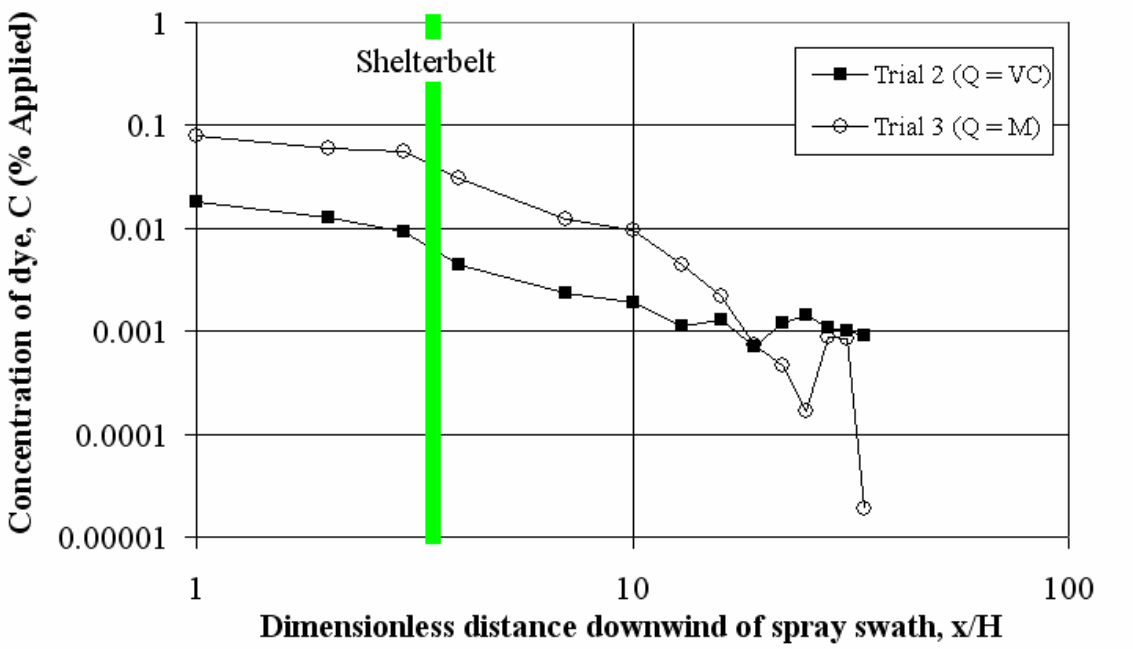

Figure 4.28 Effect of spray quality on the downwind ground deposition of drift for Trials 2 & 3

of deposition most likely occurred because the Medium spray quality had a greater driftable fraction (see Table 3.1). Past this point, the ground deposition for the Very Coarse spray quality was slightly higher.

For a comparison of the downwind ground deposition of the Medium and Fine spray qualities, Trials 5 and 6 were used (Figure 4.29). The mass of ground deposit downwind of the shelterbelt was approximately 3 times greater for the Fine spray quality compared to the Medium spray quality. This was likely because the finer spray quality had a greater driftable fraction. This observation was comparable to findings by

Fritz (2004) who observed that the deposition was 1.5 times greater for a Fine spray quality compared to a Medium spray quality. The deposition plots for the Fine and Medium spray qualities were nearly parallel downwind of the shelterbelt, which suggested that the rate of deposition with respect to downwind distance was similar for the two spray qualities.

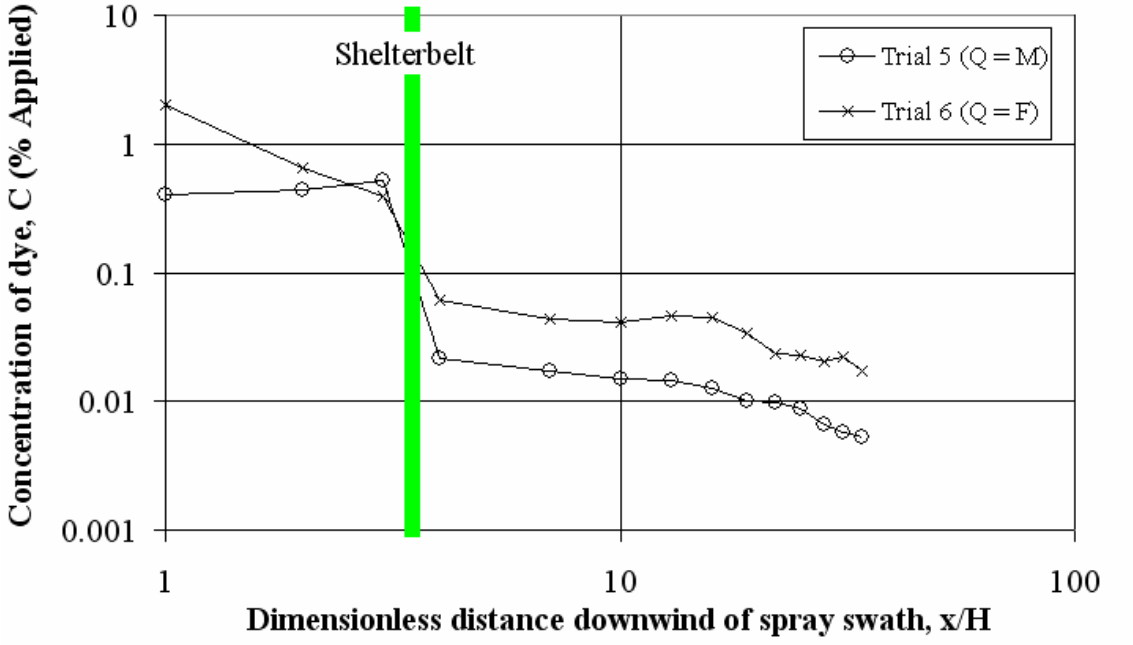

Figure 4.29 Effect of spray quality on the downwind ground deposition of drift for Trials 5 & 6

Figure 4.30 shows the downwind deposition of drift for Trials 13, 14, and 15, which had Fine, Medium, and Very Coarse spray qualities, respectively. For the three trials, a fineer spray quality led to greater mass of deposit. On the upwind side of the shelterbelt, the ground deposit of drift for the Medium and Very Coarse spray qualities was reduced by 55% and 79%, respectively, compared to the Fine spray quality. On the downwind side of the shelterbelt, the reduction in ground deposition of drift was 43% and 88% for the Medium and Very Coarse spray qualities, respectively, compared to the Fine spray quality. The rates of deposition on the up- and downwind sides of the shelterbelt were similar. Again, this indicated that the mass of deposit was dependent on the spray quality, but the movement of drift was not. This was likely because only

the driftable fraction was subjected to drift, and a coarser spray quality had a correspondingly smaller driftable fraction.

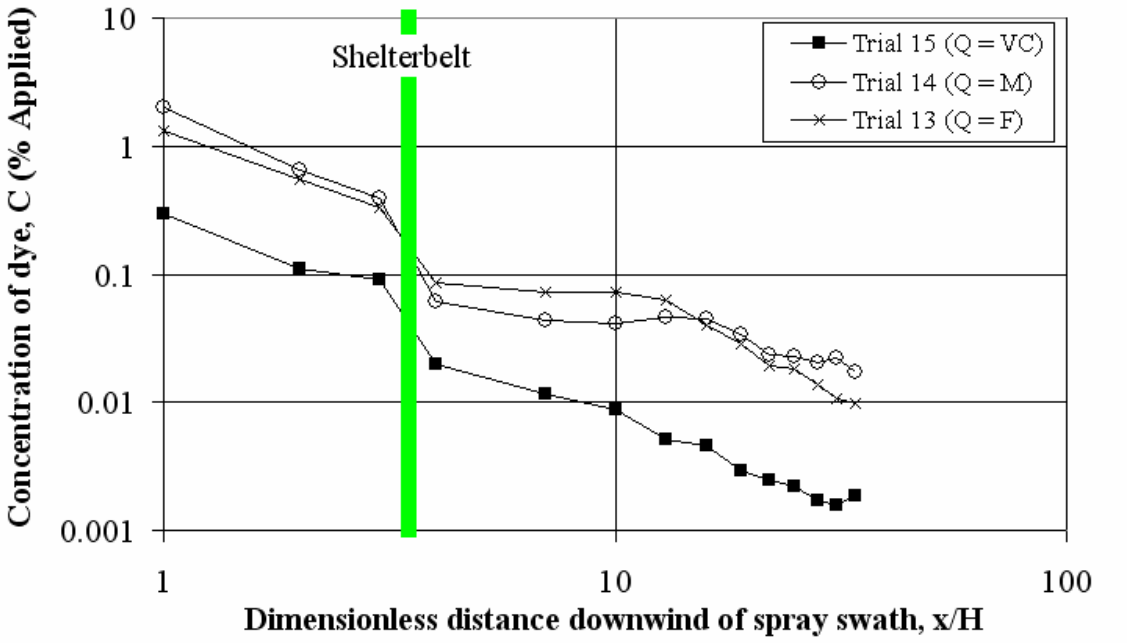

Figure 4.30 Effect of spray quality on the downwind ground deposition of drift for Trials 13, 14, & 15

The airborne concentration profiles of drift for Trials 5 & 6 and Trials 13, 14, & 15 are shown below in Figures 4.31 and 4.32, respectively. The airborne concentration profile of drift showed that the spray quality affected the mass of ground deposition but not the movement of spray drift, as was previously mentioned. The airborne concentration of drift was 30% and 18% greater on the up- and downwind sides of the shelterbelt, respectively, for the Fine spray quality compared to the Medium spray quality. The concentration of airborne drift over the top of the shelterbelt was greater for a finer spray quality, but the shape of the concentration profiles was similar for the three spray qualities, with the peak concentrations occurring at heights of approximately 0.4H upwind of the shelterbelt (Figure 4.31) and between 0.8H and 1.2 H downwind of the shelterbelt (Figure 4.32).

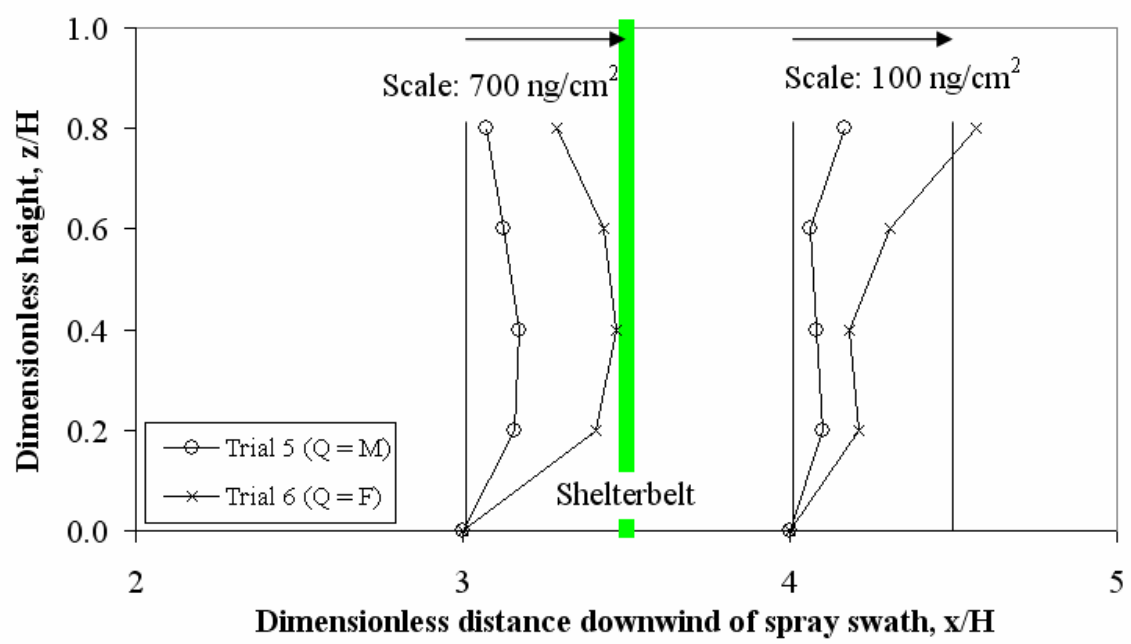

Figure 4.31 Effect of spray quality on the airborne drift concentration profiles for Trials 5 & 6

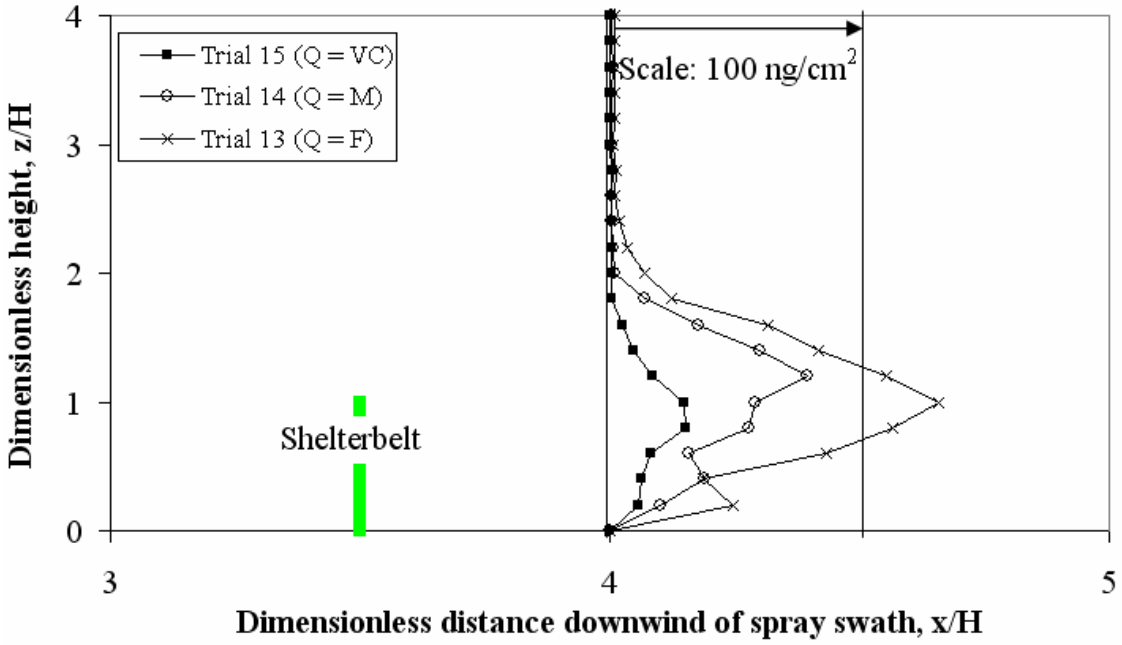

Figure 4.32 Effect of spray quality on the airborne drift over the shelterbelt for Trials 13, 14, & 15

4.7.2 Qualitative analysis of the effect of shelterbelt optical porosity

Trials 1 and 14 were the only suitable pair of trials that had a varied optical porosity with all other variables close to the same (Table 4.10). The optical porosity for Trials 1 and 14 were 0.204 and 0.483, respectively. The mass of ground deposition downwind of the shelterbelt for the less porous shelterbelt was 54% less than the deposition for the more porous shelterbelt (Figure 4.33). This reduction in ground deposition downwind was also observed by Brown et al. (2004), who found that the ground deposition was 35% less downwind of a dense snow fence ($\beta = 0.25$) compared to a more porous snow fence ($\beta = 0.50$).

Table 4.10 Conditions of trials that examine shelterbelt optical porosity

Trial #	U (km/h)	γ (°)	T (°C)	RH (%)	Ri	Q	β	α	D
1	8.8	33.0	18.5	42.2	-0.025	M	0.204	0.457	3H
14	10.3	14.4	17.7	33.5	-0.035	M	0.483	0.974	3H

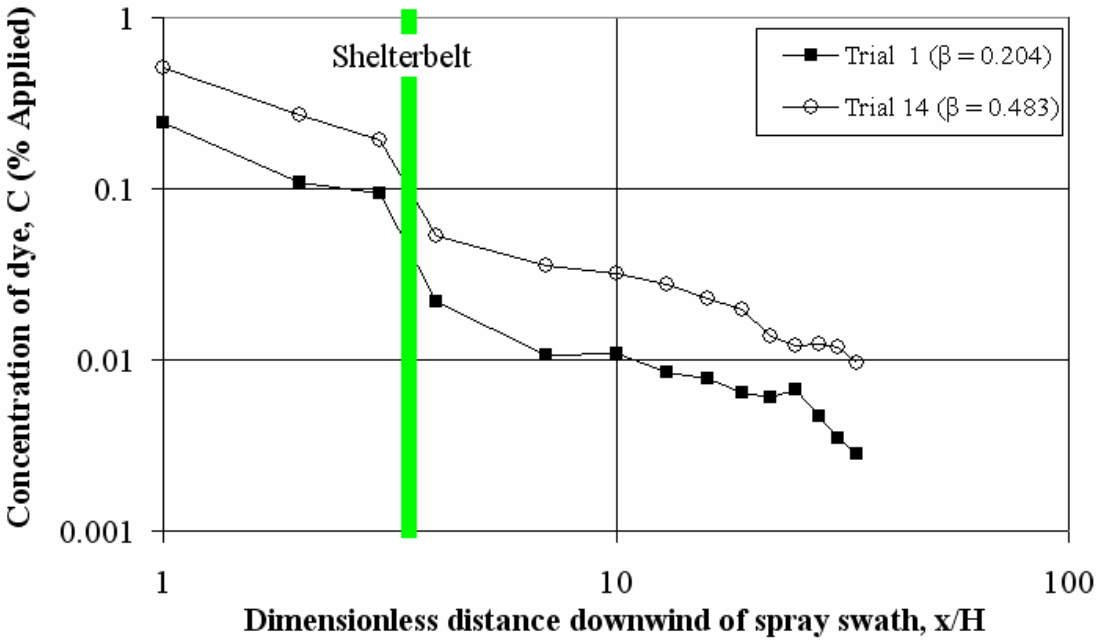

Figure 4.33 Effect of shelterbelt porosity on the downwind ground deposition of drift for Trials 1 & 14

The airborne concentration of drift on the downwind side of the shelterbelt was approximately 5 times greater for the higher shelterbelt optical porosity (Figure 4.34). Also, for a height up to 1H, the drift concentration increased with height at a greater rate

and showed less attenuation for the more porous shelterbelt. This may have been caused by two mechanisms. First, the more porous shelterbelt had more open spaces where the drift cloud could have passed through without contacting the canopy of the shelterbelt. Second, to provide the greatest porosity, the experiments were conducted when the shelterbelt was bare of leaves in the autumn. The collection efficiency of the trees to spray droplets was likely reduced in the autumn because, earlier in the season, the leaves would have had a greater efficiency to collecting droplets. The data was not available to calculate the reduction in airborne drift by the shelterbelt, but the higher degree of attenuation of the airborne concentration profile suggested that the reduction was greater for the lower porosity. In research by Richardson et al. (2004), they found the reduction in airborne drift through a windbreak decreased by 50% during the summer when the windbreak was in full leaf compared to the early spring before the windbreak was foliated.

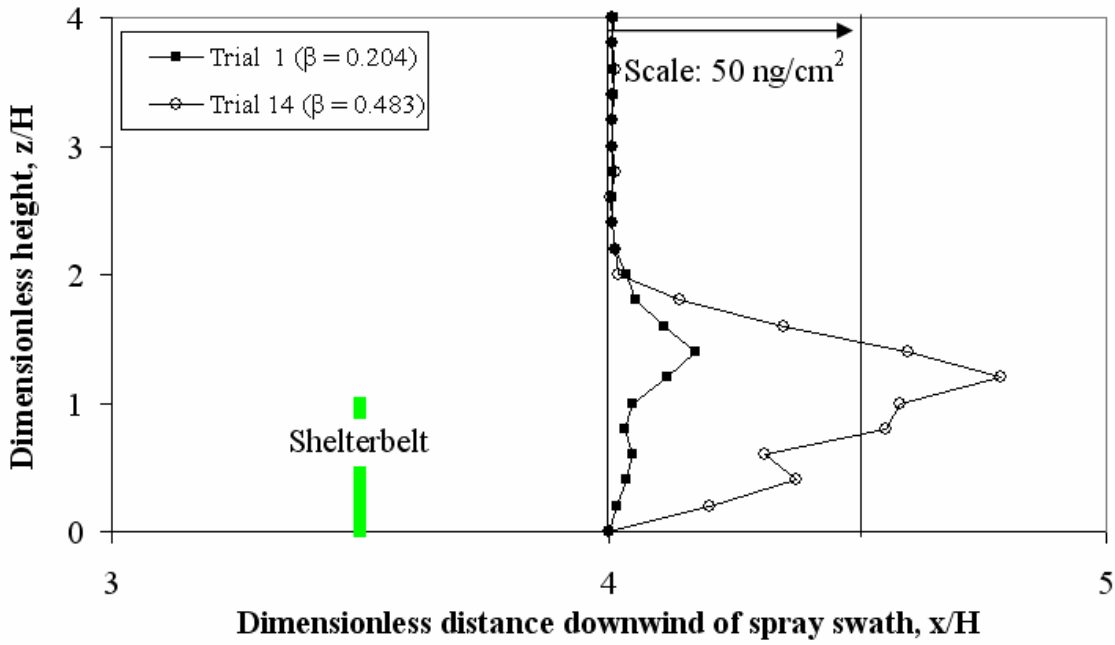

Figure 4.34 Effect of shelterbelt porosity on the airborne concentration profile of drift for Trials 1 & 14

4.7.3 Qualitative analysis of the effect of upwind sprayer distance

To examine the effect of upwind sprayer distance, two sets of trials were identified with varied upwind sprayer distance and all other conditions close to the

same. Table 4.11 gives a summary of the experimental conditions. These two sets were Trials 16, 17, & 18 and Trials 22, 23, & 24 for which the corresponding upwind sprayer distances were 1H, 3H, and 6H. These upwind sprayer distances correspond to a spray swath that was entirely within the sheltered zone, partially within the sheltered zone, and entirely outside of the sheltered zone (recall in Chapter 2 that the sheltered zone extends a distance of 5H upwind of the shelterbelt). In the following plots of ground deposition with respect to distance, the x axis was changed to a normal scale and the distance measured was relative to the shelterbelt (upwind of the shelterbelt is negative distance). In all of the previous plots, the x axis was a logarithmic scale and distance was measured relative to the spray swath. Here the x axis was changed because the shelterbelt would have been at different downwind distances for the different upwind spray distances, and subsequently, a logarithmic scale could not denote the negative upwind distances if distance was measured relative to the shelterbelt.

Table 4.11 Conditions of trials that examine upwind sprayer distance

Subset	Trial #	U (km/h)	γ (^{o})	T (^{o}C)	RH (%)	Ri	Q	β	α	D
1	16	24.1	2.2	16.6	64.9	-0.020	M	------	0.634	1H
	17	25.5	7.1	16.4	73.4	-0.020	M	------	0.528	3H
	18	27.6	5.2	17.9	55.7	-0.025	M	------	0.612	6H
2	22	11.5	12.6	20.0	53.5	-0.107	M	0.292	0.628	1H
	23	11.3	3.5	20.9	50.2	-0.087	M	0.292	0.614	3H
	24	12.6	11.2	22.1	45.6	-0.089	M	0.292	0.605	6H

On the downwind side of the shelterbelt to a distance of 30H, the corresponding integrated ground deposit for the 3H and 6H distances were 50% and 33% greater compared to the 1H distance (Figures 4.35 and 4.36). This was likely because more drift would have been diverted over the top of the shelterbelt and not subjected to the filtering action of the shelterbelt.

The airborne concentration profiles were similar over the height of the shelterbelt for Trials 23 and 24 (3H and 6H upwind sprayer distance, respectively) on the up- and downwind sides of the shelterbelt (Figure 4.37). On the upwind side of the

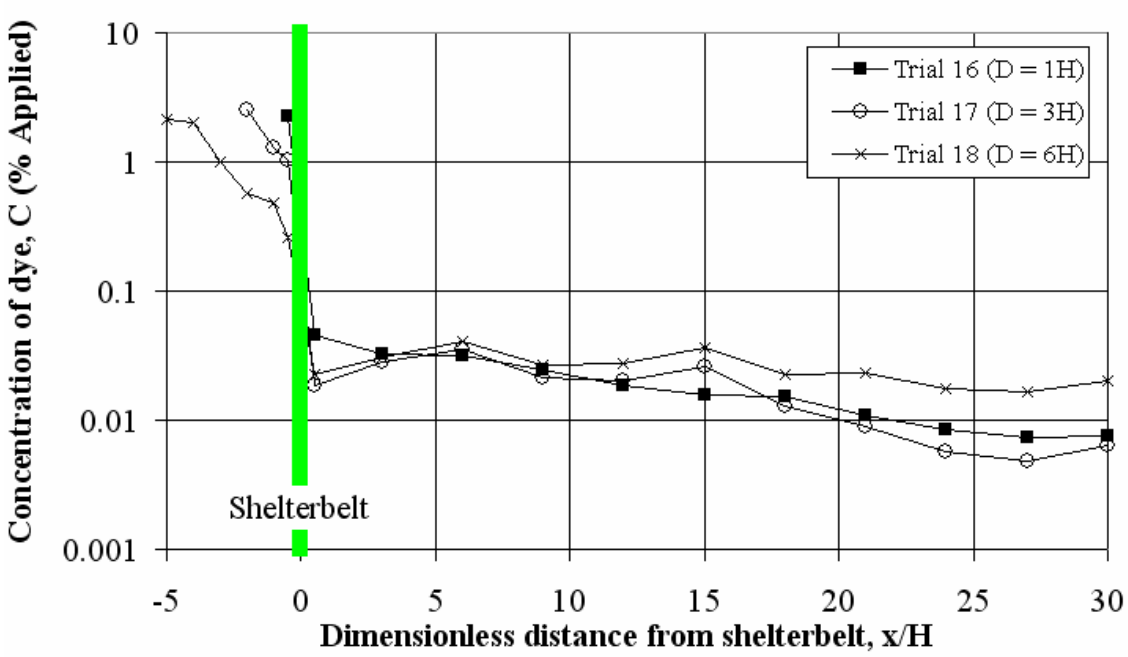

Figure 4.35 Effect of sprayer distance on the downwind ground deposition of drift for Trials 16, 17, & 18

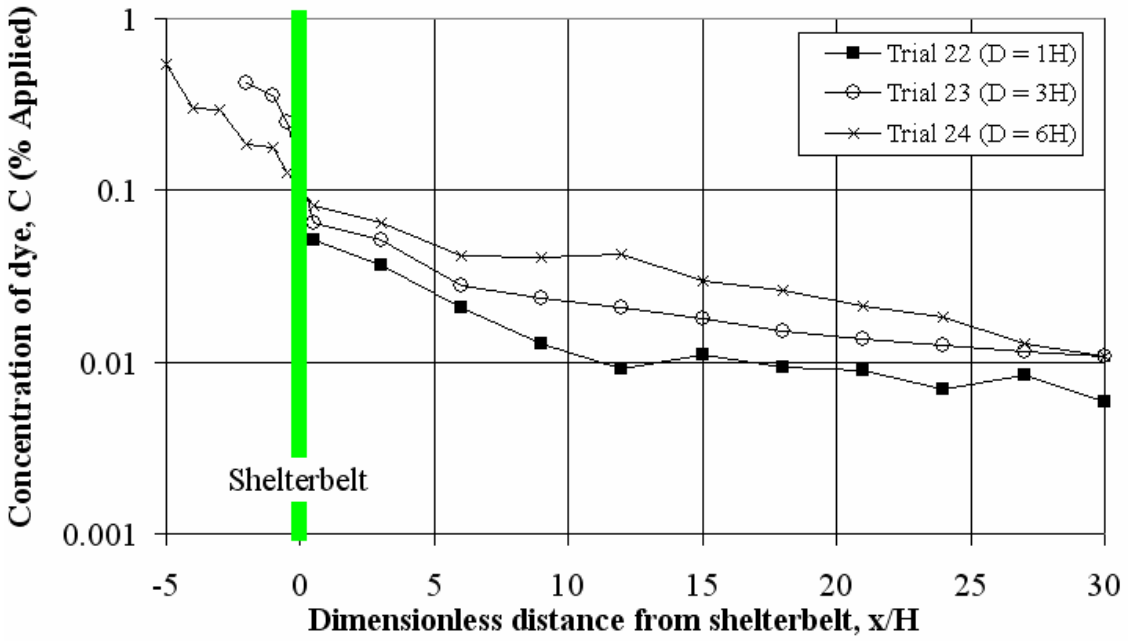

Figure 4.36 Effect of sprayer distance on the downwind ground deposition of drift for Trials 22, 23, & 24

shelterbelt, the airborne concentration of drift for Trial 22 (1H upwind sprayer distance) was approximately 7 times greater than for the 3H and 6H distances. This may have been because the drift cloud was not subjected to flow over the top and was channeled through the shelterbelt for the 1H distance. On the downwind side of the shelterbelt, the airborne concentration profile was relatively constant over the height of the shelterbelt for the 3H and 6H distances and was more pronounced for the 1H distance. For the 1H distance on the downwind side of the shelterbelt, there was a decrease in concentration at a height of 0.6H followed by an increase at 0.8H. This increase at 0.8H could be evidence of the proportion of drift cloud diverted over the top of the shelterbelt.

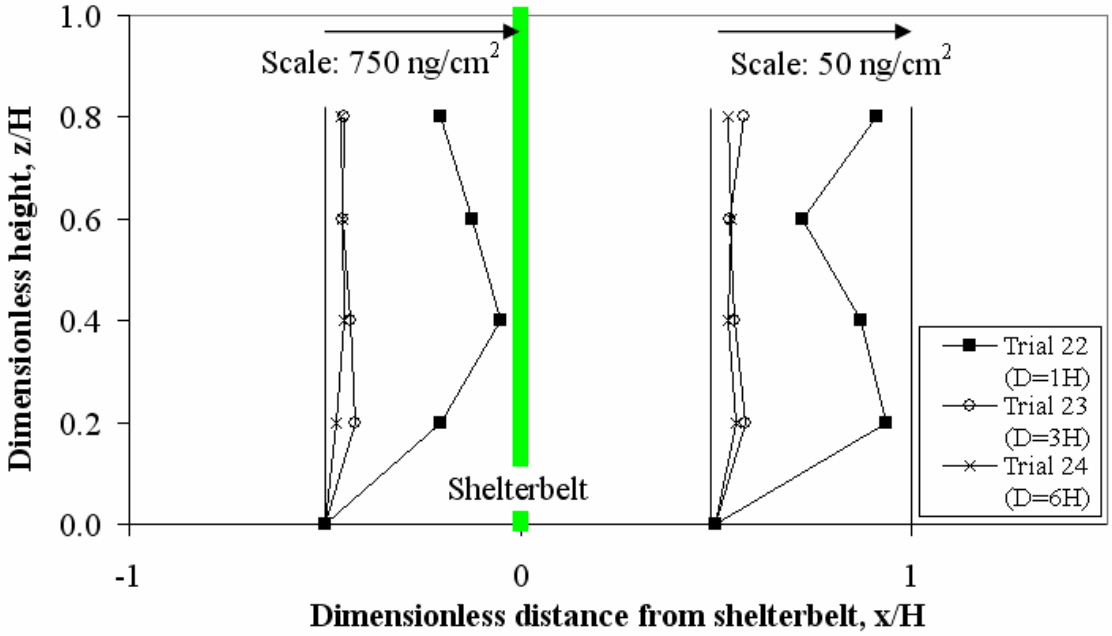

Figure 4.37 Effect of sprayer distance on the airborne concentration profile of drift for Trials 22, 23, & 24

Figure 4.38 shows that on the up- and downwind sides of the shelterbelt, there was decreasing airborne concentrations of drift for an increasing upwind sprayer distance. For the 6H upwind sprayer distance, the drift cloud had a longer distance to settle out or disperse by the time it reached the shelterbelt so there was less airborne drift. On the downwind side of the shelterbelt, there was an obvious peak concentration at a height of 1.2H and 1.4H for the 1H and 3H distances, respectively. For the 6H distance, the concentration of drift was relatively constant to a height of approximately

1.4H. This may have been because the drift cloud had more fully dispersed over a height of 2H for the 6H upwind sprayer distance. For the 1H and 3H distances, there appeared to be two distinct regions of the concentration profile with two local maxima occurring at approximately 0.4H – 1H and 1.2H – 1.4H. These two regions may represent the portion of the drift cloud that passed through the canopy of the shelterbelt and the portion that was diverted over the top of the shelterbelt. For both the 1H and 3H distances, the airborne concentration over the top of the shelterbelt was greater than the drift exiting the shelterbelt.

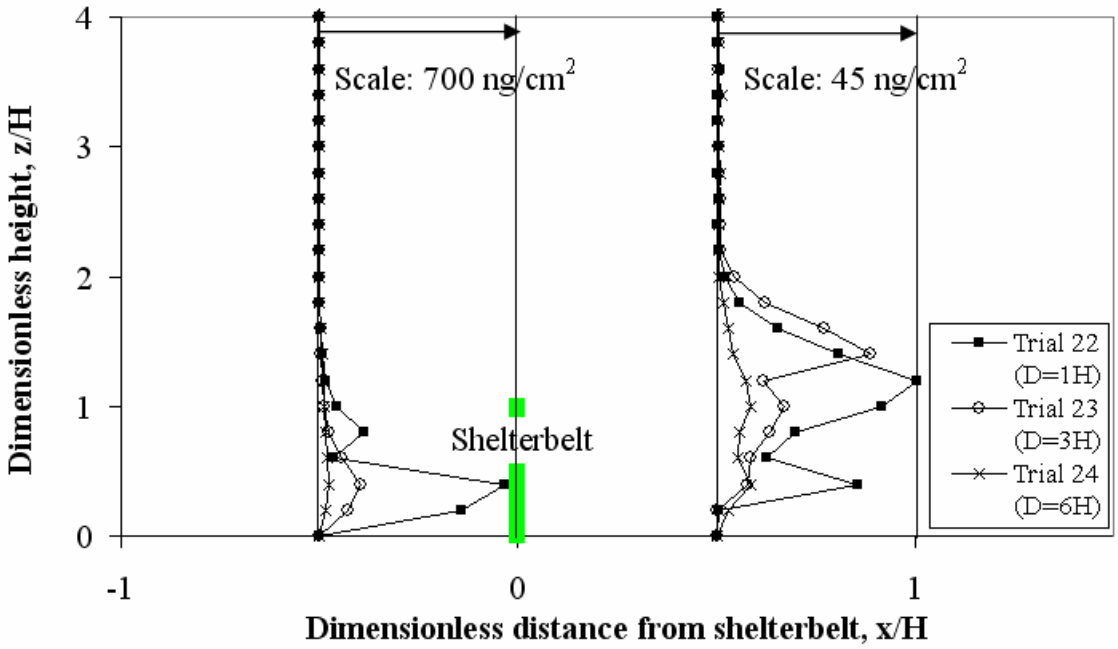

Figure 4.38 Effect of sprayer distance on the airborne drift over the top of the shelterbelt for Trials 22, 23, & 24

The shelterbelt had a noticeable effect on the movement of spray drift between the 1H and 6H upwind release distances, but for different reasons. For the 1H distance, the drift cloud was likely channeled through the shelterbelt, so there was a greater concentration of airborne drift entering and exiting the shelterbelt. For the 6H distance, the drift cloud had a longer distance to deposit to ground and disperse vertically before reaching the shelterbelt, and it was fully subjected to the diverted flow over the top of the shelterbelt. This led to an increased deposit of drift to the ground downwind of the shelterbelt (Figure 4.36).

4.7.4 Quantitative analysis of the controlled variables

The quantitative analysis of the controlled variables used the same methodology outlined in Section 4.6.4. Multiple linear regression analysis was used to identify the significance of the controlled variables in a regression model that predicted the integrated ground deposit of drift downwind of the shelterbelt. For each controlled variable under consideration, a subset of trials was chosen in which the other controlled variables were kept constant. Thus, three regression models were used, one each for spray quality, shelterbelt optical porosity, and upwind sprayer distance. This was done in order to reduce the number of variables in the regression model. It is recommended that, when using a relatively small dataset (relative to the number of independent variables), the regression analysis is more efficient using fewer independent variables (Statistica User Manual, 2001). The meteorological conditions and the controlled variable in question were entered into the analysis as independent variables, and the ground deposit of drift downwind of the shelterbelt, to a distance of 30H downwind of the shelterbelt, was the dependent variable.

The input data for the spray quality analysis was from Trials 1 to 9. These trials had a constant shelterbelt optical porosity and upwind sprayer distance. To account for the varying droplet size, the driftable fraction value was assigned to the Fine, Medium, and Coarse qualities (see Table 3.2); the corresponding driftable fraction for the three spray qualities was 56%, 26%, and 7.2%, respectively.

The results of the multiple linear regression analysis that examined the effect of spray quality are shown in Table 4.12. The adjusted r^2 value of the regression model was 0.87. The only variable of significance (p value < 0.05) identified by regression analysis was spray quality (p value = 0.022). This result was further evidence that spray quality had a significant effect on the mass of drift deposition, as was concluded in the preceding qualitative analysis. The positive sign of the calibration coefficient (0.506) indicated that the deposit downwind of the shelterbelt increased with a finer spray quality.

The input data for the optical porosity analysis was the subset of trials with a Medium spray quality and a 3H upwind release distance. The aerodynamic and optical

Table 4.12 Regression analysis of the effect of spray quality

x_i	a_i	p value
Intercept	-1.214	0.079
U	0.041	0.085
γ	0.005	0.082
T	0.033	0.088
RH	-0.002	0.615
Ri	-1.865	0.167
Q	0.506	0.022
α	0.069	0.720

porosity of the shelterbelt are dependent on each other (Guan et al., 2003), therefore the aerodynamic porosity was not included in the model. Including both variables could have introduced collinearity into the regression analysis. The results of the regression analysis are shown below (Table 4.13), and the adjusted r^2 value was 0.988. The regression analysis identified shelterbelt optical porosity as a significant variable, as well as wind speed, temperature, and relative humidity. The previous regression model that examined spray quality did not identify these meteorological variables as significant, which was likely because the model was developed from a different subset of data. These meteorological variables were identified as significant variables in Section 4.6 in both the qualitative and quantitative analysis. The conclusion that shelterbelt optical porosity had a significant effect on the deposition of drift downwind of the shelterbelt supported the observations in the preceding qualitative analysis. The model predicted that deposition downwind of the shelterbelt would increase with a higher porosity, as implied by the sign of the calibration coefficient (0.506).

Table 4.13 Regression analysis of the effect of shelterbelt optical porosity

x_i	a_i	p value
Intercept	-0.632	0.003
U	0.028	0.004
γ	0.003	0.076
T	0.021	0.017
RH	-0.004	0.012
Ri	-1.771	0.095
β	0.506	0.020

The regression analysis for the upwind sprayer distance included Trials 19 to 27, which had the same spray quality and shelterbelt optical porosity. The adjusted r^2 value of the analysis was 0.80. Table 4.14 shows the results of the regression analysis. The analysis did not identify any variables of significance where the p value was less than 0.05. This indicated that the upwind sprayer distance did not have a significant effect on the ground deposition of drift downwind of the shelterbelt, which is contrary to the observations in the preceding qualitative analysis.

Table 4.14 Regression analysis of the effect of upwind sprayer distance

x_i	a_i	p value
Intercept	0.159	0.846
U	-0.670	0.179
γ	0.005	0.490
T	0.064	0.216
RH	-0.003	0.206
Ri	1.820	0.497
α	-0.315	0.708
D	0.002	0.911

As a final quantitative assessment, the regression analysis was performed on all of the experimental variables using the mass of drift captured within the shelterbelt (SB) as the dependent variable. This data were not available for a number of trials because the rotorod data were missing. In the previous regression analyses that examined a specific variable, there were not enough trials with rotorod data to adequately perform the regression analysis using the mass of drift deposited within the shelterbelt (SB) as the dependent variable. However, in this analysis, a subset of nineteen trials was identified that had complete rotorod data and all of the meteorological and controlled variables were introduced as independent variables in the regression model. The results of the regression analysis are shown in Table 4.15.

The adjusted r^2 value was 0.80. The regression analysis identified wind speed and upwind sprayer distance as significant variables, which had p values of 0.009 and 0.00008, respectively. This is in agreement with the previous qualitative and quantitative analyses which identified wind speed as having a significant effect on the

Table 4.15 Regression analysis of mass of drift captured in the shelterbelt (SB)

x_i	a_i	p value
Intercept	-1.665	0.189
U	0.167	0.009
γ	0.016	0.458
T	0.068	0.167
RH	-0.009	0.391
Ri	-11.019	0.302
Q	2.096	0.126
β	0.0002	0.984
D	-0.579	0.00008

capture of spray drift in the shelterbelt. Although the regression analysis showed the upwind sprayer distance did not have a significant effect on the ground deposition of drift downwind of the shelterbelt, this analysis as well as the preceding qualitative assessment recognized that the upwind sprayer distance did significantly affect the capture of drift within the shelterbelt. The corresponding positive and negative calibration coefficients for wind speed and upwind sprayer distance (0.167 and -0.579, respectively) indicated that a higher wind speed or shorter upwind sprayer distance would increase the mass of drift captured within the shelterbelt.

4.8 Analysis of errors

This section provides estimates of the errors in the measured and calculated quantities presented in the preceding analyses. The error analysis was performed following Topping (1972).

The distances in the field were measured using a tape measure with a resolution of 0.01 m; however, because it was difficult to measure the distance exactly perpendicular to the shelterbelt, a reasonable estimate of the accuracy of the furthest distances (150 m) would likely be 1 m or 0.7%. The height of the instruments was measured using a tape measure with a resolution of 0.01 m; however, due to the unevenness of the ground, a likely error in this measurement would be 0.1 m. This would give a percent error of 2.5% for the 4 m height. The height of the shelterbelt was determined by scaling it against a 4 m tall pole; also, the height of the shelterbelt was

variable along its length. A reasonable estimate of the accuracy in the shelterbelt height is approximately 20%.

The wind speed was measured using a Campbell Scientific 014A cup anemometer and a R.M. Young 81000 ultrasonic anemometer, with a manufacturer-specified accuracy of 1.5% (up to 160 km/h) and 1% (up to 108 km/h), respectively. The error in the calculation of aerodynamic porosity was 3%, based on the error in the cup anemometer specifications. The wind direction, measured with the ultrasonic anemometer, was within 2^o for a wind speed up to 108 km/h. Based on the error in the three perpendicular components of the wind velocity, it follows that the percent error in the wind direction measurement was 4.5%.

The temperature and relative humidity was measured with a Campbell Scientific HMP45C212 temperature and humidity probe, with an error of 0.09^oC (up to 50^oC) and 2% RH (up to 90% RH), respectively. The minimum temperature and relative humidity experienced in the experiments were approximately 13^oC and 25%, respectively, so the maximum error corresponded to 0.7% and 8%. Using the error in the measurement of wind speed and temperature, the error in the calculation of the Richardson number was estimated to be 5.8%.

The optical porosity of the shelterbelt was determined using the method developed by Kenney (1987), who estimated the accuracy at 2%. Because of the difficulty in defining the top edge of the shelterbelt canopy, the error in calculating optical porosity was estimated at approximately 10%.

The drift deposit data was first converted from fluorescent intensity to parts per billion using a Shimadzu RF-1501 spectrofluorophotometer and standard curves. The curves were developed from standard solutions decanted from the spray tank. The volume in the spray tank was measured using a Sotera Flow Meter with a manufacturer-specified accuracy of 0.8%. The volume of dye added to the tank was measured using a 1 L graduated cylinder with a resolution of 10 mL. A total volume of 1600 mL of dye was added to the tank (requiring two fills of the cylinder), so the error in the volume measurement was 1.3%. Using these errors, it follows that the error in preparing the standard solutions was 2.1%. The standard curve developed by the spectrofluoro-

photometer had an r^2 value of at least 0.9990, so the error in converting fluorescent intensity to concentration in parts per billion was estimated as 0.1%.

The area of each sampler was assumed to be constant. The wash volume for the Petri-plates, rotorods, and string was measured to within 1 mL, 0.2 mL, and 0.1 mL, respectively. Thus, the relative error in the wash volume corresponded to 2%, 2.9%, and 3.1%. It follows that the error in converting the drift data for the three types of collectors to units of ng/cm^2 was estimated at 4.2%, 5.0%, and 3.2%, respectively.

When calibrating the spray boom, if any particular nozzle was not within 5% of the nominal flow rate, the nozzle was replaced. Thus, it is assumed that the flow rate of the sprayer was within 5%. The boom width (14.5 m) was measured to within 0.1 m or 0.7%. The travel speed of the sprayer was calculated as the time that elapsed for the sprayer to traverse the sprayer path three times. The shortest sprayer path was 150 m, measured to within 1 m, so had an estimated error of 0.7%. The shortest time of spraying was 132 s, measured to 1 s, and had an estimated error of 0.8%. The error in calculating the travel speed was estimated as 1.4%. Using these errors, the error in calculating the mass of applied spray may be estimated as 9.2%. In converting the drift data to a dimensionless form (% of Applied), the error in the deposit data for the Petri-plates, rotorods, and string can be estimated as 13.3%, 14.1%, and 12.3%, respectively.

4.9 Summary

This chapter presented the results from field experiments that investigated the movement of spray drift past a shelterbelt. There was evidence that the drift cloud was split into two components as it approached the shelterbelt: the portion that passed through the shelterbelt and the portion that flowed over the top of the shelterbelt. The drift cloud that passed through the shelterbelt was filtered by the shelterbelt's canopy and the airborne drift was reduced. This was shown by a sharp decrease in drift deposit to the ground immediately downwind of the shelterbelt and by a decrease in airborne drift immediately downwind of the shelterbelt. There was evidence that a greater proportion of drift flowed over the top of the shelterbelt than passed through with the bleed flow. This portion of the drift cloud returned to ground level at approximately 15 to 30 m (3H to 6H) downwind of the shelterbelt, which was shown as an increase in

ground deposit. Further than 6H downwind of the shelterbelt, the wind likely began to return to its upwind profile, and the drift deposit decreased at a relatively constant rate.

When compared to the open field setting, the shelterbelt had a noticeable effect on the movement of spray drift in the immediate vicinity of the shelterbelt. In the shelterbelt setting, the deposit upwind of the shelterbelt was similar to the open field. Downwind of the shelterbelt up to a distance of 10H, deposit was less than in the open field. The airborne concentration profile of the drift cloud on the immediate upwind side of the shelterbelt was similar in shape to the open field. On the immediate downwind side of the shelterbelt, the profile was relatively constant up to a height of 4 m. A greater proportion of drift was carried over the top of the shelterbelt and the peak concentration shifted up by a height of approximately 1H, compared to the open field setting.

Mass balance analysis showed the relative magnitude of deposition of drift in various locations around the shelterbelt. For the trials that examined spray quality, it was found that the finer spray quality had greater ground deposition within the shelterbelt and downwind of the shelterbelt, while the coarser spray quality had greater deposit to ground on the upwind side of the shelterbelt. For the trials that examined the upwind distance of the sprayer, there was increased deposition within the shelterbelt and decreased ground deposit downwind of the shelterbelt for the 1H upwind sprayer distance. This indicated that the drift cloud was channeled through the shelterbelt and was scrubbed by the shelterbelt's canopy.

In the repeatability analysis, the mean and standard deviation of the data points for the comparative trials were plotted and the variability was visually assessed. It was determined that the Petri-plate data was within ± 1 standard deviation between the replicate trials for most of the measurement distances, except for distances further than approximately 28H downwind of the spray swath. The rotorod data was all within ± 1 standard deviation of its replicate trial. There was only one string collector for each trial, so the variability was qualitatively examined. For the three types of collectors, there was a noticeable variance within the data, but the shape of the profiles was preserved between the replicate trials. Thus, the mass and concentration data may have differed based on random variability, but the relative shape of the data plots was similar.

Thus, it was deemed important to observe not just the mass of drift but also the shape of the plots between comparative trials.

The initial qualitative analysis could not draw any conclusions on the effect of wind direction on the movement of spray drift. It was determined that the mass of ground deposition and airborne drift increased with a greater wind speed. Temperature and relative humidity were examined together because both affected the rate of evaporation of the drift droplets. It was found that, for an increased temperature and/or decreased relative humidity, the rate of deposition decreased past a distance of 18H downwind of the shelterbelt, likely due to a more rapidly reducing droplet size that was less prone to ground deposition further than this distance.

Quantitative assessment was performed using multiple linear regression analysis to determine the significance of a specific variable on the movement and deposition of spray drift. The results from the regression model are only applicable to the range of conditions sampled. It was found that an increasing wind speed, increasing temperature, and/or decreasing relative humidity increased the ground deposition of drift downwind of the shelterbelt. It was also determined that an increased wind speed increased the drift deposited within the shelterbelt. Wind direction and atmospheric stability were found to be insignificant variables.

The final section examined the effect of spray quality, shelterbelt optical porosity, and upwind sprayer distance on the movement of spray drift past a shelterbelt. A qualitative analysis of the ground deposition and airborne movement of drift was completed first, followed by a quantitative assessment using multiple linear regression analysis.

Both the qualitative and quantitative analysis found that a finer spray quality increased the mass of airborne drift as well as the ground deposition downwind of the shelterbelt. The qualitative analysis indicated the movement of drift was not affected by spray quality, as the deposition and concentration profiles were of similar shape for the three spray qualities.

Shelterbelt optical porosity had a noticeable effect on the deposition of drift, and that an increased porosity led to increased ground deposition and airborne concentration of drift exiting the shelterbelt. This may be caused by increased bleed flow through the

shelterbelt due to its higher porosity or a decreased collection efficiency of the shelterbelt when it was bare of leaves.

The upwind sprayer distance did not have a significant effect on the ground deposition of spray drift downwind of the shelterbelt, which was indicated both by the qualitative and quantitative analyses. However, the qualitative analysis did show that the upwind sprayer distance did have a noticeable effect on the airborne movement of drift, both through the shelterbelt and over the top of the shelterbelt. This was also confirmed in the mass balance and regression analyses. When the spray was released entirely within the upwind sheltered zone, there was more drift entering and exiting the shelterbelt, as well as greater drift captured within the shelterbelt. When the spray was released entirely upwind of the sheltered zone, more of the drift cloud was diverted over the top of the shelterbelt and less traveled through the shelterbelt.

Chapter 5

CONCLUSIONS & RECOMMENDATIONS

5.1 Conclusions

The objective of this research was to investigate the movement of spray drift past a shelterbelt and to determine the effect of meteorological conditions, operator settings, and shelterbelt properties on the interaction of spray drift and a shelterbelt. Specifically, the effects of wind speed, wind direction, temperature, relative humidity, atmospheric stability, spray quality, shelterbelt optical porosity, and upwind sprayer distance on the ground deposition and airborne movement of drift past a live shelterbelt were investigated. There is limited knowledge of the behaviour of spray drift and a live shelterbelt as well as the significance of the above-mentioned variables on the drift movement near a shelterbelt.

The general movement of drift past a shelterbelt was characterized using the ground deposit and airborne concentration data; first in only the shelterbelt setting and then compared to an open field setting. The major findings of this research were:

- The drift cloud was split into two components as it approached the shelterbelt: (1) the component that passed through the shelterbelt with the bleed flow, and; (2) the component that was diverted over the top of the shelterbelt with the displaced flow. Some experiments showed that the airborne drift diverted over the top of the shelterbelt led to increased ground deposition further downwind where the displaced flow returned to ground level.
- There was less ground deposition of drift downwind of the shelterbelt compared to the open field setting. At approximately 10H downwind of the shelterbelt, the ground deposit was again similar to the open field. The airborne concentration

profile of drift upwind of the shelterbelt was similar to the open field; downwind of the shelterbelt, the peak concentration was shifted up by a height of approximately 1H.

The variables under consideration were classified as meteorological and controlled variables. The meteorological variables included wind speed, wind direction, temperature, relative humidity, and atmospheric stability. The controlled variables were spray quality, shelterbelt optical porosity, and upwind sprayer distance. The effect of the variables on the ground deposition and airborne movement of spray drift were investigated qualitatively and quantitatively. The quantitative assessment was performed using mass balance and multiple linear regression analyses. The important conclusions were as follows:

- Wind speed had a significant effect on the ground deposition of drift downwind of the shelterbelt and the mass of drift captured within the shelterbelt. The ground deposition and airborne concentration of drift increased with increasing wind speed.
- The effect of wind direction could not be determined from the qualitative analysis. It was found that wind direction had an insignificant effect on the mass of drift captured within the shelterbelt and deposited downwind of the shelterbelt for the range of conditions observed.
- Temperature and relative humidity had a noticeable effect on the airborne movement of drift. Higher temperature and/or lower RH increased the airborne concentration of drift and were found to be significant variables affecting the ground deposition of drift downwind of the shelterbelt.
- For the range of atmospheric stability sampled, it was determined to have an insignificant effect on the drift deposited within the shelterbelt as well as the ground deposition of drift downwind of the shelterbelt.
- A finer spray increased drift deposition within the shelterbelt and to the ground downwind of the shelterbelt, while a coarser spray had greater ground deposition upwind of the shelterbelt. While a finer spray produced greater amounts of airborne drift and ground deposit, as expected, the movement of the drift cloud appeared similar for the three spray qualities.

- A more porous shelterbelt increased the airborne concentration of drift exiting the shelterbelt and increased ground deposition of drift up- and downwind of the shelterbelt. It was determined that shelterbelt optical porosity had a significant effect on the mass of drift deposited downwind of the shelterbelt.
- The upwind sprayer distance had a noticeable effect on the movement of spray drift. When the spray was released entirely within the upwind sheltered zone of the shelterbelt, it was found that more drift passed through the shelterbelt which led to greater capture within the shelterbelt. When the spray was released entirely upwind of the sheltered zone of the shelterbelt, more drift was deflected over the top of the shelterbelt. Greater upwind sprayer distance significantly reduced the mass of drift captured within the shelterbelt, but did not significantly affect the mass of drift deposited to ground downwind of the shelterbelt.

There has been recent interest in the use of shelterbelts to protect vulnerable downwind areas from spray drift. This research has determined that there was some degree of protection afforded by the shelterbelt to a distance of approximately 10H downwind of the shelterbelt, where the deposition was less than in the open field. Further downwind, there is potential for increased deposition compared to the open field. This may actually cause greater damage to vulnerable downwind areas. Also, there may be a large amount of drift deposited within the shelterbelt, which could harm the shelterbelt itself or the associated ecosystem within the shelterbelt margin.

5.2 Recommendations for Future Work

The field experiments undertaken in this research were complex due to the confounding effects of the meteorological conditions while attempting to investigate the controlled variables. As a result, although an adequate number of replicate trials were done for any one variable, differing meteorological conditions introduced significant variability into the analysis. The variability inherent in field experiments may be addressed by exploring the use of wind-tunnel or numerical modelling, although a sufficient number of field experiments are still needed for calibrating these models.

There has been much research in both the areas of spray drift and the flow around a shelterbelt, but relatively few studies examining the interaction of both. Future

research should focus first on describing the general movement of spray drift past a shelterbelt by conducting replicate trials around a shelterbelt with fixed variables and similar meteorological conditions. Next, the effect of the meteorological conditions should be investigated in depth. In future research, this analysis should be expanded to include atmospheric turbulence, both mechanical and thermal, as both affect the movement of spray drift and the flow around a shelterbelt. Mechanical turbulence may be examined by varying the height of the upwind ground cover, which would change the aerodynamic roughness height. Thermal turbulence could be examined by conducting field experiments at times of the day where there is a wide variation in the degree of atmospheric stability, such as early morning and late afternoon.

Although the use of finer sprays resulted in more drift, as expected, the resulting drift cloud behaved in a similar manner to drift clouds originating from coarse sprays. As a result, there is limited need for further research studying the interacting effects of spray quality and shelterbelts. More research should be done investigating shelterbelt optical porosity, which could be expanded to include different shelterbelt species. The effect of optical porosity on the movement of drift was apparent, but the effect could not be attributed to a difference in the flow resistance of the shelterbelt or different collection characteristics of the shelterbelt's canopy. This may be further investigated by sampling shelterbelts composed of trees with much different collection efficiencies, such as coniferous and broad-leafed trees.

This research used the tracer dye technique to measure spray drift, and the tracer dye used was susceptible to photolysis. The loss of dye due to photolysis was approximately 30%, which had the potential to introduce significant error into the drift data. Further research should use more stable tracer dyes or other methods of drift measurement, such as laser-based techniques or herbicide/insecticide bioassays.

This research also concluded that a large mass of drift may be deposited within the shelterbelt. It is recognized that shelterbelts provide opportunity for biodiversity, but it should be determined whether the drift collected in the shelterbelt would prove harmful or even fatal to the shelterbelt itself, or the flora and fauna within the shelterbelt margin.

REFERENCES

Adrizal, A., Patterson, P.H., Hulet, R.M., Bates, R.M., Myers, C.A.B., Marting, G.P., Shocky, R.L., van der Grinten, M., Anderson, D.A., and Thompson, J.R. 2008. Vegetative buffers for fan emissions from poultry farms: 2. ammonia, dust, and foliar nitrogen. *Journal of Environmental Science and Health, Part B*, 43:1: 96-103.

ASAE S561.1 APR2004. 2005a. Procedure for measuring drift deposits from ground, orchard, and aerial sprayers. *ASAE Standards 2005*. pp. 432-434.

ASAE S572 FEB04. 2005b. Spray nozzle classification by droplet spectra. *ASAE Standards 2005*. pp. 435-437.

Bache, D.H. and Johnstone, D.R. 1992. *Microclimate and Spray Dispersion*. Ellis Horwood Ltd., Chichester, England. 239 pp.

Bean, A., Alperi, R.W., and Federer, C.A. 1975. A method for categorizing shelterbelt porosity. *Agricultural Meteorology*, 14: 471-429.

Bouvet, T., Wilson, J.D., and Tuzet, A. 2006. Observations and modeling of heavy particle deposition in a windbreak flow. *Journal of Applied Meteorology and Climatology*, 45: 1332-1349.

Brown, R.B., Carter, M.H., and Stephenson, G.R. 2004. Buffer zone and windbreak effects on spray drift deposition in a simulated wetland. *Pesticide Management Science*, 60: 1085-1090.

Caborn, J.M. 1965. *Shelterbelts and Windbreaks*. Faber & Faber, Ltd., London, England. 288 pp.

Caldwell, B.C. 2005. Unpublished data set. Agriculture and Agri-Food Canada. Saskatoon, Saskatchewan.

Caldwell, B.C. and Wolf, T.M. 2006. Measurement of long-distance particle drift using a fluorescent tracer – samplers, sensitivity, detection limits, and background. *Aspects of Applied Biology*, 77: 371-378.

Carlsen, S.C.K., Spliid, N.H., and Svensmark, B. 2006. Drift of 10 herbicides after tractor spray application. 2. Primary drift (droplet drift). *Chemosphere*, 64: 778-786.

Cleugh, H.A. 1998. Effects of windbreaks on airflow, microclimates, and crop yields. *Agroforestry Systems*, 41: 55-84.

Cleugh, H.A. 2002. Field measurements of windbreak effects on airflow, turbulent exchanges and microclimates. *Australian Journal of Experimental Agriculture*, 42: 665-677.

Cote, D.A., Bugg, J.D., and Wolf, T.M. 2006. Wind tunnel modeling of flow near a windbreak with vertically varying optical porosity. *Aspects of Applied Biology*, 77: 349-358.

Crowe, C.T., Sommerfeld, M., and Tsuji, Y. 1998. *Multiphase flows with droplets and particles*. CRC Press, Boca Raton, FL. 471 pp.

CSIRO 2002. S*pray Drift Management: Principles, Strategies, and Supporting Information.* CSIRO Publishing, Collingwood, Australia. 71 pp.

Davis, B.N.K., Brown, M.J., Frost, A.J., Yates, T.J., and Plant, R.A. 1994. The effects of hedges on spray deposition and on the biological impact of pesticide spray drift. *Ecotoxicology and Environmental Safety*, 27: 281-293.

Fritz, B.K. 2004. Role of Atmospheric Stability in Drift and Deposition of Aerially Applied Sprays – Preliminary Results. *Paper Number 041031*. 2004 ASAE/CSAE Annual International Meeting. Ottawa, ON.

Grover, R., Maybank, J., Caldwell, B.C., and Wolf, T.M. 1997. Airborne off-target losses and deposition characteristics from a self-propelled, high speed and high clearance ground sprayer. *Canadian Journal of Plant Science*, 77: 493-500.

Guan, D., Zhang, Y., and Zhu, T. 2003. A wind-tunnel study of windbreak drag. *Agricultural and Forest Meteorology*, 118: 75-84.

Heisler, G.M. and Dewalle, D.R. 1988. Effects of windbreak structure on wind flow. *Agriculture, Ecosystems, and Environment*, 22/23: 41-69.

Hewitt, A.J. 2001. Drift filtration by natural and artificial collectors: A literature review. *Spray Drift Task Force Publications*. [Online] Available: http://www.agdrift.com [22 November 2006].

Hoffman, W.C., Hewitt, A.J., Barber, J.A.S., Kirk, I.W., and Brown, J.R. 2003. *Field swath and drift analyses techniques*. Proc. 2003 ASAE/NAAA Technical Session. Reno, NV: AA03-007.

Holterman, H.J., van de Zande, J.C., Porskamp, H.A.J., and Huijsmans, J.F.M. 1997. Modelling spray drift from boom sprayers. *Computers and Electronics in Agriculture*, 19: 1-22.

ISO 22866:2005. 2005. Equipment for crop protection – Methods for field measurement of spray drift. International Organization for Standardization. 17 pp.

Johnstone, D.R. 1985. Physics and Meteorology. In: Haskell, P.T. (ed). *Pesticide Application: Principles and Practice*. Clarendon Press, Oxford, England. pp.35-65.

Jones, H.R. and Sudmeyer, R.A. 2002. Economic assessment of windbreaks on the south-eastern coast of Western Australia. *Australian Journal of Experimental Agriculture*, 42: 751-761.

Judd, M.J., Raupach, M.R., and Finnigan, J.J. 1996. A wind tunnel study of turbulent flow around single and multiple windbreaks, Part I: Velocity fields. *Boundary-Layer Meteorology*, 80: 127-165.

Kenney, W.A. 1987. A method for estimating windbreak porosity using digitized photographic silhouettes. *Agricultural and Forest Meteorology*, 39: 91-94.

Lefebvre, A.H. 1993. Droplet Production. In: Matthews, G.A. and Hislop, E.C. (eds). *Application Technology for Crop Protection*. CAB International, Oxon, England. pp. 101-122.

Loeffler, A.E., Gordon, A.M., and Gillespie, T.J. 1992. Optical porosity and windspeed reduction by coniferous windbreaks in Southern Ontario. *Agroforestry Systems*, 17: 117-133.

Marrs, R.H., Frost, A.J., Plant, R.A., and Lunnis, P. 1992. The effects of herbicide drift on semi-natural vegetation: the use of buffer zones to minimize risks. *Aspects of Applied Biology*, 29: 57-64.

Matthews, G.A. 2000. *Pesticide Application Methods*, 3rd Ed. Blackwell Science, Oxford, England. 432 pp.

Maybank, J., Yoshida, K., and Grover, R. 1978. Spray drift from agricultural pesticide applications. *Journal of the Air Pollution Control Association*, 28(10): 1009-1014.

Miller, P.C.H. 1993. Spray drift and its measurement. In: Matthews, G.A. and Hislop, E.C. (eds). *Application Technology for Crop Protection*. CAB International, Oxon, England. pp. 101-122.

Miller, P.C.H. and Lane, A.G. 1999. Relationship between spray characteristics and drift risk into field boundaries of different structure. *Aspects of Applied Biology*, 54: 45-51.

Miller, P.C.H., Lane, A.G., Walklate, P.J., and Richardson, G.M. 2000. The effect of plant structure on the drift of pesticides at field boundaries. *Aspects of Applied Biology*, 57: 75-82.

Montgomery, D.C., Runger G.C., and Hubele, N.F. 2004. *Engineering statistics.* 3rd Edition. John Wiley & Sons, Inc., New York, NY. 461 pp.

Nelmes, S., Belcher, R.E., and Wood, C.J. 2001. A method for routine characterisation of shelterbelts. *Agricultural and Forest Meteorology*, 106: 303-315.

Nord, M. 1991. Shelter effects of vegetation belts – Results of field measurements. *Boundary-Layer Meteorology*, 54: 363-385.

Nuyttens, D., de Schampheleire, M., Steurbaut, W., Baetens, K., Verboven, P., Nicolai, B., Ramon, H., and Sonck, B. 2006a. Experimental study of factors influencing the risk of drift from field sprayers, Part 1: Meteorological conditions. *Aspects of Applied Biology*, 77: 321-329.

Nuyttens, D., de Schampheleire, M., Steurbaut, W., Baetens, K., Verboven, P., Nicolai, B., Ramon, H., and Sonck, B. 2006b. Experimental study of factors influencing the risk of drift from field sprayers, Part 2: Spray application technique. *Aspects of Applied Biology*, 77: 331-339.

Oke, T.R. 1987. *Boundary Layer Climates.* 2nd Edition. Routledge, Methuen, NY. 463 pp.

Ozkan, H.E, Miralles, A., Sinfort, C., Zhu, H., Reichard, D.L., and Fox, R.D. 1997. Effect of shielding spray boom on spray deposition. *Pesticide Formulations and Application Systems: 17th Volume, ASTM STP 1328*, G. Robert Goss, Michael Hopkinson, and Herbert M. Collins (eds.). American Society for Testing and Materials.

Raupach, M.R., Woods, N., Dorr, G., Leys, J.F., and Cleugh, H.A. 2001. The entrapment of particles by windbreaks. *Atmospheric Environment*, 35: 3373-3383.

Richardson, G.M., Walklate, P.J., and Baker, D.E. 2004. Spray drift from apple orchards with deciduous windbreaks. *Aspects of Applied Biology*, 71: 149-156.

Richardson, G.M., Walklate, P.J., and Baker, D.E. 2002. Drift reduction characteristics of windbreaks. *Aspects of Applied Biology*, 66: 201-208.

Robinson, T.M. 1993. Large-scale ground based application techniques. In: Matthews, G.A. and Hislop, E.C. (eds). *Application Technology for Crop Protection*. CAB International, Oxon, England. pp. 163-186.

Seginer, I. 1975a. Flow around a windbreak in oblique wind. *Boundary-Layer Meteorology*, 9:133-141.

Seginer, I. 1975b. Atmospheric-stability effect on windbreak shelter and drag. *Boundary-Layer Meteorology*, 8: 383-400.

StatSoft, Inc. 2001. *Statistica (data analysis software system) User Manual, Version 6*. StatSoft, Inc., Tulsa, OK.

Topping, J. 1972. *Errors of observation and their treatment*. 4th Ed. Chapman and Hall Ltd., London, England. 119 pp.

Ucar, T. and Hall, F.R. 2001. Windbreaks as a pesticide drift mitigation strategy: A review. *Pest Management Science*, 57: 663-675.

Ucar, T., Hall, F.R., Tew, J.E., and Hacker, J.K. 2003. Wind tunnel studies on spray deposition on leaves of tree species used for windbreaks and exposure of honey bees. *Pest Management Science*, 59: 358-364.

van Eimern, J., Karschon, R., Razumova, L.A. and Robertson, G.W. 1964. *Windbreaks and Shelterbelts*. WMO Technical Note No. 59 (WMO – No. 147.TP.70), 188 pp.

Wang, H. and Takle, E.S. 1996. On shelter efficiency of shelterbelts in oblique wind. *Agricultural and Forest Meteorology*, 81: 95-117.

Wilson, J.D. 2005. Deposition of particles to a thin windbreak: The effect of a gap. *Atmospheric Environment*, 39: 5525-5531.

Wolf, T.M. 2006. Unpublished data set. Agriculture and Agri-Food Canada. Saskatoon, Saskatchewan.

Wolf, T.M., Grover, R., Wallace, K., Shewchuk, S.R., and Maybank, J. 1993. Effect of protective shields on drift and deposition characteristics of field sprayers. *Canadian Journal of Plant Science*, 73: 1261-1273.

Wolf, T.M., Caldwell, B.C., and Pederson, J.L. 2004. Interaction of riparian vegetation and nozzle type for drift deposit reduction. *Aspects of Applied Biology*, 71: 183-190.

Wolf, T.M., Cessna, A.J., Caldwell, B.C., and Pederson, J.L. 2005. Riparian vegetation reduces spray drift deposition into water bodies. Pages 201-212 in A.G. Thomas (ed.). *Field Boundary Habitats: Implications for Weed, Insect, and Disease Management. Topics in Canadian Weed Science, Volume 1*. Sainte-Anne-de-Bellevue, Québec: Canadian Weed Science Society - Société Canadienne de Malherbologie.

Zhang, H., Brandle, J.R., Meyer, G.E., and Hodges, L. 1995. The relationship between open windspeed and windspeed reduction in shelter. *Agroforestry Systems*, 32: 297-311.

Zhou, X.H., Brandle, J.R., Mize, C.W., and Takle, E.S. 2004. Three-dimensional aerodynamic structure of a tree shelterbelt: Definition, characterization, and working models. *Agroforestry Systems*, 63: 133-147.

Zhou, X.H., Brandle, J.R., Takle, E.S., and Mize, C.W. 2002. Estimation of the three-dimensional aerodynamic structure of a green ash shelterbelt. *Agricultural and Forest Meteorology*, 111: 93-108.

Appendices

Appendix A

Meteorological Data

Meteorological Data
Trials 1 - 10d

		Trial									
Distance[1]	Variable	1	2	3	4	5	6	7	8	9	10d
-12H[2]	U_{1m}[3]	8.81	7.25	6.75	7.93	15.79	15.85	13.02	15.21	12.94	7.02
	U_{2m}[4]	11.61	9.39	8.69	10.03	11.01	10.02	8.73	9.89	8.58	9.14
	U_{3m}[5]	12.74	10.52	9.75	10.96	22.72	21.45	17.90	21.21	18.15	9.75
	U_{4m}[6]	13.36	10.94	9.98	11.24	24.88	23.36	19.50	22.94	19.40	10.11
	γ[7]	33.00	57.00	52.70	52.00	25.70	33.10	37.00	33.30	30.50	2.40
	T_{1m}[8]	23.09	21.56	21.33	23.28	17.40	17.54	18.27	18.32	19.43	21.95
	T_{5m}[9]	22.65	21.38	21.29	23.41	16.86	16.73	17.40	18.00	18.48	21.29
-6H	U_{1m}	8.66	7.16	6.32	7.49	15.22	14.98	12.45	14.00	11.47	5.93
	γ	47.00	57.10	51.92	47.67	21.87	28.26	33.41	28.60	34.00	12.45
-3H	U_{1m}	7.48	5.94	5.26	6.13	13.15	13.99	10.91	12.81	11.37	5.11
	γ										
-0.5H	U_{1m}					12.16	11.99	11.14	11.88	10.51	5.99
	U_{2m}	9.62	8.65	7.42	8.89	15.66	15.28	14.02	15.12	13.09	
	U_{3m}	10.38	9.29	8.19	9.75	18.30	17.84	16.29	17.62	15.23	4.48
	U_{4m}	11.42	9.98	8.83	10.62	20.50	19.96	18.22	19.86	17.25	9.43
0.5H	U_{1m}	5.10	3.95	2.81	4.68	8.56	8.29	5.90	7.11	5.86	4.95
	U_{2m}	5.08	3.89	3.04	4.74	7.91	7.40	6.26	7.02	6.35	4.57
	U_{3m}	3.79	3.10	2.84	3.37	6.61	9.00	8.01	8.81	7.48	5.32
	U_{4m}	5.82	4.91	4.22	6.11	15.85	15.03	12.59	14.29	12.08	4.81
6H	U_{1m}					8.89	10.40		9.65	8.63	2.53
9H	U_{1m}										
12H	U_{1m}					13.64	12.95	12.68	13.43	11.99	5.04
15H	U_{1m}					15.04	14.34	13.55	14.04	12.45	5.69
18H	U_{1m}					15.64	14.68	13.34	14.23	12.84	5.96
24H	U_{1m}	7.70	6.95	6.41	7.66	15.44	16.05	13.44	14.87	13.19	6.07
30H	U_{1m}	8.06	6.47	6.62	8.01	15.12	15.33	12.75	14.87	12.97	6.91
	γ	29.41	38.31	12.47	34.02	16.08	23.59	25.66	26.99	24.19	19.32
	T_{1m}	18.51	18.05	18.02	19.18	13.21	13.35	13.63	13.54	14.47	17.26
	RH[10]	42.21	42.70	41.95	35.29	42.60	42.69	42.51	40.98	40.52	37.72

Missing data due to data logger problems

Legend

1. Distance measured relative to the shelterbelt
2. Height of the shelterbelt (5 m)
3. Wind speed measured at z = 1 m (km/h)
4. Wind speed measured at z = 2 m (km/h)
5. Wind speed measured at z = 3 m (km/h)
6. Wind speed measured at z = 4 m (km/h)
7. Wind direction measured from a line perpendicular from the shelterbelt (degree)
8. Temperature measured at z = 1 m (oC)
9. Temperature measured at z = 5 m (oC)
10. Relative humidity (%)

Meteorological Data
Trials 11d - 17

		Trial									
Distance[1]	Variable	11d	12d	10	11	12	13	14	15	16	17
-12H[2]	U_{1m}[3]	9.12	8.54	11.37	9.92	9.41	10.49	10.30	11.53	25.27	29.38
	U_{2m}[4]	12.38	11.69	7.35	6.97	7.14	7.75	7.01	8.03	28.49	32.96
	U_{3m}[5]	13.74	12.90	14.62	13.67	14.00	15.19	14.11	16.07	30.54	35.43
	U_{4m}[6]	14.56	13.70	15.57	14.56	14.79	16.06	15.08	17.05	32.09	37.44
	γ[7]	5.90	4.40	13.50	15.50	4.20	11.20	14.40	0.90	2.20	7.10
	T_{1m}[8]	21.86	21.32	15.64	17.49	17.87	22.09	22.29	24.10	18.80	19.36
	T_{5m}[9]	21.59	21.24	15.25	17.13	17.77	21.42	21.67	23.28	18.09	20.31
-6H	U_{1m}	8.47	8.42	10.62	9.39	9.97	11.01	10.23	10.87		22.89
	γ	1.01	3.68								6.78
-3H	U_{1m}	7.36	6.76	9.21	8.23	8.42	9.44	8.71	9.11	24.14	
	γ									3.31	
-0.5H	U_{1m}	7.47	7.20							18.78	18.45
	U_{2m}									23.31	22.60
	U_{3m}	6.07	5.55							26.52	25.76
	U_{4m}	13.16	11.91							13.91	13.48
0.5H	U_{1m}	6.69	6.28	9.02	8.42	8.42	9.21	8.90	9.20	20.33	19.20
	U_{2m}	6.30	5.84	12.13	11.03	11.10	12.15	11.79	12.32	20.53	19.49
	U_{3m}	8.32	7.45	13.70	12.41	12.71	13.77	13.23	14.04	18.50	17.30
	U_{4m}	8.01	7.08	15.05	13.58	14.05	15.05	14.55	15.44	12.26	11.84
6H	U_{1m}	2.14		6.67	6.40	6.87	6.51	6.10	7.84	11.21	11.56
9H	U_{1m}									15.64	16.21
12H	U_{1m}	6.62	5.83	9.70	8.92	9.14	9.29	9.02	10.25	18.49	19.65
15H	U_{1m}	7.58	6.36	10.47	9.48	9.87	9.81	9.46	11.28		
18H	U_{1m}	8.37	6.95	10.61	10.16	10.28	10.03	9.88	11.33	23.17	23.23
24H	U_{1m}	8.18	7.58								
30H	U_{1m}	9.28	9.22	11.79	11.17	9.59	12.00	11.60	12.26		
	γ	5.34	10.46	12.52	14.52	4.25	11.19	12.43	0.89	1.83	7.36
	T_{1m}	16.98	16.78	14.58	15.34	15.60	17.86	17.73	18.87	16.59	16.42
	RH[10]	36.95	36.04	42.14	40.81	40.43	34.02	33.52	30.23	64.86	73.79

Missing data due to data logger problems

Legend

1. Distance measured relative to the shelterbelt
2. Height of the shelterbelt (5 m)
3. Wind speed measured at z = 1 m (km/h)
4. Wind speed measured at z = 2 m (km/h)
5. Wind speed measured at z = 3 m (km/h)
6. Wind speed measured at z = 4 m (km/h)
7. Wind direction measured from a line perpendicular from the shelterbelt (degree)
8. Temperature measured at z = 1 m (oC)
9. Temperature measured at z = 5 m (oC)
10. Relative humidity (%)

Meteorological Data
Trials 18 - 27

		Trial									
Distance[1]	Variable	18	19	20	21	22	23	24	25	26	27
-12H[2]	U_{1m}[3]	28.34	14.52	15.68	17.51	11.99	10.94	12.83	15.92	15.93	18.04
	U_{2m}[4]	32.05	17.22	18.79	21.01	13.87	13.19	15.11	18.83	18.95	21.22
	U_{3m}[5]	34.54	18.52	20.32	23.00	15.22	14.55	16.69	20.84	21.22	23.37
	U_{4m}[6]	36.14	18.96	21.00	24.04	15.67	15.05	17.13	21.48	22.26	24.05
	γ[7]	5.20	28.00	47.70	49.40	12.60	3.50	11.20	13.60	39.00	17.60
	T_{1m}[8]	20.59	24.15	24.96	24.67	20.94	22.52	24.01	27.46	26.64	27.59
	T_{5m}[9]	19.43	23.10	23.71	23.84	19.74	21.27	22.60	25.71	25.86	26.12
-6H	U_{1m}	26.27		15.72	16.92		10.97	13.05		15.80	17.54
	γ	6.54		50.50	47.49		3.23	14.73		35.33	14.65
-3H	U_{1m}		14.04			11.68			16.24		
	γ		27.02			11.55			19.01		
-0.5H	U_{1m}	20.19	10.38	12.48	13.12	9.04	8.88	9.84	12.93	12.42	13.37
	U_{2m}	24.71	9.81	11.40	12.95	8.20	10.16	11.72	15.26	15.23	16.31
	U_{3m}	28.49					11.29	14.60		17.56	18.86
	U_{4m}	14.56	15.96	17.62	20.30	13.03	12.41		18.46	18.82	20.44
0.5H	U_{1m}	21.99	8.29	7.11	7.53	9.18	8.54	10.07	12.34	8.84	11.75
	U_{2m}	22.00	1.93	3.57	4.65	9.40	8.43	9.97	12.85	6.39	11.33
	U_{3m}	20.75	7.45	5.34	5.37	6.72	8.65	6.29	9.68	9.88	13.49
	U_{4m}	12.82	10.51	5.89	5.37	9.25	8.99	9.77	12.45	11.62	15.84
6H	U_{1m}	13.34	8.21	9.69	12.41	3.97	4.48	4.35	6.59	8.82	8.80
9H	U_{1m}	19.07	10.12	12.81	15.10	5.82	6.38	6.81	9.08	10.76	12.46
12H	U_{1m}	21.57	11.29	14.55	15.86	7.48	7.54	8.47	11.31	13.09	13.96
15H	U_{1m}										
18H	U_{1m}	25.41	13.50	14.97	18.00	9.86	9.01	10.63	13.99	15.01	16.42
24H	U_{1m}		12.95	15.46	17.68						
30H	U_{1m}		11.68	14.62	16.61						
	γ	5.12	19.23	48.82	46.36	16.41	0.54	14.46	17.28	35.98	13.04
	T_{1m}	17.87	21.97	22.86	21.94	19.86	20.93	22.05	24.76	23.91	25.46
	RH[10]	55.70				53.54	50.16	45.58	33.00	31.52	26.74

Missing data due to data logger problems

Legend

1. Distance measured relative to the shelterbelt
2. Height of the shelterbelt (5 m)
3. Wind speed measured at z = 1 m (km/h)
4. Wind speed measured at z = 2 m (km/h)
5. Wind speed measured at z = 3 m (km/h)
6. Wind speed measured at z = 4 m (km/h)
7. Wind direction measured from a line perpendicular from the shelterbelt (degree)
8. Temperature measured at z = 1 m (oC)
9. Temperature measured at z = 5 m (oC)
10. Relative humidity (%)

Meteorological Data
Open Field Trials

		Trial		
Distance[1]	Variable	Open Field 1	Open Field 2	Open Field 3
-45	U_{1m}[2]	9.86	13.35	11.84
	U_{2m}[3]	12.50	16.96	15.62
	U_{3m}[4]	13.34	17.53	16.18
	U_{4m}[5]	13.89	17.99	16.62
	γ[6]	23.69	20.34	8.02
	T_{1m}[7]	31.87	31.47	29.96
	T_{5m}[8]	30.35	30.10	31.39
20	U_{1m}	6.90	11.37	9.03
	U_{2m}	12.63	16.76	14.43
	U_{3m}	13.29	17.69	14.88
	U_{4m}	13.99	18.71	15.73
25	U_{1m}	10.65	14.28	12.17
	U_{2m}	12.43	16.53	13.80
	U_{3m}			
	U_{4m}	13.73	18.45	15.52
170	U_{1m}			
	γ	29.09	23.88	13.74
	T_{1m}	26.86	27.38	27.41
	RH[9]	35.03	34.74	34.93

Missing data due to data logger problems

Legend

1. Distance measured relative to the spray swath
2. Wind speed measured at z = 1 m (km/h)
3. Wind speed measured at z = 2 m (km/h)
4. Wind speed measured at z = 3 m (km/h)
5. Wind speed measured at z = 4 m (km/h)
6. Wind direction measured from a line perpendicular
7. from the spray swath (degree)
   Temperature measured at z = 1 m (oC)
8. Temperature measured at z = 5 m (oC)
9. Relative humidity (%)

Appendix B

Drift Data

Trial 1

Petri-plate Data

Distance	Concentration		
	Row 1	Row 2	Row 3
(m)	(ppb)	(ppb)	(ppb)
Onswath 1	17139.0	15528.8	16244.8
Onswath 2	14545.4	12332.4	12749.6
Onswath 3	15536.8	12995.0	14933.8
Onswath 4	14460.6	12366.8	13809.0
5	56.25	35.09	32.89
10	15.993	19.367	19.915
15	13.439	13.390	20.853
20	2.694	4.153	4.347
35	1.437	1.976	2.015
50	2.0477	1.7375	1.7209
65	1.0779	1.5658	1.6761
80	1.4708	1.1448	1.3670
95	0.7550	1.3161	1.1885
110	1.1916	0.8045	1.1015
125	1.0925	1.0351	1.2917
140	0.7292	0.8687	0.7728
155	0.5953	0.5971	0.5783
170	0.4990	0.4557	0.4721

String Data

Height	Concentration	
	Upwind	Downwind
(m)	(ppb)	(ppb)
30		0.592
29		0.388
28		1.291
27		2.701
26		1.643
25		0.608
24		0.467
23		1.645
22		0.551
21		0.336
20		1.049
19		0.502
18		0.508
17		0.931
16		0.484
15		0.765
14		0.660
13		0.484
12		0.708
11		1.315
10		3.605
9		5.283
8		10.997
7		17.464
6		11.600
5		4.643
4		3.021
3		4.833
2		3.476
1		1.689

Upwind string collector not used

Rotorod Data

Upwind of Shelterbelt

Height	Concentration		
	Row 1	Row 2	Row 3
(m)	(ppb)	(ppb)	(ppb)
1	17.030	22.794	36.504
2	16.851	22.050	43.374
3	14.219	39.932	25.932
4	7.815	34.622	17.334

Downwind of Shelterbelt

Height	Concentration		
	Row 1	Row 2	Row 3
(m)	(ppb)	(ppb)	(ppb)
1	0.628	0.666	0.673
2	0.612	0.874	0.513
3	0.466	0.802	0.521
4	0.241	0.461	0.404

Petri-dish Blanks

Dish #	Concentration (ppb)
1	-0.0178
2	-0.0284
3	-0.0204
4	-0.0314

Rotorod Blanks

Height (m)	Concentration (ppb)
1	-0.0196
2	-0.0146
3	-0.0269
4	-0.0194

Photolysis

Dish #	Light (ppb)	Dark (ppb)
1	792.58	1060.80
2	761.03	1080.70
3	784.99	1030.30
4	834.28	854.72

Trial 2

Petri-plate Data

Distance	Concentration		
	Row 1	Row 2	Row 3
(m)	(ppb)	(ppb)	(ppb)
Onswath 1	14077.8	14572.4	16643.0
Onswath 2	17423.0	15205.2	17564.6
Onswath 3	18586.4	14783.8	15913.4
Onswath 4	14726.6	15856.0	16643.4
5	4.18	3.21	3.21
10	1.723	3.081	2.551
15	1.455	1.487	2.422
20	0.803	0.855	0.867
35	0.414	0.505	0.432
50	0.2753	0.5231	0.2949
65	0.2554	0.1708	0.2294
80	0.3159	0.1900	0.2445
95	0.1428	0.1741	0.0886
110	0.3346	0.1843	0.1880
125	0.2444	0.2673	0.3265
140	0.2136	0.2155	0.2082
155	0.1839	0.1951	0.2058
170	0.2390	0.1763	0.1183

String Data

Height	Concentration	
	Upwind	Downwind
(m)	(ppb)	(ppb)
30		
29		
28		
27		
26		0.616
25		0.526
24		0.390
23		0.380
22		0.425
21		0.586
20		0.272
19		0.197
18		0.410
17		0.395
16		0.284
15		0.288
14		0.138
13		0.194
12		0.189
11		0.259
10		1.185
9		0.480
8		1.898
7		2.128
6		1.556
5		1.383
4		1.619
3		1.739
2		4.070
1		1.595

Upwind string collector not used

Rotorod Data

Upwind of Shelterbelt

Height	Concentration		
	Row 1	Row 2	Row 3
(m)	(ppb)	(ppb)	(ppb)
1	2.360	2.036	1.546
2	1.855	2.222	1.271
3	1.259	1.225	0.979
4	1.230	0.723	1.325

Downwind of Shelterbelt

Height	Concentration		
	Row 1	Row 2	Row 3
(m)	(ppb)	(ppb)	(ppb)
1	3.371	0.580	0.058
2	2.044	1.985	1.208
3	3.388	1.547	0.462
4	2.235	5.125	0.533

Petri-dish Blanks

Dish #	Concentration (ppb)
1	0.1137
2	0.1038
3	0.1082
4	0.1084

Rotorod Blanks

Height (m)	Concentration (ppb)
1	-0.0236
2	-0.0284
3	-0.0295
4	-0.0294

Photolysis

Dish #	Light (ppb)	Dark (ppb)
1	853.83	1057.20
2	890.37	961.24
3	857.97	852.60
4	798.86	1029.00

Trial 3

Petri-plate Data

Distance	Concentration		
	Row 1	Row 2	Row 3
(m)	(ppb)	(ppb)	(ppb)
Onswath 1	13992.8	14305.4	15677.4
Onswath 2	15441.6	12483.4	14394.0
Onswath 3	11596.8	14068.6	14904.2
Onswath 4	13494.6	14419.0	14601.4
5	13.12	15.00	16.05
10	12.781	10.577	9.577
15	9.291	8.013	14.021
20	4.299	5.151	7.439
35	1.986	2.299	2.611
50	2.0480	1.6283	1.6531
65	0.8604	0.7533	0.8793
80	0.3883	0.4270	0.4282
95	0.1539	0.0955	0.1561
110	0.1119	0.0788	0.0734
125	0.0359	0.0210	0.0369
140	0.1717	0.1519	0.1607
155	0.1806	0.1565	0.1359
170	0.0051	0.0031	0.0023

String Data

Height	Concentration	
	Upwind	Downwind
(m)	(ppb)	(ppb)
30		
29		1.132
28		0.982
27		0.958
26		1.199
25		1.129
24		1.872
23		1.917
22		1.704
21		1.906
20		2.369
19		3.352
18		2.581
17		4.073
16		3.506
15		4.707
14		5.252
13		5.129
12		7.040
11		8.609
10		7.047
9		11.414
8		9.889
7		10.623
6		10.966
5		8.984
4		5.509
3		3.128
2		3.461
1		3.081

Upwind string collector not used

Rotorod Data

Upwind of Shelterbelt

Height	Concentration		
	Row 1	Row 2	Row 3
(m)	(ppb)	(ppb)	(ppb)
1	4.271	4.782	7.201
2	3.399	5.536	4.120
3	2.115	3.678	1.709
4	2.717	1.643	4.247

Downwind of Shelterbelt

Height	Concentration		
	Row 1	Row 2	Row 3
(m)	(ppb)	(ppb)	(ppb)
1	3.723	1.529	4.814
2	2.189	3.031	4.996
3	0.960	2.199	4.916
4	1.336	2.364	3.216

Petri-dish Blanks

Dish #	Concentration (ppb)
1	0.0934
2	0.1072
3	0.1030
4	0.1010

Rotorod Blanks

Height (m)	Concentration (ppb)
1	0.0297
2	-0.0285
3	-0.0327
4	-0.0333

Photolysis

Dish #	Light (ppb)	Dark (ppb)
1	808.32	1061.00
2	810.19	1078.90
3	842.86	1033.10
4	844.47	1139.50

Trial 4

Petri-plate Data

Distance	Concentration		
	Row 1	Row 2	Row 3
(m)	(ppb)	(ppb)	(ppb)
Onswath 1	15650.4	15555.2	14857.4
Onswath 2	15051.6	13242.4	14501.2
Onswath 3	13726.6	13402.2	12863.0
Onswath 4	14576.2	13236.4	16069.8
5	4.47	5.02	4.46
10	2.050	2.339	2.223
15	1.378	1.212	1.398
20	0.630	0.775	0.561
35	0.431	0.437	0.399
50	0.4602	0.5197	0.5092
65	0.3672	0.4823	0.3543
80	0.4941	0.3212	0.2927
95	0.3742	0.4631	0.3903
110	0.4844	0.4098	0.2460
125	0.4333	0.4417	0.3244
140	0.1105	0.2660	0.1815
155	0.0830	0.1182	0.0952
170	0.1228	0.1339	0.1713

String Data

Height	Concentration	
	Upwind	Downwind
(m)	(ppb)	(ppb)
30		0.490
29		0.246
28		0.178
27		0.149
26		0.191
25		0.134
24		0.125
23		0.177
22		0.220
21		0.128
20		0.155
19		0.244
18		0.160
17		0.161
16		0.149
15		0.138
14		0.126
13		0.137
12		0.221
11		0.258
10		0.184
9		0.311
8		0.649
7		1.210
6		0.853
5		0.932
4		0.906
3		0.992
2		0.963
1		0.567

Upwind string collector not used

Rotorod Data

Upwind of Shelterbelt

Height	Concentration		
	Row 1	Row 2	Row 3
(m)	(ppb)	(ppb)	(ppb)
1	0.708	0.740	0.799
2	0.779	0.751	0.944
3	0.663	1.075	0.626
4	0.654	1.756	0.983

Downwind of Shelterbelt

Height	Concentration		
	Row 1	Row 2	Row 3
(m)	(ppb)	(ppb)	(ppb)
1	0.282	0.361	0.382
2	0.239	0.474	0.279
3	0.205	0.246	0.301
4	0.127	0.264	0.444

Petri-dish Blanks

Dish #	Concentration (ppb)
1	0.0991
2	0.1178
3	0.1146
4	0.1096

Rotorod Blanks

Height (m)	Concentration (ppb)
1	0.0232
2	0.0087
3	0.1116
4	0.0132

Photolysis

Dish #	Light (ppb)	Dark (ppb)
1	796.45	1111.60
2	825.58	1095.40
3	796.96	1067.90
4	818.25	1027.50

Trial 5

Petri-plate Data

Distance	Concentration		
	Row 1	Row 2	Row 3
(m)	(ppb)	(ppb)	(ppb)
Onswath 1	12506.8	12577.8	15267.2
Onswath 2	14916.6	14605.8	13985.0
Onswath 3	12432.0	14413.4	14358.6
Onswath 4	14365.6	14469.8	15199.4
5	105.23	59.32	44.65
10	142.110	52.736	27.214
15	158.430	81.874	28.204
20	2.112	5.316	3.712
35	4.514	2.286	2.116
50	2.8865	2.0967	2.6550
65	3.0855	2.7959	1.5264
80	2.5006	2.5151	1.5229
95	2.0464	1.5038	1.6471
110	1.3068	1.8647	1.8637
125	1.5257	1.4961	1.4815
140	1.2044	1.2968	0.9050
155	0.6816	1.1526	1.1031
170	1.1564	0.9231	0.6557

String Data

Height	Concentration	
	Upwind	Downwind
(m)	(ppb)	(ppb)
30		
29		
28		
27		
26		
25		
24		
23		
22		
21		
20		
19		
18		
17		
16		
15		
14		
13		
12		
11		
10		
9		
8		
7		
6		
5		
4		
3		
2		
1		

Upwind string collector not used
Downwind string collector data not available

Rotorod Data

Upwind of Shelterbelt

Height	Concentration		
	Row 1	Row 2	Row 3
(m)	(ppb)	(ppb)	(ppb)
1	84.913	95.313	117.560
2	83.514	71.996	100.870
3	48.030	44.222	63.444
4	19.756	25.475	38.005

Downwind of Shelterbelt

Height	Concentration		
	Row 1	Row 2	Row 3
(m)	(ppb)	(ppb)	(ppb)
1	13.740	17.675	3.746
2	10.807	18.412	2.293
3	22.302	0.500	6.389
4	11.147	9.651	10.211

Petri-dish Blanks

Dish #	Concentration (ppb)
1	-0.0883
2	-0.0924
3	-0.0921
4	-0.0809

Rotorod Blanks

Height (m)	Concentration (ppb)
1	0.1973
2	0.1024
3	0.1008
4	0.1081

Photolysis

Dish #	Light (ppb)	Dark (ppb)
1	254.32	335.07
2	235.57	375.61
3	244.28	361.33
4	259.85	372.39

Trial 6

Petri-plate Data

Distance	Concentration		
	Row 1	Row 2	Row 3
(m)	(ppb)	(ppb)	(ppb)
Onswath 1	2380.7	2192.0	3839.0
Onswath 2	3837.0	2350.7	3809.0
Onswath 3	3853.3	6485.7	4242.0
Onswath 4	3733.5	3687.2	3071.8
5	114.30	120.44	149.58
10	40.742	37.171	46.741
15	30.884	29.048	14.936
20	2.327	5.582	3.710
35	2.228	3.639	2.591
50	2.6871	2.2936	2.8045
65	3.4052	3.1632	2.2519
80	3.1265	2.9801	2.5205
95	2.1907	2.2354	2.1140
110	1.7418	1.3238	1.4237
125	1.2163	1.6161	1.5519
140	1.3947	1.0861	1.3902
155	1.3196	1.4094	1.5091
170	0.9635	1.1480	1.1749

String Data

Height	Concentration	
	Upwind	Downwind
(m)	(ppb)	(ppb)
30		
29		
28		
27		
26		
25		
24		
23		
22		
21		
20		
19		
18		
17		
16		
15		
14		
13		
12		
11		
10		
9		
8		
7		
6		
5		
4		
3		
2		
1		

Upwind string collector not used
Downwind string collector data not available

Rotorod Data

Upwind of Shelterbelt

Height	Concentration		
	Row 1	Row 2	Row 3
(m)	(ppb)	(ppb)	(ppb)
1	114.320	88.342	57.520
2	99.419	81.247	55.058
3	67.450	70.669	48.238
4	40.058	43.567	26.698

Downwind of Shelterbelt

Height	Concentration		
	Row 1	Row 2	Row 3
(m)	(ppb)	(ppb)	(ppb)
1	7.926	19.799	1.701
2	7.621	14.855	1.429
3	25.024	12.674	5.980
4	14.888	30.709	7.372

Petri-dish Blanks

Dish #	Concentration (ppb)
1	-0.0632
2	-0.0641
3	-0.0604
4	-0.0503

Rotorod Blanks

Height (m)	Concentration (ppb)
1	0.1697
2	0.1039
3	0.1202
4	0.0885

Photolysis

Dish #	Light (ppb)	Dark (ppb)
1	267.99	343.56
2	294.76	365.71
3	278.32	375.63
4	277.63	364.47

Trial 7

Petri-plate Data

Distance	Concentration		
	Row 1	Row 2	Row 3
(m)	(ppb)	(ppb)	(ppb)
Onswath 1	12397.0	13875.6	14082.4
Onswath 2	12140.4	11285.0	15034.4
Onswath 3	11211.0	11401.6	14911.6
Onswath 4	14108.2	9588.2	13818.0
5	93.50	137.08	109.43
10	48.045	44.126	36.098
15	15.175	22.057	25.764
20	3.017	2.518	1.380
35	5.305	1.720	1.142
50	4.9878	1.5936	1.1496
65	3.2358	2.0896	1.3146
80	2.2650	1.6401	1.3103
95	3.1705	1.6490	1.3443
110	3.5469	1.7120	1.3311
125	2.2552	1.1347	1.4833
140	2.3313	0.9869	0.9281
155	2.5114	1.3537	1.1688
170	2.5244	0.8588	0.9410

String Data

Height	Concentration	
	Upwind	Downwind
(m)	(ppb)	(ppb)
30		
29		
28		
27		
26		
25		
24		
23		
22		
21		
20		
19		
18		
17		
16		
15		
14		
13		
12		
11		
10		
9		
8		
7		
6		
5		
4		
3		
2		
1		

Upwind string collector not used
Downwind string collector data not available

Rotorod Data

Upwind of Shelterbelt

Height	Concentration		
	Row 1	Row 2	Row 3
(m)	(ppb)	(ppb)	(ppb)
1	59.067	90.542	105.070
2	53.154	70.613	90.656
3	55.605	53.510	80.196
4	33.751	31.530	62.169

Downwind of Shelterbelt

Height	Concentration		
	Row 1	Row 2	Row 3
(m)	(ppb)	(ppb)	(ppb)
1	4.444	12.668	3.163
2	7.902	10.508	1.824
3	17.294	10.677	3.519
4	10.557	28.302	4.895

Petri-dish Blanks

Dish #	Concentration (ppb)
1	-0.0903
2	-0.0907
3	0.0978
4	-0.0760

Rotorod Blanks

Height (m)	Concentration (ppb)
1	0.1276
2	0.1296
3	0.1129
4	0.1186

Photolysis

Dish #	Light (ppb)	Dark (ppb)
1	281.87	367.98
2	255.00	375.18
3	243.75	368.15
4	261.45	366.04

Trial 8

Petri-plate Data

Distance	Concentration		
	Row 1	Row 2	Row 3
(m)	(ppb)	(ppb)	(ppb)
Onswath 1	4022.1	3433.4	4375.1
Onswath 2	4077.7	3556.5	4309.1
Onswath 3	3875.6	3997.8	3746.3
Onswath 4	3720.6	4953.2	4075.9
5	116.31	126.44	73.08
10	34.769	44.014	42.227
15	17.796	27.028	14.303
20	2.315	8.513	5.652
35	2.229	4.977	2.964
50	2.2611	2.2287	2.4823
65	2.2946	2.3766	1.7997
80	2.1925	1.5054	1.5415
95	2.5909	1.6210	2.2275
110	1.4512	1.2296	1.4068
125	1.2951	1.3456	1.0283
140	1.0658	0.8666	1.1449
155	1.0844	1.0074	0.8977
170	0.7365	0.8348	0.7802

String Data

Height	Concentration	
	Upwind	Downwind
(m)	(ppb)	(ppb)
30		
29		
28		
27		
26		
25		
24		
23		
22		
21		
20		
19		
18		
17		
16		
15		
14		
13		
12		
11		
10		
9		
8		
7		
6		
5		
4		
3		
2		
1		

Upwind string collector not used
Downwind string collector data not available

Rotorod Data

Upwind of Shelterbelt

Height	Concentration		
	Row 1	Row 2	Row 3
(m)	(ppb)	(ppb)	(ppb)
1	71.209	75.645	59.520
2	71.394	68.441	55.171
3	41.060	62.662	40.452
4	27.070	36.010	29.656

Downwind of Shelterbelt

Height	Concentration		
	Row 1	Row 2	Row 3
(m)	(ppb)	(ppb)	(ppb)
1	4.943	8.116	2.376
2	6.377	10.654	1.338
3	10.343	8.760	3.398
4	3.806	13.451	5.238

Petri-dish Blanks

Dish #	Concentration (ppb)
1	-0.0642
2	-0.0585
3	-0.0587
4	-0.0603

Rotorod Blanks

Height (m)	Concentration (ppb)
1	0.1239
2	0.0707
3	0.0670
4	0.0843

Photolysis

Dish #	Light (ppb)	Dark (ppb)
1	303.66	369.97
2	299.97	368.95
3	288.02	347.85
4	293.40	362.31

Trial 9

Petri-plate Data

Distance	Concentration		
	Row 1	Row 2	Row 3
(m)	(ppb)	(ppb)	(ppb)
Onswath 1	13956.0	15646.0	15124.0
Onswath 2	16243.0	13779.0	13430.0
Onswath 3	13147.0	14313.0	13484.0
Onswath 4	14693.0	16649.0	14724.0
5	24.30	37.80	10.16
10	16.687	14.471	11.717
15	11.238	9.510	36.029
20	1.005	1.519	0.934
35	0.573	0.982	0.934
50	0.4901	0.6833	0.8940
65	0.4670	0.2363	0.2814
80	0.3667	0.3892	0.4074
95	0.2425	0.2353	0.3374
110	0.2348	0.2732	0.1884
125	0.3704	0.2806	0.2653
140	0.1647	0.2084	0.2240
155	0.2339	0.3480	0.1003
170	0.0655	0.1173	0.1107

String Data

Height	Concentration	
	Upwind	Downwind
(m)	(ppb)	(ppb)
30		
29		
28		
27		
26		
25		
24		
23		
22		
21		
20		
19		
18		
17		
16		
15		
14		
13		
12		
11		
10		
9		
8		
7		
6		
5		
4		
3		
2		
1		

Upwind string collector not used
Downwind string collector data not available

Rotorod Data

Upwind of Shelterbelt

Height	Concentration		
	Row 1	Row 2	Row 3
(m)	(ppb)	(ppb)	(ppb)
1	71.209	75.645	59.520
2	71.394	68.441	55.171
3	41.060	62.662	40.452
4	27.070	36.010	29.656

Downwind of Shelterbelt

Height	Concentration		
	Row 1	Row 2	Row 3
(m)	(ppb)	(ppb)	(ppb)
1	4.943	8.116	2.376
2	6.377	10.654	1.338
3	10.343	8.760	3.398
4	3.806	13.451	5.238

Petri-dish Blanks

Dish #	Concentration (ppb)
1	-0.0597
2	-0.0594
3	-0.0597
4	-0.0532

Rotorod Blanks

Height (m)	Concentration (ppb)
1	3.8247
2	2.5890
3	4.0770
4	4.8080

Photolysis

Dish #	Light (ppb)	Dark (ppb)
1	287.75	410.29
2	290.46	371.77
3	284.61	376.21
4	306.43	376.98

Trial 10d

Petri-plate Data

Distance	Concentration		
	Row 1	Row 2	Row 3
(m)	(ppb)	(ppb)	(ppb)
Onswath 1	4194.7	4214.5	3867.7
Onswath 2	4797.9	3948.7	4844.5
Onswath 3	3924.3	3962.6	3799.4
Onswath 4	4582.8	4312.0	4703.3
5	41.69	66.41	48.61
10	23.199	28.651	21.939
15	20.877	18.118	15.467
20	6.675	5.331	5.626
35	2.215	2.024	2.924
50	2.1760	2.5866	3.8775
65	2.6748	2.9098	2.7375
80	2.6116	2.9167	2.4249
95	1.9504	2.3591	2.1714
110	2.1775	2.1631	1.9171
125	1.6022	1.7515	1.6136
140	2.9547	1.8241	1.6700
155	0.9344	1.1976	0.6322
170	0.8451	0.8244	0.4637

String Data

Height	Concentration	
	Upwind	Downwind
(m)	(ppb)	(ppb)
30		0.463
29		0.464
28		0.309
27		0.844
26		0.723
25		0.509
24		2.429
23		0.485
22		0.309
21		0.558
20		0.341
19		0.396
18		0.306
17		0.556
16		2.373
15		0.845
14		0.474
13		0.903
12		0.915
11		1.539
10		5.249
9		5.888
8		11.621
7		13.759
6		12.237
5		7.866
4		5.593
3		4.675
2		7.623
1		5.744

Upwind string collector not used
Rotorod collector not used

Rotorod Data

Upwind of Shelterbelt

Height	Concentration		
	Row 1	Row 2	Row 3
(m)	(ppb)	(ppb)	(ppb)
1			
2			
3			
4			

Downwind of Shelterbelt

Height	Concentration		
	Row 1	Row 2	Row 3
(m)	(ppb)	(ppb)	(ppb)
1			
2			
3			
4			

Petri-dish Blanks

Dish #	Concentration (ppb)
1	0.1982
2	0.1076
3	0.1009
4	0.1235

Rotorod Blanks

Height (m)	Concentration (ppb)
1	
2	
3	
4	

Photolysis

Dish #	Light (ppb)	Dark (ppb)
1	356.34	785.09
2	363.17	740.47
3	407.06	733.29
4	466.42	825.06

Trial 11d

Petri-plate Data

Distance	Concentration		
	Row 1	Row 2	Row 3
(m)	(ppb)	(ppb)	(ppb)
Onswath 1	4536.9	5235.6	3750.1
Onswath 2	4288.0	4548.2	4787.5
Onswath 3	5660.2	4952.0	5107.9
Onswath 4	4533.4	4678.6	5380.0
5	123.70	96.78	87.45
10	61.813	62.356	35.107
15	31.576	40.372	24.468
20	7.105	6.217	16.414
35	5.810	4.396	5.232
50	5.4800	2.8530	4.8865
65	3.2923	3.4953	4.7151
80	3.1577	3.0420	3.6096
95	2.6315	2.2661	2.4036
110	2.1653	2.4748	2.0938
125	1.9187	2.3925	2.1889
140	1.4387	1.2500	1.9125
155	1.6213	1.2620	1.6092
170	1.7763	1.3361	1.2377

String Data

Height	Concentration	
	Upwind	Downwind
(m)	(ppb)	(ppb)
30		1.809
29		0.792
28		0.429
27		1.609
26		0.593
25		0.209
24		0.642
23		0.288
22		0.351
21		0.264
20		0.552
19		0.978
18		0.302
17		0.633
16		0.226
15		0.248
14		0.427
13		0.598
12		0.318
11		0.727
10		1.275
9		2.635
8		5.928
7		6.061
6		11.266
5		7.068
4		7.382
3		9.807
2		12.962
1		20.145

Rotorod Data

Upwind of Shelterbelt

Height	Concentration		
	Row 1	Row 2	Row 3
(m)	(ppb)	(ppb)	(ppb)
1			
2			
3			
4			

Downwind of Shelterbelt

Height	Concentration		
	Row 1	Row 2	Row 3
(m)	(ppb)	(ppb)	(ppb)
1			
2			
3			
4			

Upwind string collector not used
Rotorod collector not used

Petri-dish Blanks		**Rotorod Blanks**	
Dish #	Concentration (ppb)	Height (m)	Concentration (ppb)
1	-0.0903	1	
2	0.0235	2	
3	0.0597	3	
4	0.0278	4	

Photolysis

Dish #	Light (ppb)	Dark (ppb)
1	699.98	926.79
2	796.88	910.44
3	722.41	875.49
4	675.78	859.05

Trial 12d

Petri-plate Data

Distance	Concentration		
	Row 1	Row 2	Row 3
(m)	(ppb)	(ppb)	(ppb)
Onswath 1	4707.9	4515.4	4802.9
Onswath 2	4953.3	4619.6	5253.7
Onswath 3	6212.1	6299.5	5351.6
Onswath 4	5543.4	5683.8	5056.2
5	90.92	70.06	69.52
10	25.255	41.398	31.185
15	15.681	30.963	31.503
20	16.485	9.114	6.188
35	4.240	3.815	3.220
50	4.3238	4.0616	3.1126
65	4.7657	4.6003	2.8225
80	4.5617	3.7572	3.4305
95	3.9914	3.9198	3.3340
110	3.2682	3.7515	3.0627
125	3.1367	4.0471	3.5592
140	3.7244	3.0713	3.6634
155	2.4649	2.4397	2.8595
170	1.9860	2.2548	2.3984

String Data

Height	Concentration	
	Upwind	Downwind
(m)	(ppb)	(ppb)
30		1.234
29		0.389
28		0.707
27		0.663
26		0.481
25		0.365
24		0.286
23		1.452
22		0.254
21		1.311
20		0.868
19		0.559
18		0.476
17		0.466
16		0.385
15		0.542
14		0.266
13		0.434
12		0.486
11		0.776
10		1.417
9		2.972
8		7.233
7		10.301
6		8.906
5		6.903
4		9.284
3		7.857
2		6.423
1		14.408

Upwind string collector not used
Rotorod collector not used

Rotorod Data

Upwind of Shelterbelt

Height	Concentration		
	Row 1	Row 2	Row 3
(m)	(ppb)	(ppb)	(ppb)
1			
2			
3			
4			

Downwind of Shelterbelt

Height	Concentration		
	Row 1	Row 2	Row 3
(m)	(ppb)	(ppb)	(ppb)
1			
2			
3			
4			

Petri-dish Blanks

Dish #	Concentration (ppb)
1	-0.0048
2	-0.0299
3	-0.0133
4	-0.0160

Rotorod Blanks

Height (m)	Concentration (ppb)
1	
2	
3	
4	

Photolysis

Dish #	Light (ppb)	Dark (ppb)
1	727.42	805.43
2	716.27	915.40
3	690.61	832.66
4	751.73	887.13

Trial 10

Petri-plate Data

Distance	Concentration		
	Row 1	Row 2	Row 3
(m)	(ppb)	(ppb)	(ppb)
Onswath 1	4466.6	4579.8	4322.1
Onswath 2	5495.0	4532.4	4591.3
Onswath 3	5594.7	4862.5	4918.0
Onswath 4	5131.5	4930.7	4943.3
5	46.55	67.24	69.83
10	38.262	50.178	25.111
15	22.173	22.558	15.572
20	1.736	6.846	2.230
35	4.557	3.124	2.047
50	1.8069	2.8699	2.8967
65	2.1959	2.0483	1.4748
80	1.9939	2.3115	1.7086
95	0.9681	0.9913	1.3948
110	1.3981	1.6560	1.6977
125	1.6345	1.3575	1.5015
140	0.8612	0.8568	1.3562
155	0.7362	1.0657	1.0920
170	1.3081	1.3452	1.0686

String Data

Height	Concentration	
	Upwind	Downwind
(m)	(ppb)	(ppb)
30		1.483
29		0.688
28		0.506
27		0.964
26		1.094
25		0.539
24		0.478
23		0.425
22		0.439
21		0.378
20		0.564
19		0.438
18		0.551
17		0.642
16		0.469
15		0.443
14		0.427
13		0.516
12		0.487
11		0.252
10		0.418
9		0.459
8		6.120
7		17.237
6		29.410
5		30.686
4		19.353
3		14.406
2		14.036
1		1.417

Upwind string collector not used

Rotorod Data

Upwind of Shelterbelt

Height	Concentration		
	Row 1	Row 2	Row 3
(m)	(ppb)	(ppb)	(ppb)
1	53.994	61.234	34.538
2	37.409	48.263	25.700
3	18.454	26.640	22.915
4	19.636	15.748	22.675

Downwind of Shelterbelt

Height	Concentration		
	Row 1	Row 2	Row 3
(m)	(ppb)	(ppb)	(ppb)
1	11.661	19.310	6.974
2	11.033	10.183	8.789
3	25.258	17.881	10.346
4	22.177	15.833	10.842

Petri-dish Blanks

Dish #	Concentration (ppb)
1	1.1293
2	0.0048
3	-0.0772
4	-0.0753

Rotorod Blanks

Height (m)	Concentration (ppb)
1	-0.0720
2	-0.0710
3	-0.0779
4	0.0122

Photolysis

Dish #	Light (ppb)	Dark (ppb)
1	571.31	845.10
2	531.80	921.58
3	565.19	799.18
4	594.62	831.20

Trial 11

Petri-plate Data

Distance	Concentration		
	Row 1	Row 2	Row 3
(m)	(ppb)	(ppb)	(ppb)
Onswath 1	11692.8	14765.2	14713.4
Onswath 2	15584.8	15434.8	14755.4
Onswath 3	16617.4	15835.4	15227.0
Onswath 4	14692.6	15845.2	16413.6
5	48.90	63.01	107.84
10	25.242	44.933	35.715
15	22.060	18.638	19.112
20	5.363	5.759	4.381
35	4.663	3.477	2.672
50	3.3387	3.9314	4.0110
65	2.9685	3.6824	3.9401
80	1.6163	3.0367	2.3920
95	2.3581	2.3081	1.9693
110	1.8698	2.2683	2.5864
125	2.1344	1.7027	2.3102
140	2.1708	1.3884	1.6364
155	1.5381	1.6211	1.6341
170	2.4541	1.3458	1.3878

String Data

Height	Concentration	
	Upwind	Downwind
(m)	(ppb)	(ppb)
30		
29		1.119
28		0.993
27		1.199
26		0.942
25		0.497
24		0.399
23		0.377
22		1.427
21		0.515
20		0.782
19		0.742
18		1.587
17		1.258
16		0.941
15		0.741
14		0.493
13		0.502
12		0.477
11		1.157
10		2.035
9		4.395
8		9.095
7		22.418
6		39.928
5		61.918
4		49.049
3		27.213
2		19.555
1		2.467

Upwind string collector not used

Rotorod Data

Upwind of Shelterbelt

Height	Concentration		
	Row 1	Row 2	Row 3
(m)	(ppb)	(ppb)	(ppb)
1	53.994	61.234	34.538
2	37.409	48.263	25.700
3	18.454	26.640	22.915
4	19.636	15.748	22.675

Downwind of Shelterbelt

Height	Concentration		
	Row 1	Row 2	Row 3
(m)	(ppb)	(ppb)	(ppb)
1	11.661	19.310	6.974
2	11.033	10.183	8.789
3	25.258	17.881	10.346
4	22.177	15.833	10.842

Petri-dish Blanks

Dish #	Concentration (ppb)
1	-0.1471
2	-0.1210
3	-0.1755
4	-0.1813

Rotorod Blanks

Height (m)	Concentration (ppb)
1	-0.0850
2	-0.0708
3	-0.0571
4	-0.0318

Photolysis

Dish #	Light (ppb)	Dark (ppb)
1	659.93	799.60
2	691.10	874.55
3	647.51	814.85
4	628.69	842.08

Trial 12

Petri-plate Data

Distance	Concentration		
	Row 1	Row 2	Row 3
(m)	(ppb)	(ppb)	(ppb)
Onswath 1	16047.2	18206.0	17541.8
Onswath 2	18807.8	16222.2	16980.6
Onswath 3	19248.6	16671.2	19166.2
Onswath 4	19968.2	15520.4	14373.4
5	14.32	31.05	35.04
10	7.630	14.007	13.873
15	4.424	6.596	7.311
20	1.087	1.556	0.858
35	0.740	0.492	1.249
50	1.2736	1.5120	0.6147
65	0.7293	0.6028	0.4631
80	0.5886	0.5162	0.3630
95	0.3163	0.2818	0.2707
110	0.1750	0.0749	0.3167
125	0.1443	0.4091	0.4284
140	0.0107	0.0978	0.0412
155	0.1393	0.1133	0.1387
170	0.1489	0.1586	0.0100

String Data

Height	Concentration	
	Upwind	Downwind
(m)	(ppb)	(ppb)
30		
29		0.416
28		0.251
27		0.222
26		0.142
25		0.144
24		0.140
23		0.171
22		0.139
21		0.231
20		0.265
19		0.148
18		0.247
17		0.239
16		0.194
15		0.106
14		0.112
13		0.109
12		0.231
11		0.232
10		0.229
9		0.515
8		1.356
7		3.501
6		7.189
5		13.755
4		15.880
3		12.147
2		13.169
1		8.569

Upwind string collector not used

Rotorod Data

Upwind of Shelterbelt

Height	Concentration		
	Row 1	Row 2	Row 3
(m)	(ppb)	(ppb)	(ppb)
1	53.994	61.234	34.538
2	37.409	48.263	25.700
3	18.454	26.640	22.915
4	19.636	15.748	22.675

Downwind of Shelterbelt

Height	Concentration		
	Row 1	Row 2	Row 3
(m)	(ppb)	(ppb)	(ppb)
1	11.661	19.310	6.974
2	11.033	10.183	8.789
3	25.258	17.881	10.346
4	22.177	15.833	10.842

Petri-dish Blanks

Dish #	Concentration (ppb)
1	-0.1701
2	-0.1651
3	-0.1860
4	-0.2012

Rotorod Blanks

Height (m)	Concentration (ppb)
1	-0.0671
2	-0.0607
3	-0.0702
4	-0.0461

Photolysis

Dish #	Light (ppb)	Dark (ppb)
1	647.84	899.90
2	675.90	867.66
3	747.02	843.91
4	714.36	858.64

Trial 13

Petri-plate Data

Distance	Concentration		
	Row 1	Row 2	Row 3
(m)	(ppb)	(ppb)	(ppb)
Onswath 1	5177.0	4541.1	5132.8
Onswath 2	3947.1	2904.6	4369.1
Onswath 3	4633.9	4633.3	4196.2
Onswath 4	4551.9	3787.1	4622.9
5	82.10	96.69	82.56
10	39.292	42.939	27.427
15	27.500	18.635	20.050
20	6.635	4.273	5.947
35	3.850	7.619	2.940
50	6.2978	4.9997	3.0727
65	3.2395	4.0601	5.2627
80	2.6092	2.1546	3.1428
95	1.9958	2.2357	1.4516
110	1.0414	1.2250	1.5766
125	1.2340	1.2545	1.1178
140	1.1808	0.7658	0.8004
155	0.6678	0.8919	0.5763
170	0.6870	0.6030	0.6676

String Data

Height	Concentration	
	Upwind	Downwind
(m)	(ppb)	(ppb)
30		
29		1.094
28		0.452
27		0.568
26		0.820
25		0.790
24		0.574
23		0.596
22		0.248
21		0.567
20		0.596
19		0.555
18		0.725
17		0.554
16		0.727
15		0.503
14		0.884
13		0.604
12		1.211
11		2.320
10		4.652
9		8.160
8		21.187
7		27.791
6		37.011
5		43.851
4		37.722
3		28.814
2		12.476
1		16.477

Upwind string collector not used

Rotorod Data

Upwind of Shelterbelt

Height	Concentration		
	Row 1	Row 2	Row 3
(m)	(ppb)	(ppb)	(ppb)
1	53.994	61.234	34.538
2	37.409	48.263	25.700
3	18.454	26.640	22.915
4	19.636	15.748	22.675

Downwind of Shelterbelt

Height	Concentration		
	Row 1	Row 2	Row 3
(m)	(ppb)	(ppb)	(ppb)
1	11.661	19.310	6.974
2	11.033	10.183	8.789
3	25.258	17.881	10.346
4	22.177	15.833	10.842

Petri-dish Blanks

Dish #	Concentration (ppb)
1	-0.0481
2	-0.1741
3	-0.2023
4	-0.1920

Rotorod Blanks

Height (m)	Concentration (ppb)
1	-0.0858
2	-0.0866
3	-0.0927
4	-0.0869

Photolysis

Dish #	Light (ppb)	Dark (ppb)
1	649.99	811.05
2	712.56	888.52
3	664.99	829.69
4	778.08	919.94

Trial 14

Petri-plate Data

Distance	Concentration		
	Row 1	Row 2	Row 3
(m)	(ppb)	(ppb)	(ppb)
Onswath 1	15179.6	14851.4	14333.0
Onswath 2	17952.4	13063.4	13806.8
Onswath 3	13634.6	14392.4	13141.2
Onswath 4	13976.8	14312.8	14821.2
5	62.91	99.71	130.73
10	44.795	46.923	62.836
15	30.760	40.035	38.930
20	10.669	11.488	8.200
35	5.824	7.784	6.800
50	6.0814	5.2505	6.8632
65	5.3818	5.2032	5.1979
80	4.1208	5.4322	3.4789
95	3.1719	4.0269	4.0092
110	2.5019	2.6205	2.6773
125	1.5212	2.6833	2.7733
140	2.2438	2.9503	1.9508
155	2.0737	2.2901	2.4693
170	1.8009	2.3229	1.4286

String Data

Height	Concentration	
	Upwind	Downwind
(m)	(ppb)	(ppb)
30		
29		1.104
28		0.972
27		0.606
26		0.724
25		0.463
24		0.623
23		0.477
22		1.228
21		0.391
20		0.520
19		0.602
18		1.270
17		0.658
16		0.615
15		0.744
14		1.267
13		0.379
12		0.591
11		1.216
10		2.043
9		14.182
8		35.237
7		60.272
6		78.953
5		58.509
4		55.784
3		31.409
2		37.690
1		20.407

Upwind string collector not used

Rotorod Data

Upwind of Shelterbelt

Height	Concentration		
	Row 1	Row 2	Row 3
(m)	(ppb)	(ppb)	(ppb)
1	53.994	61.234	34.538
2	37.409	48.263	25.700
3	18.454	26.640	22.915
4	19.636	15.748	22.675

Downwind of Shelterbelt

Height	Concentration		
	Row 1	Row 2	Row 3
(m)	(ppb)	(ppb)	(ppb)
1	11.661	19.310	6.974
2	11.033	10.183	8.789
3	25.258	17.881	10.346
4	22.177	15.833	10.842

Petri-dish Blanks

Dish #	Concentration (ppb)
1	-0.1937
2	-0.2018
3	-0.2096
4	-0.2134

Rotorod Blanks

Height (m)	Concentration (ppb)
1	-0.0918
2	-0.0874
3	-0.0856
4	-0.0754

Photolysis

Dish #	Light (ppb)	Dark (ppb)
1	621.68	798.34
2	630.99	755.29
3	642.42	798.29
4	592.87	785.13

Trial 15

Petri-plate Data

Distance	Concentration		
	Row 1	Row 2	Row 3
(m)	(ppb)	(ppb)	(ppb)
Onswath 1	18888.2	18012.8	13783.0
Onswath 2	15801.2	16206.0	18628.4
Onswath 3	16878.4	16785.8	15319.8
Onswath 4	19740.0	17066.2	16801.6
5	35.79	31.08	72.33
10	20.353	8.933	22.761
15	21.558	11.308	9.971
20	2.186	6.046	1.191
35	1.926	1.844	1.864
50	1.9257	0.9749	1.2437
65	1.0120	0.6901	0.7635
80	0.7914	0.7511	0.6404
95	0.4451	0.5375	0.4166
110	0.4126	0.3735	0.3985
125	0.4311	0.3912	0.2199
140	0.2645	0.3312	0.2152
155	0.1306	0.2992	0.3170
170	0.5360	0.0999	0.2369

String Data

Height	Concentration	
	Upwind	Downwind
(m)	(ppb)	(ppb)
30		
29		
28		0.447
27		0.161
26		0.193
25		0.231
24		0.244
23		0.239
22		0.702
21		0.179
20		0.138
19		0.273
18		0.176
17		0.250
16		0.195
15		0.278
14		0.367
13		0.323
12		0.437
11		0.400
10		0.786
9		0.932
8		5.226
7		9.493
6		17.032
5		29.455
4		30.440
3		16.352
2		12.707
1		11.203

Upwind string collector not used

Rotorod Data

Upwind of Shelterbelt

Height	Concentration		
	Row 1	Row 2	Row 3
(m)	(ppb)	(ppb)	(ppb)
1	53.994	61.234	34.538
2	37.409	48.263	25.700
3	18.454	26.640	22.915
4	19.636	15.748	22.675

Downwind of Shelterbelt

Height	Concentration		
	Row 1	Row 2	Row 3
(m)	(ppb)	(ppb)	(ppb)
1	11.661	19.310	6.974
2	11.033	10.183	8.789
3	25.258	17.881	10.346
4	22.177	15.833	10.842

Petri-dish Blanks

Dish #	Concentration (ppb)
1	-0.2163
2	-0.0974
3	-0.2030
4	-0.2008

Rotorod Blanks

Height (m)	Concentration (ppb)
1	-0.0783
2	-0.0968
3	-0.0980
4	-0.0985

Photolysis

Dish #	Light (ppb)	Dark (ppb)
1	527.35	777.60
2	510.27	773.29
3	516.31	777.69
4	554.75	881.90

Trial 16

Petri-plate Data

Distance	Concentration		
	Row 1	Row 2	Row 3
(m)	(ppb)	(ppb)	(ppb)
Onswath 1	12044.8	11361.8	14937.0
Onswath 2	11127.0	9066.6	9872.2
Onswath 3	10273.0	12499.2	15555.2
Onswath 4	13474.2	9669.4	10841.2
5	365.26	184.69	339.02
10	1.337	14.089	2.230
25	4.781	4.021	3.764
40	4.451	5.404	2.595
55	4.692	2.625	2.114
70	2.0691	2.1314	2.9551
85	1.6342	1.8349	2.6871
100	1.3605	2.7391	1.8175
115	1.6854	0.9998	1.5960
130	1.2263	0.9141	1.1396
145	0.9351	0.7068	1.2191
160	0.9949	1.0388	0.8970

String Data

Height	Concentration	
	Upwind	Downwind
(m)	(ppb)	(ppb)
30		
29		
28		
27		
26		
25		
24		
23		
22		
21		
20		
19		
18		
17		
16		
15		
14		
13		
12		
11		
10		
9		
8		
7		
6		
5		
4		
3		
2		
1		

Rotorod Data

Upwind of Shelterbelt

Height	Concentration		
	Row 1	Row 2	Row 3
(m)	(ppb)	(ppb)	(ppb)
1	404.940	455.080	
2	309.080	232.440	
3	107.990	127.030	
4	53.485	56.989	

Downwind of Shelterbelt

Height	Concentration		
	Row 1	Row 2	Row 3
(m)	(ppb)	(ppb)	(ppb)
1	30.930	27.278	
2	47.380	34.367	
3	15.761	14.008	
4	30.974	32.187	

Upwind string collector data not available
Downwind string collector data not available
Third rotorod pole not used

Petri-dish Blanks

Dish #	Concentration (ppb)
1	-0.0773
2	-0.0778
3	-0.0754
4	-0.0778

Rotorod Blanks

Height (m)	Concentration (ppb)
1	-0.0028
2	-0.0261
3	-0.0329
4	-0.0143

Photolysis

Dish #	Light (ppb)	Dark (ppb)
1	352.31	543.17
2	382.13	567.53
3	319.49	567.04
4	441.02	590.63

Trial 17

Petri-plate Data

Distance	Concentration		
	Row 1	Row 2	Row 3
(m)	(ppb)	(ppb)	(ppb)
Onswath 1	10555.0	16362.8	12348.6
Onswath 2	9885.4	13551.0	13393.0
Onswath 3	9523.6	13186.6	8679.0
Onswath 4	11023.2	14893.6	12751.0
5	240.06	297.36	336.88
10	176.004	158.890	113.752
15	29.634	244.860	80.873
20	1.028	4.178	1.241
35	1.926	3.692	4.183
50	2.9464	3.7202	5.5871
65	2.4867	2.2904	2.6548
80	2.7855	1.7087	2.6035
95	1.6060	3.9482	3.4495
110	1.6155	1.1640	1.6336
125	0.9082	0.7349	1.4626
140	0.8897	0.4496	0.6556
155	0.5290	0.4219	0.7394
170	1.0345	0.6583	0.5016

String Data

Height	Concentration	
	Upwind	Downwind
(m)	(ppb)	(ppb)
30		
29		
28		
27		
26		
25		
24		
23		
22		
21		
20		
19		
18		
17		
16		
15		
14		
13		
12		
11		
10		
9		
8		
7		
6		
5		
4		
3		
2		
1		

Rotorod Data

Upwind of Shelterbelt

Height	Concentration		
	Row 1	Row 2	Row 3
(m)	(ppb)	(ppb)	(ppb)
1	195.564	184.402	
2	171.188	176.250	
3	132.560	127.740	
4	47.314	76.393	

Downwind of Shelterbelt

Height	Concentration		
	Row 1	Row 2	Row 3
(m)	(ppb)	(ppb)	(ppb)
1	30.634	24.929	
2	40.717	31.415	
3	17.522	10.225	
4	28.248	14.530	

Upwind string collector data not available
Downwind string collector data not available
Third rotorod pole not used

Petri-dish Blanks

Dish #	Concentration (ppb)
1	-0.0893
2	-0.0917
3	-0.0993
4	-0.0973

Rotorod Blanks

Height (m)	Concentration (ppb)
1	-0.0013
2	-0.0010
3	0.0326
4	0.0379

Photolysis

Dish #	Light (ppb)	Dark (ppb)
1	No photolysis data available	
2	Use average of Trials 16 & 18	
3		
4		

Trial 18

Petri-plate Data

Distance	Concentration		
	Row 1	Row 2	Row 3
(m)	(ppb)	(ppb)	(ppb)
Onswath 1	7782.4	8585.8	4700.8
Onswath 2	5933.6	8833.8	7083.4
Onswath 3	11485.4	11864.6	10186.4
Onswath 4	10176.8	8210.0	8955.8
5	264.84	246.10	213.70
10	180.170	353.600	158.452
15	120.950	114.260	104.950
20	38.106	50.028	108.370
25	20.775	21.138	121.970
30	21.9520	20.3080	46.9730
35	1.0754	4.2679	2.4401
50	2.4448	3.3638	4.6350
65	4.5724	5.9702	3.4801
80	4.0597	2.5987	2.4743
95	1.5458	3.1817	4.6265
110	3.4036	4.0577	4.8950
125	2.6948	2.5928	2.4990
140	2.8026	2.2936	2.8344
155	2.1968	1.8676	1.9441
170	1.8136	1.3251	2.4770
185	1.9493	2.6176	2.2430

Rotorod Data

Upwind of Shelterbelt

Height	Concentration		
	Row 1	Row 2	Row 3
(m)	(ppb)	(ppb)	(ppb)
1	172.610	62.552	
2	105.260	55.996	
3	64.130	35.335	
4	43.366	25.250	

Downwind of Shelterbelt

Height	Concentration		
	Row 1	Row 2	Row 3
(m)	(ppb)	(ppb)	(ppb)
1	10.845	15.457	
2	18.229	13.283	
3	20.008	2.949	
4	9.626	7.935	

String Data

Height	Concentration	
	Upwind	Downwind
(m)	(ppb)	(ppb)
30		
29		
28		
27		
26		
25		
24		
23		
22		
21		
20		
19		
18		
17		
16		
15		
14		
13		
12		
11		
10		
9		
8		
7		
6		
5		
4		
3		
2		
1		

Upwind string collector data not available
Downwind string collector data not available
Third rotorod pole not used

Petri-dish Blanks

Dish #	Concentration (ppb)
1	-0.0982
2	-0.1016
3	-0.1010
4	-0.1012

Rotorod Blanks

Height (m)	Concentration (ppb)
1	0.0012
2	0.0376
3	0.0059
4	0.0380

Photolysis

Dish #	Light (ppb)	Dark (ppb)
1	372.30	603.60
2	341.21	537.89
3	347.36	575.18
4	291.87	540.44

Trial 19

Petri-plate Data

Distance	Concentration		
	Row 1	Row 2	Row 3
(m)	(ppb)	(ppb)	(ppb)
Onswath 1	8843.2	14462.4	10678.2
Onswath 2	10071.2	12192.4	12956.4
Onswath 3	11558.6	10553.0	11827.8
Onswath 4	13502.8	11464.8	14187.6
5	61.56	50.11	56.46
10	5.661	7.395	10.866
25	4.574	3.893	3.776
40	2.475	3.222	5.101
55	2.379	2.378	3.303
70	1.9130	1.8498	2.7432
85	0.9963	1.4233	1.0386
100	1.2063	1.2321	0.9563
115	0.9838	1.1595	0.8982
130	0.9458	0.9755	0.7718
145	0.8322	0.8433	0.7852
160	0.9454		1.3903

String Data

Height	Concentration	
	Upwind	Downwind
(m)	(ppb)	(ppb)
30	0.742	0.469
29	0.177	0.091
28	0.125	0.181
27	0.100	0.277
26	0.594	0.256
25	0.107	0.071
24	0.090	0.116
23	0.086	0.325
22	1.104	0.075
21	0.271	0.287
20	0.306	0.044
19	0.130	0.293
18	0.042	0.197
17	0.047	0.080
16	1.282	0.121
15	0.075	2.048
14	0.093	0.207
13	0.180	0.509
12	0.522	0.479
11	1.750	0.169
10	0.422	0.760
9	3.933	4.117
8	0.465	9.255
7	1.163	14.604
6	8.572	31.362
5	35.692	21.570
4	68.497	11.716
3	159.330	8.164
2	243.560	12.594
1	243.810	12.066

Rotorod Data

Upwind of Shelterbelt

Height	Concentration		
	Row 1	Row 2	Row 3
(m)	(ppb)	(ppb)	(ppb)
1			
2			
3			
4			

Downwind of Shelterbelt

Height	Concentration		
	Row 1	Row 2	Row 3
(m)	(ppb)	(ppb)	(ppb)
1	8.708	1.653	
2	14.529	3.420	
3	7.326	1.917	
4	8.510	5.776	

Upwind rotorod data unavailable
Third rotorod pole not used
Petri-dish data missing on Row 2 at x = 160 m

Petri-dish Blanks

Dish #	Concentration (ppb)
1	0.0645
2	0.0845
3	0.7470
4	0.1986

Rotorod Blanks

Height (m)	Concentration (ppb)
1	
2	
3	
4	

Photolysis

Dish #	Light (ppb)	Dark (ppb)
1	192.61	479.40
2	289.65	539.95
3	277.20	499.87
4	213.44	511.62

Trial 20

Petri-plate Data

Distance	Concentration		
	Row 1	Row 2	Row 3
(m)	(ppb)	(ppb)	(ppb)
Onswath 1	10206.2	10478.0	15204.4
Onswath 2	16006.4	9225.8	11361.8
Onswath 3	9259.0	10727.4	10873.2
Onswath 4	9091.6	9100.8	10980.6
5	35.12	89.65	119.20
10	35.380	25.137	21.113
15	20.881	15.194	16.784
20	3.644	12.714	6.571
35	4.983	8.389	9.588
50	5.1683	6.5205	5.0574
65	4.5427	5.5049	4.8401
80	3.6815	4.1399	3.2156
95	3.7481	3.4966	2.0474
110	2.0477	1.9235	1.7735
125	1.4424	1.4901	1.3652
140	0.6184	0.9144	0.7719
155	0.6808	0.7363	0.4842
170	0.8480	0.8240	0.2076

String Data

Height	Concentration	
	Upwind	Downwind
(m)	(ppb)	(ppb)
30	3.140	0.512
29	1.046	0.239
28	0.538	0.375
27	0.318	0.508
26	0.593	0.529
25	1.616	0.240
24	0.399	0.146
23	0.214	0.676
22	0.470	0.129
21	0.363	0.217
20	0.423	1.403
19	0.190	0.336
18	0.190	0.569
17	0.541	0.597
16	0.414	0.789
15	0.357	1.551
14	0.489	2.238
13	0.450	2.854
12	0.989	2.347
11	0.525	4.775
10	1.321	8.194
9	3.039	9.401
8	5.659	13.267
7	9.563	22.834
6	20.151	16.310
5	23.907	9.436
4	31.695	5.182
3	50.966	4.186
2	56.098	5.607
1	23.962	6.082

Rotorod Data

Upwind of Shelterbelt

Height	Concentration		
	Row 1	Row 2	Row 3
(m)	(ppb)	(ppb)	(ppb)
1			
2			
3			
4			

Downwind of Shelterbelt

Height	Concentration		
	Row 1	Row 2	Row 3
(m)	(ppb)	(ppb)	(ppb)
1	4.383	0.498	
2	9.187	0.333	
3	3.530	0.644	
4	2.028	2.473	

Upwind rotorod data unavailable
Third rotorod pole not used

Petri-dish Blanks

Dish #	Concentration (ppb)
1	-0.0115
2	-0.0039
3	-0.0087
4	-0.0264

Rotorod Blanks

Height (m)	Concentration (ppb)
1	
2	
3	
4	

Photolysis

Dish #	Light (ppb)	Dark (ppb)
1	297.37	535.47
2	312.17	549.46
3	332.65	528.88
4	307.94	527.72

Trial 21

Petri-plate Data

Distance	Concentration		
	Row 1	Row 2	Row 3
(m)	(ppb)	(ppb)	(ppb)
Onswath 1	11718.4	10804.4	9044.8
Onswath 2	11252.0	13845.4	11381.0
Onswath 3	10585.0	8908.8	12066.0
Onswath 4	8235.0	8316.2	7793.8
5	75.39	57.96	57.00
10	36.063	46.034	50.364
15	28.607	28.706	29.367
20	25.341	17.713	23.963
25	24.675	21.471	19.395
30	23.2000	23.2110	16.9030
35	5.2989	14.0650	9.3609
50	2.5330	3.7462	5.4401
65	2.3975	2.7212	2.7930
80	1.6469	1.9037	2.0710
95	1.5110	2.2874	1.8192
110	1.5934	1.9134	1.8656
125	0.7219	1.0642	2.7014
140	0.6889	0.9366	0.8283
155	0.6179	0.6797	0.5301
170	0.3185	0.3783	0.5293
185	0.2055	0.6153	0.5312

Rotorod Data

Upwind of Shelterbelt

Height	Concentration		
	Row 1	Row 2	Row 3
(m)	(ppb)	(ppb)	(ppb)
1	18.513	12.728	
2	13.837	13.609	
3	11.143	11.082	
4	10.634	10.788	

Downwind of Shelterbelt

Height	Concentration		
	Row 1	Row 2	Row 3
(m)	(ppb)	(ppb)	(ppb)
1	0.806	0.267	
2	1.141	0.492	
3	1.377	0.676	
4	0.908	0.939	

String Data

Height	Concentration	
	Upwind	Downwind
(m)	(ppb)	(ppb)
30	1.966	0.378
29	0.683	0.198
28	0.388	0.166
27	0.349	0.169
26	0.290	0.814
25	0.562	0.248
24	0.236	0.338
23	0.219	0.735
22	0.458	0.858
21	0.340	0.810
20	0.370	0.722
19	0.422	0.639
18	0.419	1.562
17	1.016	2.108
16	0.619	3.591
15	0.852	4.499
14	0.547	5.424
13	0.805	6.128
12	1.511	9.504
11	3.524	11.022
10	5.013	16.672
9	7.922	17.885
8	9.665	23.896
7	15.631	28.703
6	20.246	18.063
5	24.974	9.308
4	29.644	5.373
3	30.522	5.023
2	36.813	6.335
1	23.700	3.915

Third rotorod pole not used

Petri-dish Blanks

Dish #	Concentration (ppb)
1	0.1303
2	0.1773
3	0.1191
4	0.0296

Rotorod Blanks

Height (m)	Concentration (ppb)
1	-0.1355
2	-0.1414
3	-0.1119
4	-0.1208

Photolysis

Dish #	Light (ppb)	Dark (ppb)
1	353.02	495.14
2	368.97	552.23
3	378.02	518.01
4	393.90	559.24

Trial 22

Petri-plate Data

Distance	Concentration		
	Row 1	Row 2	Row 3
(m)	(ppb)	(ppb)	(ppb)
Onswath 1	8691.0	10787.0	15946.4
Onswath 2	12714.8	16529.8	16271.8
Onswath 3	10582.4	12492.6	15640.4
Onswath 4	11565.0	15560.2	14242.0
5			
10	6.342	7.626	8.554
25	5.801	5.927	4.440
40	2.997	3.142	2.951
55	1.757	2.103	1.773
70	1.0414	1.5023	1.4293
85	1.5443	1.5898	1.7118
100	1.1788	1.5731	1.3581
115	1.4276	1.3234	1.1798
130	1.1765	1.0074	0.8390
145	1.0965	1.0155	1.5489
160	0.9350	0.8707	0.7844

String Data

Height	Concentration	
	Upwind	Downwind
(m)	(ppb)	(ppb)
30	5.301	2.182
29	2.134	0.256
28	3.091	0.396
27	1.887	0.997
26	1.791	0.125
25	2.453	0.129
24	1.166	0.340
23	0.926	0.146
22	0.576	0.220
21	0.644	0.164
20	0.803	0.171
19	0.806	0.101
18	0.481	0.829
17	1.244	0.161
16	1.192	0.213
15	1.080	0.574
14	0.388	0.151
13	0.890	0.344
12	1.064	0.214
11	1.720	0.519
10	0.960	2.012
9	1.267	5.254
8	5.105	13.846
7	9.490	27.504
6	22.419	45.367
5	65.604	37.418
4	165.640	17.836
3	51.142	11.295
2	701.570	32.106
1	533.950	0.382

Rotorod Data

Upwind of Shelterbelt

Height	Concentration		
	Row 1	Row 2	Row 3
(m)	(ppb)	(ppb)	(ppb)
1	187.370	313.980	
2	648.070	285.410	
3	501.860	46.842	
4	278.450	69.632	

Downwind of Shelterbelt

Height	Concentration		
	Row 1	Row 2	Row 3
(m)	(ppb)	(ppb)	(ppb)
1	40.499	8.284	
2	32.691	7.585	
3	12.817	11.706	
4	29.090	16.605	

Petri-dish data missing at x = 5 m
Third rotorod pole not used

Petri-dish Blanks

Dish #	Concentration (ppb)
1	-0.0612
2	-0.1337
3	0.0254
4	0.0226

Rotorod Blanks

Height (m)	Concentration (ppb)
1	-0.1460
2	-0.1474
3	-0.1436
4	-0.1464

Photolysis

Dish #	Light (ppb)	Dark (ppb)
1	416.42	511.17
2	401.90	601.99
3	416.82	537.61
4	374.79	562.73

Trial 23

Petri-plate Data

Distance	Concentration		
	Row 1	Row 2	Row 3
(m)	(ppb)	(ppb)	(ppb)
Onswath 1	6625.2	9954.4	10988.0
Onswath 2	9616.0	10478.6	14474.8
Onswath 3	9682.6	12244.8	11497.2
Onswath 4	10228.4	13025.6	11328.2
5	42.55	70.21	59.96
10	40.561	56.500	48.110
15	22.559	30.229	50.435
20	7.532	11.982	6.881
35	7.634	5.655	7.796
50	3.5420	4.4249	3.4697
65	2.6831	3.6255	3.4004
80	2.4486	3.3496	2.7572
95	2.0518	2.2654	3.0293
110	1.6127	2.1848	2.3913
125	1.6612	1.5527	2.3190
140	1.6068	1.6109	1.9325
155	2.0050	1.0476	1.6742
170	1.8442	0.9902	1.6189

String Data

Height	Concentration	
	Upwind	Downwind
(m)	(ppb)	(ppb)
30		2.266
29	2.991	0.807
28	1.697	0.155
27	1.711	0.517
26	0.667	1.255
25	0.455	1.977
24	0.279	0.934
23	0.448	0.672
22	0.487	0.547
21	0.579	1.127
20	1.271	0.455
19	0.375	0.494
18	0.717	0.372
17	0.569	0.587
16	0.823	0.590
15	0.439	0.648
14	0.514	0.685
13	0.874	0.726
12	0.950	0.708
11	0.613	0.751
10	0.744	4.009
9	1.242	10.897
8	1.836	24.299
7	5.148	35.068
6	9.841	10.720
5	18.448	15.317
4	35.839	12.273
3	85.211	7.653
2	153.410	7.080
1	107.240	0.071

Rotorod Data

Upwind of Shelterbelt

Height	Concentration		
	Row 1	Row 2	Row 3
(m)	(ppb)	(ppb)	(ppb)
1	60.880	76.199	
2	47.628	51.559	
3	29.881	29.588	
4	29.290	31.364	

Downwind of Shelterbelt

Height	Concentration		
	Row 1	Row 2	Row 3
(m)	(ppb)	(ppb)	(ppb)
1	5.975	3.093	
2	3.793	1.763	
3	1.864	2.406	
4	5.007	3.284	

Third rotorod pole not used

Petri-dish Blanks		**Rotorod Blanks**	
Dish #	Concentration (ppb)	Height (m)	Concentration (ppb)
1	-0.0866	1	-0.1445
2	-0.0693	2	-0.1426
3	-0.0644	3	-0.1139
4	-0.0736	4	-0.1432

Photolysis

Dish #	Light (ppb)	Dark (ppb)
1	387.28	505.42
2	376.28	571.03
3	431.12	556.71
4	454.27	631.81

Trial 24

Petri-plate Data

Distance	Concentration		
	Row 1	Row 2	Row 3
(m)	(ppb)	(ppb)	(ppb)
Onswath 1	6529.4	7594.8	6551.4
Onswath 2	6431.0	6428.8	6715.0
Onswath 3	7614.6	7663.4	9916.4
Onswath 4	8383.6	8036.4	7235.6
5	69.23	49.32	63.59
10	27.358	39.468	34.770
15	33.884	34.762	30.380
20	24.811	17.323	19.963
25	21.121	19.993	18.251
30	12.2720	11.5470	19.0690
35	7.7712	12.5910	6.8279
50	6.1063	9.3895	6.1065
65	5.6841	4.2382	4.1080
80	4.7820	5.2222	3.5998
95	4.6273	4.9219	4.6091
110	2.2055	4.3727	3.4512
125	2.9009	3.6653	2.1596
140	2.5982	2.6218	1.9599
155	2.4762	2.1761	1.5509
170	1.5396	1.3058	1.4219
185	1.5935	0.7908	1.2499

String Data

Height	Concentration	
	Upwind	Downwind
(m)	(ppb)	(ppb)
30		
29		0.705
28	7.137	0.143
27	0.775	0.121
26	0.404	0.575
25	0.374	0.195
24	0.573	0.205
23	0.498	0.286
22	0.408	0.225
21	0.400	0.152
20	0.146	0.343
19	0.347	0.487
18	0.450	0.263
17	0.133	1.171
16	0.202	0.254
15	0.250	0.413
14	0.234	0.782
13	0.190	0.688
12	0.436	0.380
11	0.268	0.422
10	0.166	0.430
9	0.283	1.484
8	6.368	2.631
7	11.051	3.687
6	14.113	6.735
5	18.861	7.750
4	20.957	5.223
3	29.184	4.981
2	35.377	7.637
1	20.836	2.857

Rotorod Data

Upwind of Shelterbelt

Height	Concentration		
	Row 1	Row 2	Row 3
(m)	(ppb)	(ppb)	(ppb)
1	26.724	22.003	
2	40.895	22.236	
3	34.655	11.347	
4	26.214	10.423	

Downwind of Shelterbelt

Height	Concentration		
	Row 1	Row 2	Row 3
(m)	(ppb)	(ppb)	(ppb)
1	4.345	0.921	
2	2.606	0.510	
3	1.979	1.878	
4	2.489	0.844	

Third rotorod pole not used

Petri-dish Blanks

Dish #	Concentration (ppb)
1	-0.0837
2	-0.0957
3	-0.0364
4	-0.0687

Rotorod Blanks

Height (m)	Concentration (ppb)
1	-0.1415
2	-0.1451
3	-0.1421
4	-0.1453

Photolysis

Dish #	Light (ppb)	Dark (ppb)
1	341.13	548.81
2	354.55	568.23
3	329.72	587.64
4	303.21	567.34

Trial 25

Petri-plate Data

Distance	Concentration		
	Row 1	Row 2	Row 3
(m)	(ppb)	(ppb)	(ppb)
Onswath 1	19715.2	12516.0	13068.6
Onswath 2	15863.8	18197.6	12178.4
Onswath 3	13332.6	13743.2	16510.6
Onswath 4	15311.2	15716.8	13185.0
5	269.79	256.67	216.48
10	14.267	17.370	14.189
25	12.859	14.339	1.634
40	9.372	7.315	6.805
55	5.731	7.151	6.004
70	5.7312	4.7288	6.4090
85	4.5973	3.7981	5.0997
100	2.5559	2.4562	2.3850
115	2.1783	2.2437	2.6064
130	1.9303	1.6197	1.3614
145	1.2295	0.8125	1.5906
160	1.3054	1.2501	1.7114

String Data

Height	Concentration	
	Upwind	Downwind
(m)	(ppb)	(ppb)
30		
29	0.822	3.249
28	0.520	7.187
27	0.264	0.590
26	0.297	0.583
25	0.572	0.446
24	0.206	0.608
23	0.268	0.273
22	0.400	0.355
21	0.216	0.547
20	0.371	0.841
19	0.549	0.381
18	0.496	0.114
17	0.386	0.078
16	0.829	0.434
15	0.624	0.210
14	0.185	0.208
13	0.575	0.236
12	0.540	0.416
11	0.693	3.631
10	3.776	4.166
9	7.360	10.344
8	15.908	19.574
7	42.898	38.482
6	60.711	61.109
5	125.180	47.977
4	267.870	37.274
3	445.390	31.005
2	844.710	52.009
1	1440.500	10.570

Rotorod Data

Upwind of Shelterbelt

Height	Concentration		
	Row 1	Row 2	Row 3
(m)	(ppb)	(ppb)	(ppb)
1	857.860	486.170	
2	589.830	354.860	
3	328.330	179.730	
4	66.214	69.793	

Downwind of Shelterbelt

Height	Concentration		
	Row 1	Row 2	Row 3
(m)	(ppb)	(ppb)	(ppb)
1	24.659	9.812	
2	32.619	6.174	
3	21.838	12.544	
4	47.198	17.095	

Third rotorod pole not used

Petri-dish Blanks

Dish #	Concentration (ppb)
1	-0.0947
2	0.1777
3	-0.0454
4	-0.1106

Rotorod Blanks

Height (m)	Concentration (ppb)
1	-0.1412
2	-0.1430
3	-0.1470
4	-0.1388

Photolysis

Dish #	Light (ppb)	Dark (ppb)
1	381.23	514.90
2	404.59	480.12
3	374.25	560.62
4	409.84	547.16

Trial 26

Petri-plate Data

Distance	Concentration		
	Row 1	Row 2	Row 3
(m)	(ppb)	(ppb)	(ppb)
Onswath 1	13199.0	13764.0	9244.8
Onswath 2	13076.2	13802.6	13982.0
Onswath 3	12903.8	15617.4	8058.4
Onswath 4	13810.2	14458.6	13632.8
5	328.52	446.44	127.79
10	216.830	72.577	96.451
15	83.234	68.794	94.055
20	10.692	2.593	9.843
35	12.991	15.147	11.008
50	14.4520	13.6120	8.8804
65	9.2448	11.7000	10.1530
80	6.4110	9.5162	9.4444
95	7.5861	8.1072	10.0140
110	6.1421	6.9990	7.8807
125	5.5881	4.9824	7.0123
140	4.6723	3.6150	4.5805
155	2.9150	3.0942	5.2102
170	2.6993	3.9129	5.6523

String Data

Height	Concentration	
	Upwind	Downwind
(m)	(ppb)	(ppb)
30		1.261
29	6.507	0.547
28	2.726	1.137
27	3.519	1.724
26	3.227	0.935
25	2.537	0.410
24	2.244	0.273
23	1.744	0.788
22	1.857	0.240
21	1.730	0.206
20	1.735	0.163
19	1.796	0.212
18	1.827	1.152
17	1.472	0.348
16	1.273	0.135
15	2.208	0.246
14	1.803	0.172
13	2.130	0.652
12	1.687	1.356
11	2.691	2.447
10	3.262	0.702
9	3.183	5.788
8	12.277	21.148
7	33.143	47.336
6	43.474	70.518
5	78.452	55.273
4	154.800	46.100
3	258.300	38.281
2	313.500	20.156
1	287.610	29.660

Rotorod Data

Upwind of Shelterbelt

Height	Concentration		
	Row 1	Row 2	Row 3
(m)	(ppb)	(ppb)	(ppb)
1	178.620	171.070	
2	118.480	153.390	
3	68.711	113.460	
4	19.045	51.384	

Downwind of Shelterbelt

Height	Concentration		
	Row 1	Row 2	Row 3
(m)	(ppb)	(ppb)	(ppb)
1	4.937	11.205	
2	11.782	9.910	
3	4.896	7.289	
4	11.744	12.065	

Third rotorod pole not used

Petri-dish Blanks

Dish #	Concentration (ppb)
1	-0.0603
2	-0.1145
3	-0.0629
4	-0.1179

Rotorod Blanks

Height (m)	Concentration (ppb)
1	-0.1377
2	-0.1338
3	-0.1214
4	-0.1390

Photolysis

Dish #	Light (ppb)	Dark (ppb)
1	425.86	498.79
2	441.07	539.67
3	454.54	551.22
4	453.96	617.30

Trial 27

Petri-plate Data

Distance	Concentration		
	Row 1	Row 2	Row 3
(m)	(ppb)	(ppb)	(ppb)
Onswath 1	11962.0	12747.0	11242.8
Onswath 2	10409.8	16024.0	12737.4
Onswath 3	17450.0	14887.0	17071.8
Onswath 4	13813.2	11478.6	10595.6
5	404.90	142.06	89.68
10	77.319	151.290	115.570
15	50.124	80.768	85.279
20	49.876	54.060	57.835
25	45.609	60.780	64.599
30	22.6610	28.8660	39.3520
35	8.8980	1.8846	10.7900
50	14.4450	7.2246	11.0660
65	7.7993	6.4807	6.5819
80	4.5158	5.0425	5.6947
95	3.8562	3.8589	4.7785
110	2.1335	3.6973	4.9266
125	1.6134	1.6620	2.0101
140	1.6472	1.6360	1.8067
155	0.4706	0.5804	0.9482
170	0.1482	0.2240	0.4439
185	0.1280	0.1494	0.1229

String Data

Height	Concentration	
	Upwind	Downwind
(m)	(ppb)	(ppb)
30		
29		0.997
28	0.736	0.683
27	0.647	0.830
26	1.899	0.846
25	0.557	0.622
24	0.648	0.481
23	0.370	1.367
22	0.564	0.432
21	0.734	0.944
20	0.727	1.344
19	1.172	0.935
18	0.328	0.544
17	0.465	1.118
16	2.135	0.543
15	0.639	0.845
14	0.635	1.925
13	0.520	1.311
12	1.748	1.312
11	2.928	2.487
10	4.931	2.487
9	9.333	3.055
8	18.692	4.903
7	22.812	11.090
6	40.097	9.552
5	41.503	9.436
4	48.669	9.389
3	58.744	5.514
2	69.985	7.019
1	71.443	4.425

Rotorod Data

Upwind of Shelterbelt

Height	Concentration		
	Row 1	Row 2	Row 3
(m)	(ppb)	(ppb)	(ppb)
1	76.099	42.455	
2	56.838	32.129	
3	38.389	28.501	
4	19.093	20.923	

Downwind of Shelterbelt

Height	Concentration		
	Row 1	Row 2	Row 3
(m)	(ppb)	(ppb)	(ppb)
1	2.998	1.881	
2	3.808	2.985	
3	2.699	2.959	
4	3.612	4.210	

Third rotorod pole not used

Petri-dish Blanks

Dish #	Concentration (ppb)
1	-0.0036
2	-0.0018
3	-0.0460
4	0.0008

Rotorod Blanks

Height (m)	Concentration (ppb)
1	-0.0978
2	-0.1110
3	-0.0769
4	-0.1298

Photolysis

Dish #	Light (ppb)	Dark (ppb)
1	393.99	489.87
2	400.03	500.26
3	443.57	549.91
4	435.63	597.84

Trial 1 - Open Field (Wolf, 2006)

Petri-plate Data

Distance	Concentration		
	Row 1	Row 2	Row 3
(m)	(ppb)	(ppb)	(ppb)
Onswath 1	12956.8	10896.8	12882.8
Onswath 2	14844.2	12266.0	12195.8
Onswath 3	14530.0	13733.2	14512.6
Onswath 4	14695.8	17267.8	14034.2
5	88.24	67.03	40.33
10	23.103	25.444	34.295
15	17.001	23.387	19.190
20	18.238	16.049	15.217
35	22.179	14.930	13.020
50	5.7570	3.9537	7.4561
65	2.6838	3.3688	3.3103
80	2.8368	3.1485	2.9939
95	6.1375	5.2421	5.0276
110	1.3026	1.1159	1.3680
125	0.8323	0.8658	1.2048
140	1.1472	1.0206	1.0583
155	0.8775	0.9303	0.8104
170	0.6952	0.8088	0.6720

String Data

Height	Concentration	
	Upwind	Downwind
(m)	(ppb)	(ppb)
30	3.548	1.050
29	4.153	0.889
28	3.881	0.776
27	2.402	0.849
26	2.708	0.478
25	1.876	0.773
24	1.865	0.282
23	0.912	0.505
22	2.862	0.423
21	2.181	0.831
20	1.556	0.639
19	0.951	0.538
18	0.904	2.164
17	0.858	1.637
16	1.091	0.585
15	0.869	0.251
14	2.194	2.412
13	3.350	1.897
12	2.532	0.252
11	0.820	1.294
10	1.107	0.988
9	0.978	0.537
8	4.519	0.561
7	1.831	1.190
6	1.660	2.701
5	5.276	8.162
4	13.712	18.633
3	41.526	36.950
2	37.629	37.119
1	36.489	22.758

Rotorod Data

Upwind of Shelterbelt

Height	Concentration		
	Row 1	Row 2	Row 3
(m)	(ppb)	(ppb)	(ppb)
1	33.053	36.400	
2	24.629	16.754	
3	12.695	6.248	
4	4.657	5.257	

Downwind of Shelterbelt

Height	Concentration		
	Row 1	Row 2	Row 3
(m)	(ppb)	(ppb)	(ppb)
1	7.815	10.139	
2	10.248	5.851	
3	5.842	4.102	
4	3.130	1.302	

Third rotorod pole not used

Petri-dish Blanks

Dish #	Concentration (ppb)
1	0.0551
2	0.0098
3	0.0465
4	0.0863

Rotorod Blanks

Height (m)	Concentration (ppb)
1	-0.0311
2	-0.0378
3	-0.0157
4	-0.0598

Photolysis

Dish #	Light (ppb)	Dark (ppb)
1	348.23	518.74
2	385.30	494.72
3	361.17	518.56
4	371.13	470.62

Trial 2 - Open Field (Wolf, 2006)

Petri-plate Data

Distance	Concentration		
	Row 1	Row 2	Row 3
(m)	(ppb)	(ppb)	(ppb)
Onswath 1	10665.2	11531.4	14106.6
Onswath 2	9581.0	10871.4	11349.0
Onswath 3	11753.8	11227.4	16402.0
Onswath 4	12748.0	14450.2	13355.2
5	167.36	109.28	93.69
10	47.578	56.999	40.193
15	24.213	38.597	23.299
20	20.039	18.845	20.243
35	19.859	19.409	14.774
50	8.5744	7.9963	8.4776
65	8.1846	7.4591	7.7692
80	7.9770	7.6639	5.2587
95	6.6987	4.7748	3.0934
110	4.4279	3.3869	4.2352
125	2.5423	3.0999	3.9023
140	2.9216	2.1752	2.6776
155	3.5002	2.7164	2.8270
170	2.6308	2.3168	1.7250

String Data

Height	Concentration	
	Upwind	Downwind
(m)	(ppb)	(ppb)
30		1.746
29		1.281
28	2.536	3.719
27	2.659	0.573
26	1.065	1.881
25	0.566	0.706
24	0.563	1.284
23	0.743	1.334
22	2.752	0.867
21	1.114	1.683
20	0.735	0.853
19	0.862	1.206
18	0.541	1.056
17	0.483	0.640
16	0.732	0.506
15	0.607	0.871
14	0.518	0.919
13	1.335	0.886
12	5.215	0.835
11	0.857	0.866
10	1.784	0.929
9	0.402	1.350
8	0.751	1.809
7	1.517	3.000
6	3.673	9.856
5	12.819	27.111
4	33.378	36.844
3	71.600	45.630
2	149.120	53.769
1	49.269	58.974

Rotorod Data

Upwind of Shelterbelt

Height	Concentration		
	Row 1	Row 2	Row 3
(m)	(ppb)	(ppb)	(ppb)
1	69.335	63.093	
2	100.500	53.493	
3	33.674	27.325	
4	29.007	15.174	

Downwind of Shelterbelt

Height	Concentration		
	Row 1	Row 2	Row 3
(m)	(ppb)	(ppb)	(ppb)
1	45.116	34.878	
2	27.554	26.704	
3	13.843	14.216	
4	7.178	6.292	

Third rotorod pole not used

Petri-dish Blanks

Dish #	Concentration (ppb)
1	0.0044
2	0.0058
3	0.0174
4	0.0101

Rotorod Blanks

Height (m)	Concentration (ppb)
1	-0.0258
2	-0.0279
3	-0.0217
4	-0.0410

Photolysis

Dish #	Light (ppb)	Dark (ppb)
1	422.41	524.75
2	404.20	520.58
3	409.32	562.76
4	379.80	506.67

Trial 3 - Open Field (Wolf, 2006)

Petri-plate Data

Distance	Concentration		
	Row 1	Row 2	Row 3
(m)	(ppb)	(ppb)	(ppb)
Onswath 1	12844.4	13213.0	14913.4
Onswath 2	12639.8	13521.6	17002.4
Onswath 3	14658.0	14473.2	14654.4
Onswath 4	14158.2	17315.6	16058.4
5	89.42	118.97	100.85
10	25.885	45.641	37.737
15	22.497	30.483	33.300
20	27.774	19.229	26.791
35	12.511	10.110	18.683
50	11.1240	7.5505	6.0631
65	5.9939	6.0822	4.9925
80	4.1843	6.0971	4.2507
95	1.9047	2.4143	1.7809
110	4.3018	3.5369	4.4162
125	2.8279	3.7253	3.3697
140	3.8149	3.3288	3.1855
155	2.3751	2.5133	2.4015
170	1.9695	1.2832	1.5267

String Data

Height	Concentration	
	Upwind	Downwind
(m)	(ppb)	(ppb)
30	1.260	0.016
29	1.271	1.911
28	1.154	2.557
27	0.861	0.538
26	5.332	0.964
25	0.528	0.398
24	0.354	0.279
23	0.373	0.570
22	0.670	0.417
21	0.532	0.624
20	0.295	0.511
19	0.239	0.496
18	0.083	0.297
17	0.514	0.601
16	0.319	0.693
15	0.264	0.655
14	2.089	0.627
13	1.773	0.423
12	0.854	0.289
11	0.810	0.418
10	0.849	1.163
9	0.549	3.584
8	0.841	7.545
7	3.059	21.712
6	10.101	32.311
5	8.732	35.143
4	20.406	34.627
3	51.929	31.638
2	64.908	51.368
1	143.830	44.726

Rotorod Data

Upwind of Shelterbelt

Height	Concentration		
	Row 1	Row 2	Row 3
(m)	(ppb)	(ppb)	(ppb)
1	83.098	97.824	
2	87.516	67.967	
3	43.676	32.484	
4	58.315	10.560	

Downwind of Shelterbelt

Height	Concentration		
	Row 1	Row 2	Row 3
(m)	(ppb)	(ppb)	(ppb)
1	68.890	22.410	
2	57.592	19.517	
3	51.216	14.690	
4	40.407	8.103	

Third rotorod pole not used

Petri-dish Blanks

Dish #	Concentration (ppb)
1	0.1794
2	0.1449
3	0.2463
4	0.2716

Rotorod Blanks

Height (m)	Concentration (ppb)
1	-0.0337
2	-0.0139
3	-0.0163
4	0.0191

Photolysis

Dish #	Light (ppb)	Dark (ppb)
1	379.80	546.92
2	429.76	561.86
3	426.54	566.03
4	379.31	585.09

Appendix C

Sample Calculations

Richardson number

Trial 1

U_{1m} = 8.81 km/h
U_{4m} = 13.36 km/h
T_{1m} = 23.09°C = 296.24 K
T_{5m} = 22.65°C = 295.80 K

$$\xi = T_k + \Gamma z$$

$$\xi_{1m} = 296.24K + \left(0.01\frac{K}{m}x1m\right) \qquad \xi_{5m} = 295.80K + \left(0.01\frac{K}{m}x5m\right)$$

ξ_{1m} = 296.25 K $\qquad$ ξ_{5m} = 295.85 K

$$\frac{d\xi}{dz} = \frac{\left(\xi_{5m} - \xi_{1m}\right)}{\left(z_{5m} - z_{1m}\right)}$$

$$\frac{d\xi}{dz} = \frac{\left(295.85K - 296.25K\right)}{\left(5m - 1m\right)}$$

$$\frac{d\xi}{dz} = \text{-0.100 K/m}$$

$$\frac{dU}{dz} = \frac{\left(U_{4m} - U_{1m}\right)}{\left(z_{4m} - z_{1m}\right)}$$

$$\frac{dU}{dz} = \frac{\left(13.36 - 8.81\right)km/h}{\left(4m - 1m\right)}x\frac{1000m}{1km}x\frac{1h}{3600s}$$

$$\frac{dU}{dz} = 0.4213\ 1/s$$

$$Ri = \frac{g\left(d\xi/dz\right)}{T_K\left(dU/dz\right)^2}$$

$$Ri = 9.81\frac{m}{s^2}x - 0.100\frac{K}{m}x\frac{1}{296.25K}\left(\frac{1s}{0.4213}\right)^2$$

***Ri* = -0.0187**

Mass of Spray Applied

Trial 1

Sprayer speed, v

Length of sprayer path, L = 250 m
Time of spraying, t = 76 s

$$v = \frac{L}{t}$$

$$v = \frac{250m}{76s}$$

v = 3.29 m/s

Flow rate from sprayer, $\dot{Q}$

Flow rate per nozzle = 0.3 gpm

$$\dot{Q} = \frac{0.3gpm}{nozzle} x30nozzlesx \frac{3.785L}{gal}$$

$$\dot{Q} = 34.07\ L/min$$

Mass of Applied Spray, $M_{Applied}$

C = 0.2% v/v
ρ = 1000 g/L
W = 14.5 m

$$M_{Applied} = \frac{\dot{Q}}{vW} C\rho$$

$$M_{Applied} = \frac{34.07L}{1\min} x \frac{1s}{3.29m} x \frac{1\min}{60s} x \frac{1}{14.5m} x \left(\frac{1m}{100cm}\right)^2 x3passesx \frac{0.002Ldye}{1L} x \frac{1000g}{1L} x \frac{10^9 ng}{1g}$$

$M_{Applied}$ = 7142 ng/cm^2

Drift data – Petri-plates

Trial 1

Photolysis

$$P_h = \frac{C_{Light}}{C_{Dark}}$$

$$P_h = \frac{793.22\,ppb}{1006.63\,ppb}$$

P_h = 0.788

Petri-plate area

$$A = \frac{\pi}{4} d^2$$

$$A = \frac{\pi}{4} (15cm)^2$$

A = 176.71 cm^2

Convert drift data to ng/cm^2

Onswath1
Row 1 = 17139.0 ppb
Row 2 = 15528.8 ppb
Row 3 = 16244.8 ppb
Average = 16304.2 ppb
Corrected for photolysis = 16304.2 ppb/0.788

C_{ppb} = 20691 ppb
V_{Wash} = 50 mL
ρ = 1 g/mL

$$C_{ng/cm^2} = \frac{C_{ppb} V_{Wash} \rho}{A}$$

$$C_{ng/cm^2} = 20691 \frac{ng}{g} x 50\,mL x \frac{1}{176.71 cm^2} x \frac{1g}{1mL}$$

C_{ng/cm^2} = 5854 ng/cm^2

Convert drift data to % of Applied

$$C_{\%Applied} = \frac{C_{ng/cm^2}}{M_{Applied}}$$

$$C_{\%Applied} = \frac{5854 ng/cm^2}{7142 ng/cm^2} x100\%$$

***$C_{\%Applied}$* = 82.0%**

Drift data – Rotorods

Trial 1

Upwind of shelterbelt, z = 2 m

U = 9.62 km/h

Row 1 = 1.8553 ppb
Row 3 = 1.271 ppb
Average = 1.563 ppb
Corrected for photolysis = 1.563 ppb/0.788
C_{ppb} = 1.984 ppb

V_{Wash} = 14 mL
Sampling Volume = 120 L/min
ρ = 1 g/mL

$$C_{ng/cm^2} = \frac{C_{ppb} V_{Wash} U \rho}{SamplingVolume}$$

$$C_{ng/cm^2} = 1.984 \frac{ng}{g} x 9.62 \frac{km}{h} x \frac{\min}{120L} x \frac{1hr}{60\min} x 14mL x \frac{1g}{1mL} x \frac{1000L}{1m^3} x \frac{1000m}{1km} x \left(\frac{1m}{100cm} \right)^2$$

C_{ng/cm^2} = 3.710 ng/cm^2

Drift Data - String

Trial 1

z = 1m

C_{ppb} = 1.689 ppb
Corrected for photolysis = 1.689 ppb/0.788
C_{ppb} = 2.143 ppb
V_{Wash} = 20 mL
A = 20 cm^2

$$C_{ng/cm^2} = \frac{C_{ppb} V_{Wash} \rho}{A}$$

$$C_{ng/cm^2} = 1.689 \frac{ng}{g} x 20mL x \frac{1}{20cm^2} x \frac{1g}{1mL}$$

C_{ng/cm^2} = 2.143 ng/cm^2